POLITECNICO DI TORINO

Department of Mechanical Engineering

Master's Degree in Automotive Engineering

MASTER THESIS

Investigation of engine concepts with regard to their potential to meet the Euro 7 emission standard using 1D-CFD software

Candidate:
Calogero Limblici

Advisor:
Prof. Dr.-Ing Federico Millo

Company Supervisors:
M.Sc. Alessandro Gallo
Dipl. Ing. Vincenzo Bevilacqua

Porsche Engineering
driving technologies

Academic year 2019 - 2020

CONFIDENTIALITY CLAUSE

This master thesis contains information that is not intended for publishing. All rights to the master thesis, including distribution on electronic media, belong to Porsche Engineering Services GmbH.

In exceptional circumstances and with the explicit written permission of Porsche Engineering Services GmbH, the contents of the master thesis may be passed on to third parties during a barring period of 5 years from the date of submission. After expiration of the barring period, this approval is no longer required.

SPERRKLAUSEL

Sperrklausel Die vorliegende Masterarbeit enthält zum Teil Informationen, die nicht für die Öffentlichkeit bestimmt sind. Alle Rechte an der Masterarbeit einschließlich der Verbreitung auf elektronischen Medien liegen bei der Porsche Engineering Services GmbH.

Abweichend hiervon darf der Inhalt der Masterarbeit während einer Sperrzeit von 5 Jahren ab dem Abgabedatummit der ausdrücklichen schriftlichen Genehmigung der Porsche Engineering Services GmbH an Dritte weitergegeben werden. Nach Ablauf der Sperrzeit ist diese Genehmigung nicht mehr erforderlich.

CLAUSOLA DI RISERVATEZZA

Questa relazione contiene alcune informazioni non destinate alla pubblicazione. Tutti i diritti sul lavoro di tesi, inclusa la diffusione attraverso mezzi multimediali, sono detenuti dalla Porsche Engineering Services GmbH.

Il contenuto di questo lavoro non può essere pubblicato o trasmesso a terzi senza un’approvazione esplicita e scritta da parte della Porsche Engineering Services GmbH, per 5 anni dalla data della sua pubblicazione. Dopo questo periodo, l’autorizzazione non è più obbligatoria.

ACKNOWLEDGMENTS

First of all, I am very grateful to Porsche Engineering Services GbmH for giving me the possibility to write my Master Thesis, providing the resources and knowledge for successfully complete the work.

I would like to hugely thank my company supervisors Vincenzo and Alessandro, for the brilliant support, not only from technical side but also from human side, which was essential during the hard times due to Covid19.

A big thank goes to the whole simulation team, with special regards to M. Penzel, Matthias, David, Michal and Johannes for the great time you shared with me, even virtually in the coffee meetings.

Thanks also to Oliviero and Mara, for making amazing the time we had together, even in the difficult period of Coronavirus.

To professor Millo, for the guidance, the support and the possibility of making possible such a wonderful experience in Porsche.

To all my friends, that always believe in me and support me, with special thanks to Simone.

To my family, whose endless support is and will always be the base of every success in my life.

To Clara, for being always at my side and for her tireless support.

CONTENT

ABSTRACT

With the next Euro 7 emission standard, the fuel enrichment strategy, widely adopted in high-performance gasoline engines will be banned. This will set a new challenge in the development of internal combustion engine that will be required to run with lambda 1 in the whole engine map.

In this thesis, engine concepts capable of run with lambda 1 in full load condition, without jeopardizing the performance of the engine have been proposed. Initially, the causes of fuel enrichment have been analyzed according to the latest development in component thermal resistance, so that a new strategy of lambda control, based on the maximum temperature at catalyst inlet was considered. With the aim of reducing the fuel enrichment, several innovative engine technologies have been individually investigated on a V8 twin-turbocharged GDI engine, using a 1D-CFD simulation code capable of reliable results with limited simulation time. With this regard, the reference engine model has been updated with a new turbocharger in order to let the engine to fully exploit the potential of the technologies considered.

Subsequently, by combining the most promising technologies in terms of enrichment reduction and engine efficiency increase, i.e. E-Turbo, turbulent jet ignition, Miller cycle, A/C supporter charge air cooler and water injection, Euro 7 engine concepts have been defined and tested. On them, also a part load analysis and dynamic response investigation have been carried out, aimed at evaluating the goodness of the solution even in different operative conditions.

Moreover, thanks to the high knock mitigation potential reachable increasing the number of technologies present in the concepts, it has been possible to define Evo concepts versions which are capable of enable the stochiometric operations in the whole engine map increasing the specific power as well.

LIST OF FIGURES

LIST OF TABLES

LIST OF SYMBOLS AND ABBREVIATIONS

Symbols

α	Air-fuel ratio	n	Engine speed
c_p	Specific heat at constant pressure	η	Efficiency, effectiveness
D	Diameter	P	Power
δ	Hydrogen fraction	p	Pressure
h	Specific enthalpy	$\dot{Q}$	Heat transfer rate
i	Number of cylinders	Q_{LHV}	Lower heating value
J	Polar moment of inertia	ρ	Density
k	Isentropic coefficient	T	Torque, temperature
λ	Lambda	t	Time
m	Mass	V	Cylinder displacement, volume
$\dot{m}$	Mass flow rate	ω	Angular speed

Subscripts

a	Air	g	Gasoline
b	Brake	h	Hydrogen
c	Compressor	i	Indirect
cool	Coolant	inj	Injector
d	Direct	m	Mechanical, mixture
e	Exhaust	st	Stoichometric
eq	Equivalent	t	Turbine
f	Fuel	w	Water

Abbreviations

A/C	Naturally aspirated	IVLM	Intake valve lift multiplier
ATDCf	After top dead centre firing	LIVC	Late intake valve closure
BDC	Bottom dead centre	MFB	Mass fraction burned
BMEP	Brake mean effective pressure	NA	Naturally aspirated
BSFC	Brake specific fuel consumption	NEDC	New European driving cycle
CAC	Charge air cooler	PID	Proportional-integrative-derivative
CCV	Cycle to cycle variability	PMEP	Pumping mean effective pressure
CF	Conformity factor	PWI	Port water injection
CFD	Computational fluid dynamics	RDE	Real driving emissions
CR	Compression Ratio	RON	Research octane number
DIN	Deutsches Institut für Normung	SOC	State of charge
DOE	Design of experiment	TC	Turbocharger, turbocharged
DWI	Direct water injection	TDC	Top dead centre
EIVC	Early intake valve closure	TJI	Turbulent jet ignition
EM	Electric motor	TWC	Three way catalyst
GA	Generic algorithm	VVT	Variable valve timing
GDI	Gasoline direct injection	WG	Wastegate
ICE	Internal combustion engine	WI	Water injection
IMEP	Indicated mean effective pressure	WLTC	Worldwide harmonized light duty test cycle
IV	Intake valve		
IVAM	Intake valve angle multiplier	WOT	Wide open throttle

1. INTRODUCTION

In the recent years, the light-duty transportation sector is undergoing deep changes, mostly driven by the social need to reduce pollutants and greenhouse gases emissions. Electrification seems to be the mandatory solution in shaping a green future, where energy management is brought to a higher level with low pollutants and high efficiency in energy conversion. Although the trending pathway in electric vehicle development, improvements in the energy production plant and transportation grid, still more than the 97 % of passenger cars sold last year were equipped with an internal combustion engine (ICE) [1]. Regardless of that, the trend toward the electrification is further pushed by the periodic tightening of emission regulation standards, with always lower tailpipe emission restrictions that introduces new challenges for ICE development. As a matter of fact, in Europe since 2016 with the introduction of Euro 6 emission regulation, the New European Driving cycle (NEDC) was replaced by the new Worldwide Harmonized Light Duty Test Cycle (WLTC), more representative of real driving condition. Together with the new driving cycle, Euro 6 regulation introduced the on-road Real Driving Emission (RDE) measurements, with the aim of concretely assess the vehicle pollutant emission regulation compliance. Initially, due to the mismatch registered between dyno tests and real drive emission measurements, conformity factors (CF) were introduced, useful during the defined transition phase that will be concluded with Euro 6d temp in 2025, and periodically reviewed according to actual improvement measured in on-road emissions. Together with emission standards, CO_2 target set on fleet average and significant reduced during the years, will lead the car industry to struggle to meet the incoming 2021 target of 95 g/km [2], above which fines will be applied. Therefore, pure electric vehicles represent a concrete solution to leverage the CO_2 reduction, whilst ICE vehicle are always improving in the way of increased brake efficiency. As a matter of fact, the CO_2 targets directly reflect on the engine fuel consumption because of the carbon content present in common commercial fuels. Best gasoline ICE for light duty application nowadays reaches value of brake thermal efficiency up to 40% [3], which is a great value if compared to those of one decade ago. However, good margins of improvement are still present thanks to the introduction and development of new engine technologies aiming at maximizing the combustion as well as the fuel enrichment reduction, the heat recovery and advanced after treatment systems.

1.1. EURO 7 EMISSION STANDARDS

Europe is considering several changes in “post Euro 6d temp” regulation from 2025 on, in the optics of lower tailpipe emissions and compliance with real vehicle usage emissions. In this regard, for the incoming Euro 7 emission regulation several measures have been proposed, most of which introduce new challenge in the development of high performance turbo gasoline engine, i.e.:

- Fuel and technologies neutral standards;
- Reduction of NOx tailpipe emissions;
- Low temperature chassis dyno test at -7°C including particulates and gas emissions;
- Not to exceed limit on CO during RDE test;
- Limit on fuel enrichment.

All the proposals are somehow linked to the fuel enrichment that characterize the high load - high speed operations of gasoline engines, as shown in the engine map represented in Figure 1.1.

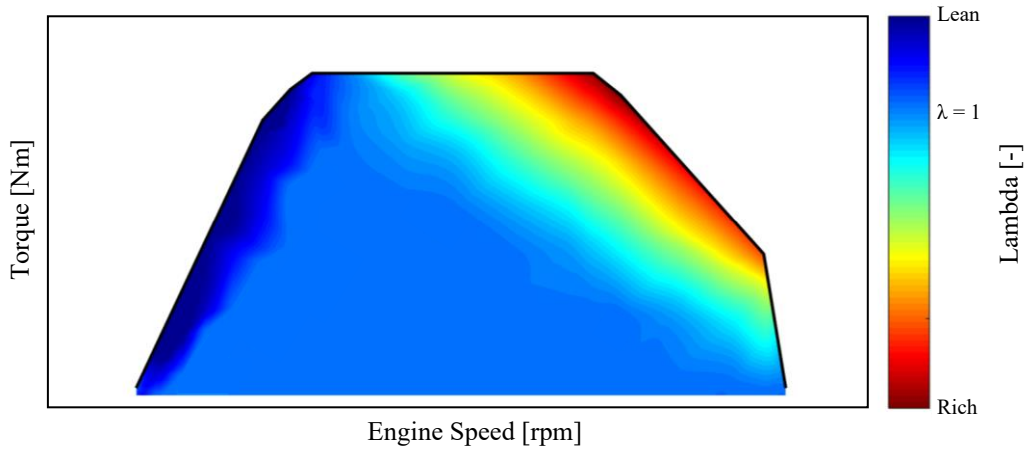

Figure 1.1: Lambda distribution over the engine map.

To evidences the correlation of the proposed measure with fuel enrichment, it is important to give some detail on the gasoline aftertreatment system. Almost all the gasoline-engine powered vehicles are equipped with the so-called three way catalyst (TWC), a very effective and affordable device which is capable to abate the main gasoline pollutant, reducing the tailpipe emissions up to the 80% [4]. However, its conversion efficiency strongly depends on the exhaust gas stoichiometric ratio or on the lambda value, defined as:

$$\lambda = \frac{\frac{\dot{m}_a}{\dot{m}_f}}{\left(\frac{\dot{m}_a}{\dot{m}_f}\right)_{st}} = \frac{\alpha}{\alpha_{st}} \tag{1.1}$$

where $\dot{m}_a$ and $\dot{m}_f$ are respectively the air mass flow rate and the fuel mass flow rate. The three way catalyst provides the highest conversion efficiencies for lambda values very close to 1, as depicted in Figure 1.2, therefore it is of paramount importance to let the engine work as close as possible to stoichiometric mixtures, preventing fuel enrichment strategies. Thus, in Euro 7 perspective, the first step in gasoline engine development is to enable the lambda 1 operation in the whole engine map, without jeopardizing the engine performance and keeping high specific power output. In fact, the reduction of performance target cannot be considered as an optimal solution, since it represents a key marketing factor as well as a decisive factor for customer value and expectation satisfaction.

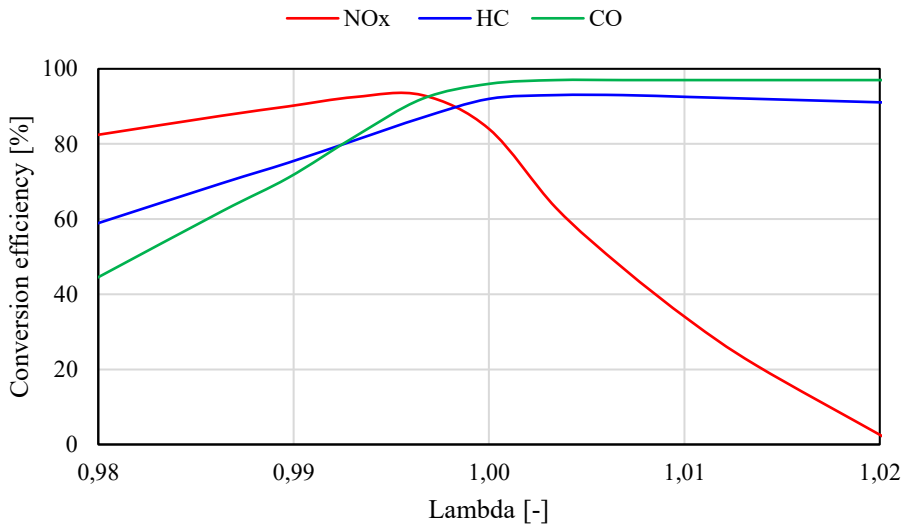

Figure 1.2: Three way catalyst pollutants conversion efficiency at varying the lambda.

1.2. TASK OF THE THESIS

The task of the thesis will be to propose *Euro 7 compliant engine concepts*, which are able to run with stoichiometric air fuel ratio in the whole engine map. The analysis was performed using a 1D-CFD code that allows to simulate the engine running in different operative condition. The definition of Euro 7 engine concepts required the investigation of several engine technologies that, according to the level of fuel enrichment reduction they are able to achieve, are combined to reach the target. The work will be developed as follows:

- Fuel enrichment strategy: motivation, analysis and understanding.
- Reference engine presentation.
- Engine model update according to the latest component and strategies development.
- Investigation of innovative engine technologies.
- Euro 7 engine concepts definition.
- Additional analysis on proposed concept.
- Conclusions.

2. PERFORMANCES OF A TURBO GASOLINE ICE

The rated power of an internal combustion engine can be expressed with the formula:

$$P_{ICE} = \eta_b \dot{m}_f Q_{LHV} \tag{2.1}$$

Where the fuel mass flow rate $\dot{m}_f$ can be replaced by:

$$\dot{m}_f = \frac{\dot{m}_a}{\alpha} = \eta_v \frac{\rho_a}{\alpha} iV \frac{n}{2} \tag{2.2}$$

Combining Formula (2.1) with Formula (1.1), then the ICE power became:

$$P_{ICE} = \eta_b \eta_v \frac{\rho_a}{\lambda \alpha_{st}} iV \frac{n}{2} Q_{LHV} \tag{2.3}$$

Fixing the engine displacement V, the cylinders number i and the engine speed n, for a naturally aspirated (NA) engine, the main parameters on which it is possible to act in order to increase the brake power are the brake efficiency η_b and the volumetric efficiency η_v, increasing the amount of trapped air into the cylinder at the end of the intake phase. However, it is also possible to increase the amount of intake air by forcing it to get into the cylinder by means of a compressor, which rises the air pressure at engine inlet. Therefore, turbocharging the engine to increase its brake power directly act on the air density ρ_a, which is increased so that more fuel can be burned, generating more power [4]. However, the air density value cannot be infinitely increased, because of mechanical and thermodynamic components limitation. Specifically, looking at the engine brake torque curve in Figure 2.1, it is possible to individuate the phenomena that limit the maximum achievable power [5], that from low to high speeds are:

- *Compressor surge*: the maximum pressure ratio that the compressor can achieve is limited by the surge limit, which must be avoided to prevent unstable behavior of the compressor. At very low engine speeds, where the air mass flow is limited, compressor surging became the limiting factor in the maximum achievable power.
- *Knock*: increasing the engine speed it is possible to increase the boost pressure, because of the higher exploitable compressor pressure ratio, but it will cause the rise of temperature at engine inlet, increasing the knock likelihood, which is further enhanced by the longer combustion time.
- *Target torque*: at mid-engine speed, the maximum torque is usually the design target torque, since combustion time shortens so that knock becomes less critical.
- *Component protection*: the maximum power at this point is limited by the maximum thermal stress that the components can withstand without damage.
- *Turbocharger maximum speed*: when the air mass flow increases a lot, compressor chocking may prevent the build-up of higher pressures.

However, among the described phenomena, the knock tendency is the most severe limit because it directly affects the maximum low-end torque and indirectly affect the maximum high-end torque, since it leads to a later combustion that in turns increases the exhaust temperature T_3, detrimental for component protection.

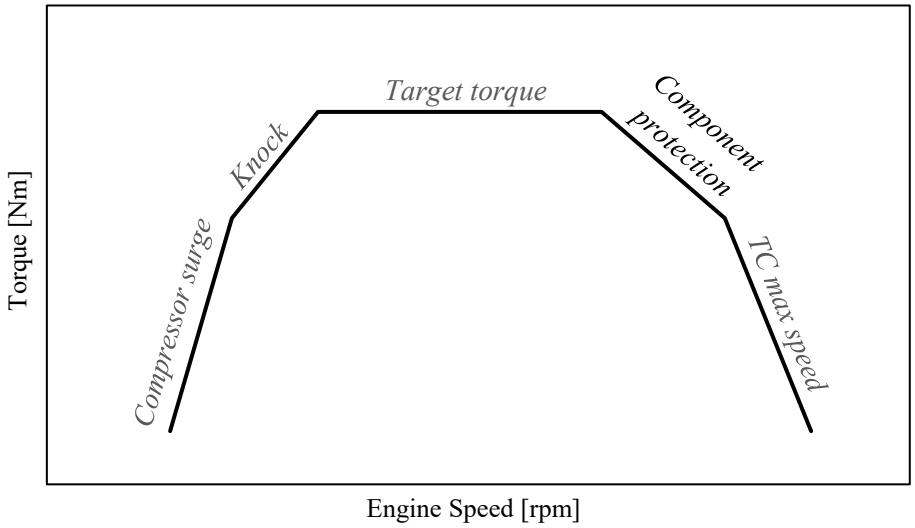

Figure 2.1: Torque limitation of a turbocharged gasoline engine.

2.1. COMPONENT PROTECTION

The component that usually sets the limit in maximum achievable power is the turbine, which has a maximum sustainable gas inlet temperature, above which irreversible component damage occurs. With the aim to avoid components failure or damage, some countermeasures are taken in order to always keep the maximum exhaust gas temperature below critical values. The most used countermeasure typically adopted in turbocharged (TC) gasoline engine is the fuel enrichment, which exploit the high vaporization heat of the fuel to cood down the mixture during compression stroke: the results of the cooler compression-end temperature is a reduced knock tendency that in turns allows to advance the combustion phasing, reducing the T_3 as a consequence.

Over the deteriorated fuel consumption, the enriched mixture leads also to an increase of carbon monoxide and unburned hydrocarbons emissions at engine out and, since lambda is lower than 1, it prevents the correct working of the three ways catalyst (TWC) as well [4]. As mentioned in Paragraph 1.1, Euro 7 emission standards will not allow any kind of fuel enrichment in the whole engine map and so different solution must be adopted in order to let the internal combustion engine working always with lambda 1, as is going to be analyzed in Chapter 5.

2.1.1. TURBINE

As mentioned, the most critical element for which fuel enrichment is required is the turbine, whose maximum inlet temperature is typically limited to about 930-980 °C, depending on the application [4]. The excessive temperature might irreversibly damage the component exceeding its material thermal limit, where structural modification may occur.

The lambda value is then controlled directly looking at the maximum T_3, which is affected by a series of factors that all together play a role in the enrichment level, but that are all related to a key

factor: the knock. In fact, increasing the knock resistance will ultimately reduce the T_3 and increase the engine efficiency.

However, in the last years lot of efforts have been spent in turbine optimization with the target of pushing the ICE performance to higher level, achieving important improvement in turbine design and on top in turbines thermal resistance. In this perspective, according to Porsche experience and in agreement with turbocharger manufacturer supplier, the maximum turbine temperature limits deriving from the optimized designs and improved materials can be now set up to 1050 °C, which represent an important result for ICE efficiency improvement potential. However, shifting the T_3 limit toward higher values, moves the needs of protection to another component that now risks of being damaged, which is the TWC. As well as for the turbine, the TWC needs some actions aiming to limits the maximum inlet temperature T_4 to prevent the component failure.

2.1.2. THREE WAY CATALYST

The three way catalyst is nowadays the most common exhaust emission control device used in gasoline engine, due to its strong capabilities of simultaneous convert the three main pollutants HC, CO and NOx into harmless component, and to the technology robustness. The temperature of exhaust gas in a spark-ignition engine vary from 300 °C for idle up to about 1000 °C for high power operation whilst in normal vehicle driving condition, the exhaust gas temperature stays in the range of about 400-600 °C that, together with a stoichiometric mixture, represent the best working condition for the TWC. However, the TWC conversion efficiency is function of the temperature as shown in Figure 2.2, so in cold start operation the catalyst is unactive up to the *light-off temperature* T_{50}, the temperature at which the conversion efficiency reaches the 50% [4]. The direct consequence is that in driving cycle emission tests or in normal cold starts, the highest pollutant quantity will be emitted in the first instants, where TWC have not reached the light-off yet. In order to speed up the catalyst warm-up, different solutions are adopted, like for example the installation of the TWC in close coupled position: it means that the TWC is placed into the engine bay, as close as possible to the exhaust runners in a NA engine and to the turbine outlet in a turbocharged engine. Although the benefits in catalyst heating times, such a position exposes the TWC to higher temperature in full load operations, that may cause the *catalyst thermal deactivation*. The catalyst design is typically oriented to the maximum exploitation of the noble materials in order to enhance its conversion capabilities: this is realized with a high dispersion of the precious materials into the carrier, but whenever exposed to high temperatures (i.e. close to 700°C), particle migration and coalescence can occur, reducing the catalyst conversion efficiency. Moreover, the exposure to higher temperature (i.e. close to 1000 °C) may also act on the carrier, causing the conversion from γ-Al_2O_3 to α- or δ-Al_2O_3 reducing the active surface. Typically, stabilizing substances are added to prevent such phenomena, nevertheless catalytic converter temperature must be kept below 950 °C to avert any damage or aging. Taking into account the heat generated into the catalyst to convert the pollutant emissions, it is possible to set an engineering limit on *maximum* T_4 *of 870 °C*.

Due to the higher turbine T_3 limits then, the more critical component became the TWC, which require actions in order to do not exceed the T_4 limit.

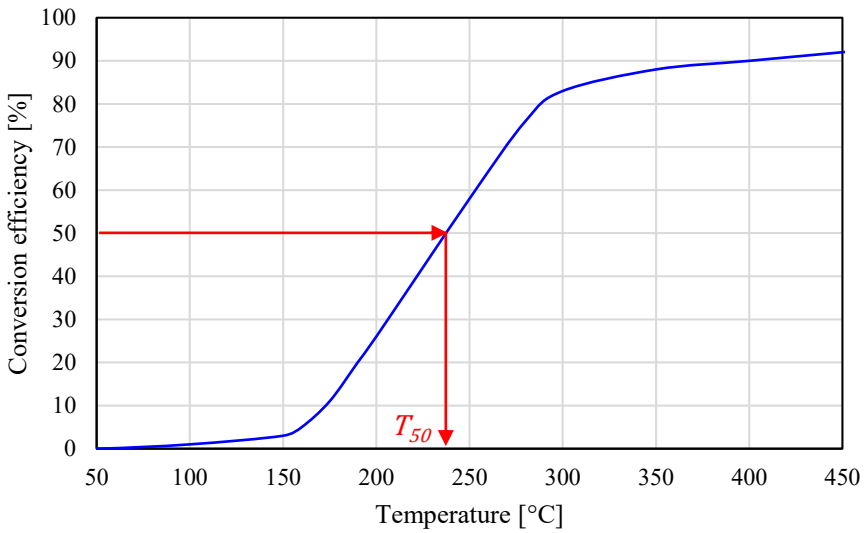

Figure 2.2: Three ways catalyst overall conversion efficiency at varying the temperature.

3. REFERENCE ENGINE

The reference engine adopted in the following analysis is a 90° V8 twin-turbocharged gasoline direct injection (GDI) engine, where detailed engine characteristics are reported in Table 3.1, and performance targets are reported in Figure 3.1. The engine has a cross-plane crankshaft that, despite its characteristic smooth running due to the intrinsic balancing, it causes a series of gas exchange problems determined by the uneven firing distance on each bank [6]. This translates in a series of blowdown interferences among cylinders on the same bank, which causes an uneven filling and mixture composition in the cylinders (different residual content), which is detrimental for final performance optimization of the engine. With this regard, the *4-2-1 exhaust manifold* in Figure 3.2 (a) and the *twisted camshaft* [7] in Figure 3.2 (b) were adopted on the engine, so that to overcame the issues related to the blowdown pulses interferences of subsequent firing cylinders.

	SPECIFICATION	DATA
Engine block	Cylinders	V8 90°
	Displacement	4.4 L
	Bore	88 mm
	Stroke	90 mm
	Compression ratio	9.5:1
	Crankshaft	Cross-Plane
Mixture preparation & Combustion	Firing order	1-3-7-2-6-5-4-8 According to DIN 73021
	Fuel supply	Direct Injection
	Air supply	Twin-Turbocharger monoscroll
Gas Exchange	Camshaft	Twisted Camshaft
	Valve train	Double VVT
	Intake valve opening duration	190 CAdeg
	Intake valve maximum lift	10.5 mm
	Exhaust valve opening duration	210 CAdeg
	Exhaust valve maximum lift	10 mm

Table 3.1: Reference engine specifications.

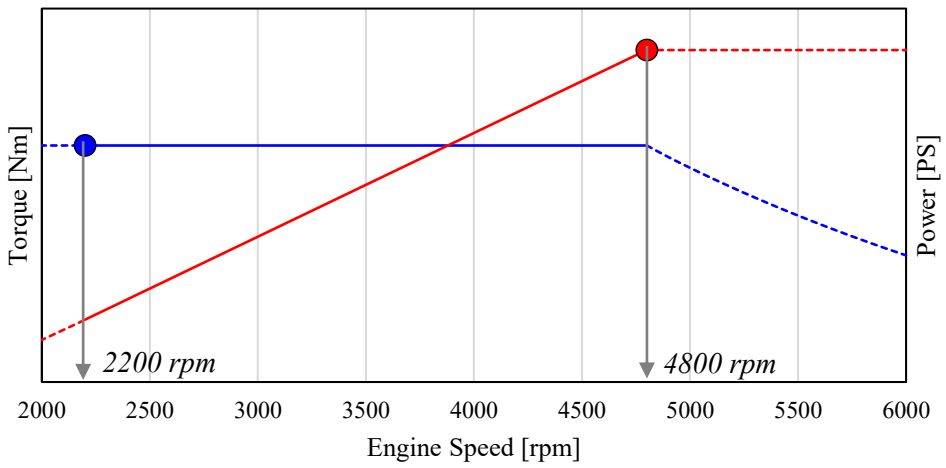

Figure 3.1: Reference engine target performance. Low-end torque target at 2200 rpm and peak power target at 4800 rpm.

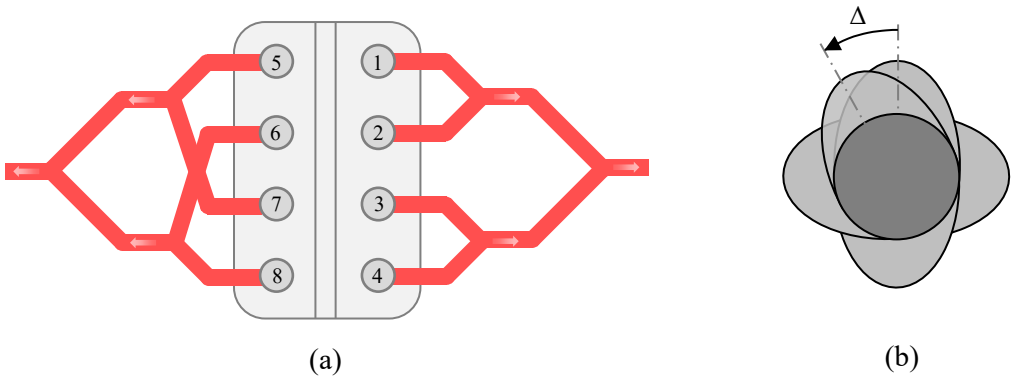

Figure 3.2: (a) 4-2-1 Exhaust manifolds. (b) Twisted Camshaft.

3.1. HYBRID ARCHITECTURE

The vehicle on which the reference V8 engine is installed is a mild hybrid, where a high voltage electric motor is positioned between gearbox and clutch, realizing a *P2 hybrid powertrain*, as shown in Figure 3.3. In a P2 hybrid configuration, being the electric motor connected to the gearbox input shaft, it is possible to run the vehicle in pure electric mode and to have a good kinetic energy recovery in braking. Thus, the described hybrid architecture gives more degree of freedom to the powertrain in traction, braking and energy management, and furthermore, it improves the pollutant emissions by aiding the ICE in transient manoeuvre. The P2 electric motor (P2 EM) is going to be exploited together with engine technologies studied, to realize the Euro 7 compliant engine concepts.

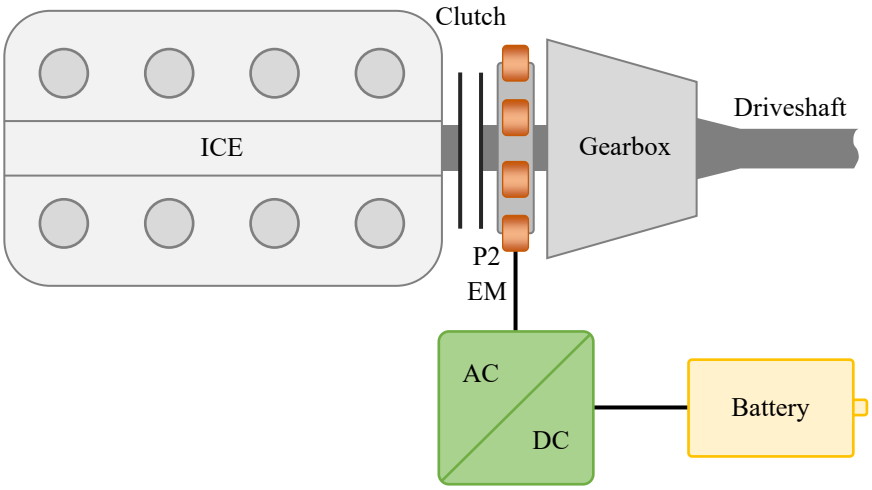

Figure 3.3: Reference engine powertrain hybrid layout.

4. SIMULATION METHODOLOGY

Nowadays internal combustion engines development is widely supported by 1D and 3D CFD simulation codes. In fact, an extensive experimental activity at test bench involves increased engine development costs and longer time-to-market for a new engine. For this reason, a numerical methodology capable to provide a reliable estimation of engine performance starting from a reduced set of measured data represents a very promising approach. Thus, the increasing refinement of 1D and 3D simulation codes make the engine simulation essential in the early development phase, thanks to their high results predictivity and costs. To the aim of the project, a 1D simulation code was used, due to its results robustness and short simulation time, which allows to investigate the system behavior under different conditions and with different technologies solutions. Specifically, the simulation code that was used is GT-POWER™, a one-dimensional fluid-dynamic code developed by Gamma Technologies Inc. for engine performance simulation [8].

4.1. ENGINE MODEL CHARACTERISTICS

The 1D engine model was originally developed by Porsche Engineering and subsequently updated up to the last engine version. However, the engine model had some features which had been modified before the analysis starts, in optic of result reliability with the investigated technologies.

That initial engine model is characterized by an imposed Wiebe combustion profile accurately calibrated against test bench data, and a phenomenological knock model to predict in cylinder autoignition occurrence. The knock model implemented is the Douaud and Eyzat, whilst the in-cylinder heat transfer is computed with Woschni correlation [9], a semi predictive equation for the instantaneous heat transfer coefficient. The detailed 1D engine model also integrates a control logic that coordinate the overall engine systems, that is illustrated in Figure 4.1. In this regards, proportional-integrative-derivative (PID) controllers are utilized. Their purpose is to achieve and maintain a target value of a certain input quantity from the system by controlling and actuating a so-called output quantity [8]. In particular, three different PID controllers were implemented:

- *Boost controller*: an internal combustion turbocharger engine is able to work with intake air pressure higher than atmospheric pressure because of the turbocharger group, where the compressor driven by the turbine force the fresh air to the engine intake manifold. Of course, the amount of air required to produce the desired output power must be finely controlled. This is done thanks to the wastegate valve that regulates the turbine extracted work from the exhaust stream and thus the power delivered to the compressor. However, it may happen that to reach the target power more air than that the compressor can provide is required. In such a condition the compressor may work in regions of the map which would be dangerous for the component and according to that, the wastegate valve is controlled also to ensure a proper safety of the whole turbocharger group: surge, overspeed and chocking are constantly monitored.
- *Lambda controller*: as already mentioned, the lambda value is controlled according to component protection constraint, whose limit working temperature require to enrich the mixture. The lambda controller enriches the mixture whenever the maximum T_3 set to 950°C

is approached, up to a minimum lambda value of 0.7, below which combustion stability dramatically deteriorates [4].

- *Knock Controller*: the knock model used for predicting the knock onset, generates an index called Knock Index whose value is related to the autoignition occurrence probability. This value was tuned according to test bench data recorded with the engine running at knock limited conditions. The PID controller controls the combustion anchor angle (which corresponds to the 50% of mass of fuel burned or MFB50) between 8° ATDCf (best thermodynamical efficiency timing) and 35° ATDCf (combustion stability acceptance limit) so that the engine runs always at knock limit combustion timing.

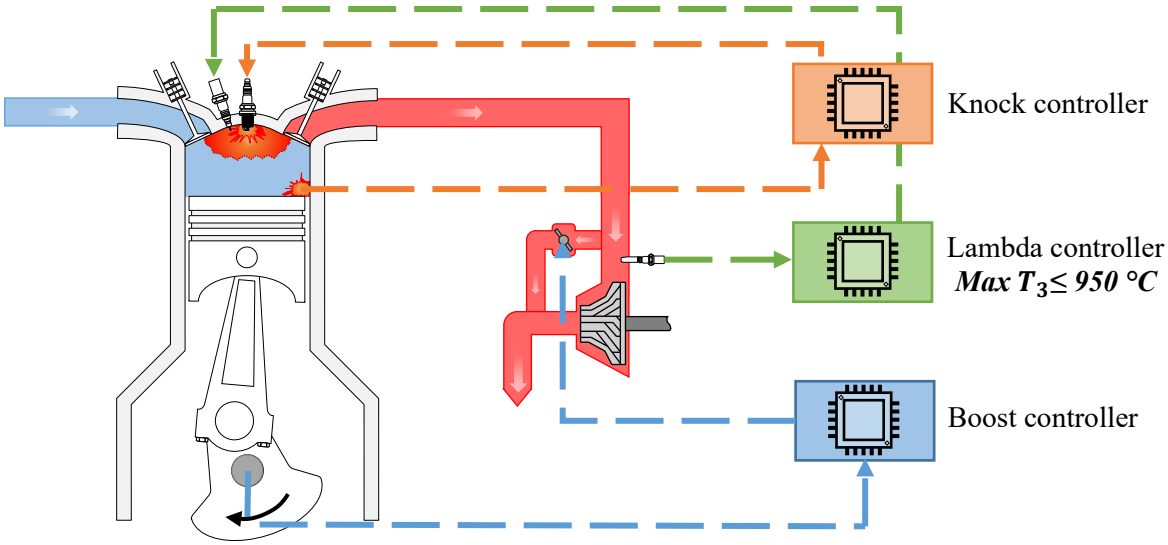

Figure 4.1: 1D engine model control logic operation scheme.

4.2. INPUT MODEL SET UP

The original engine model was modified to make it more predictable and compatible with the investigated engine technologies. Current engine works in full load and low engine speeds conditions with lean lambda values in order to improve the low-end torque, thanks to the scavenging effect. In fact, high cylinder scavenging results to be beneficial for low-end performance due to the higher air mass flow rate which let the compressor to exploit higher pressure ratio, with a consequently increased trapped air in the cylinder. Moreover, the scavenging allows to reduce the residual gas content at the beginning of the intake stroke, which has a very positive effect on knock tendency reduction and combustion stability improvement. However, the excess air forced in the exhaust system would deteriorate the TWC conversion efficiency, which is of paramount importance to have the highest tailpipe emission reduction in Euro 7 perspective. With such aim, the cam timing in the initial engine model was consequently modified in order to prevent low engine speed scavenging, keeping the trapping ratio equal to one at any engine speed. The result of the scavenging removal as expected, is a low-end torque reduction, as reported in Figure 4.2 where now low-end target torque is no longer meet.

Furthermore, the original Douaud and Eyzat knock model was substituted with the Gasoline Kinetics Fit model, developed by Gamma Technologies Inc., which is capable to consider the effects on knock probability of the mixture dilution [8]. As for the original knock model, Gasoline Kinetics Fit model was calibrated against engine test bench data. Finally, the engine model without scavenging and with the new knock model reported in Figure 4.2 was considered as the *input engine model,* on which all the analysis were carried out.

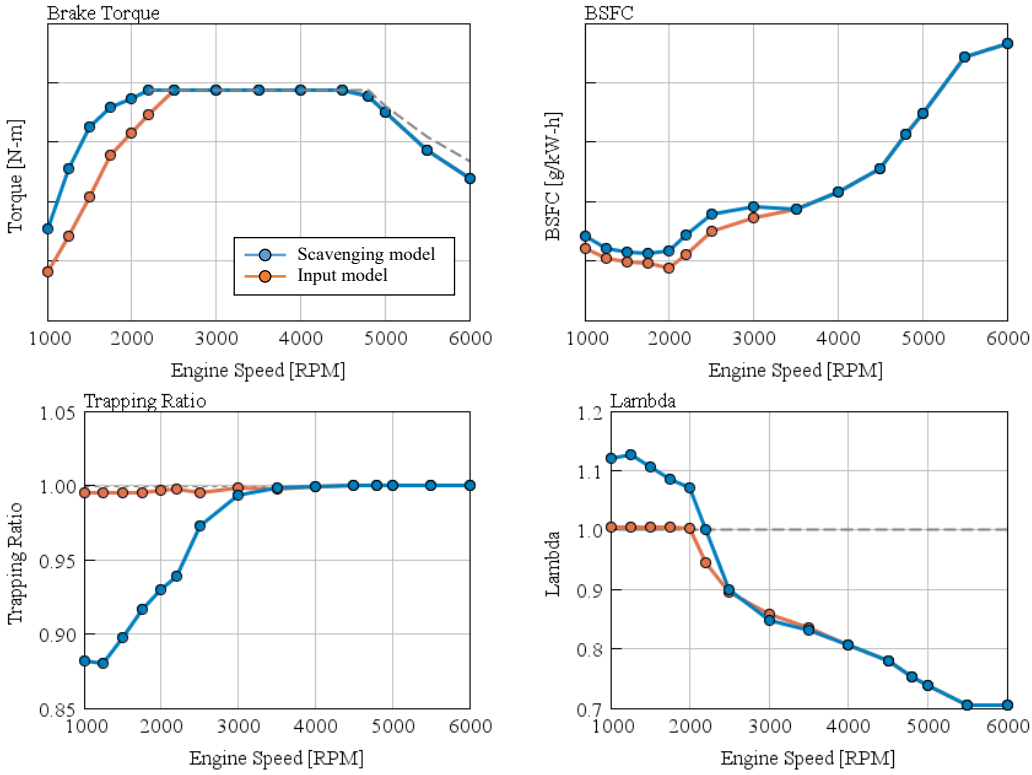

Figure 4.2: Current engine model with scavenging and input model without scavenging, performance.

4.3. T4 CONTROL

Starting from the input engine model just described, where the lambda value is controlled on maximum T_3 of 950 °C and according to what discussed in Paragraph 2.1.2, as a first step of the thesis work, the new lambda control strategy acting on maximum T_4 was implemented, in order to take into account the TWC protection requirement aroused with the higher limit on maximum T_3. As depicted in Figure 4.3, the air fuel ratio is now controlled in such a way to keep the T_4 below the threshold of 870 °C. Nevertheless, the control on T_3 was not removed at all, but modified with a new engineering limit on maximum T_3 of 1030 °C, where below that, the control stays inactive, keeping the major concern on the TWC protection.

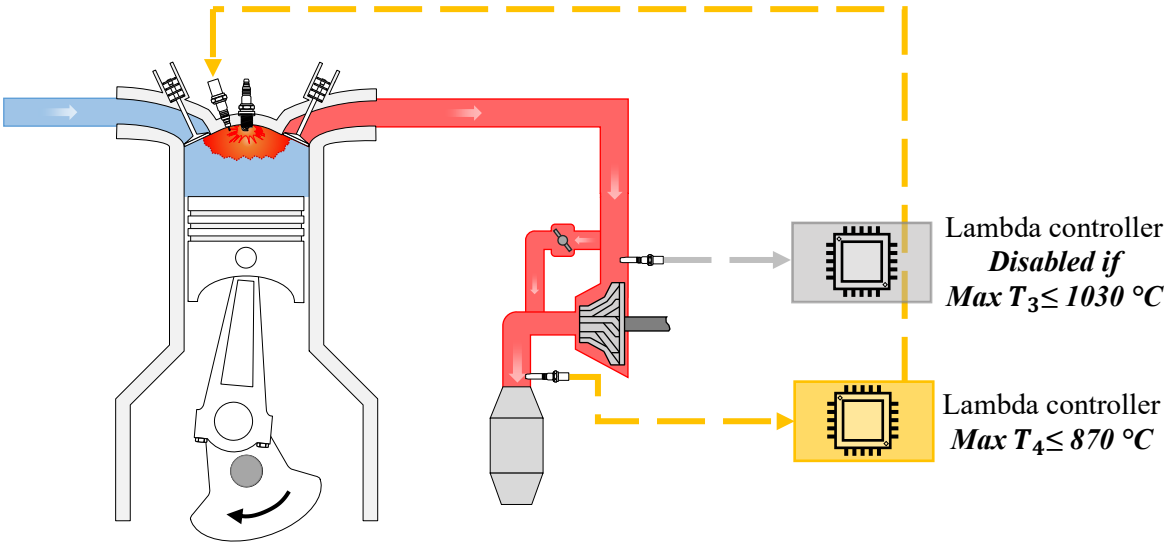

Figure 4.3: New T_4 lambda control logic operation scheme.

The result of such new control strategy is reported in Figure 4.4 where engine performance is shown. Thanks to the increased T3 limit, at peak power the lambda value increased of +0.06. The higher air fuel ratio values therefore lead to an overall higher engine efficiency, which is beneficial for the high-end torque increase, as shown in the upper left plot.

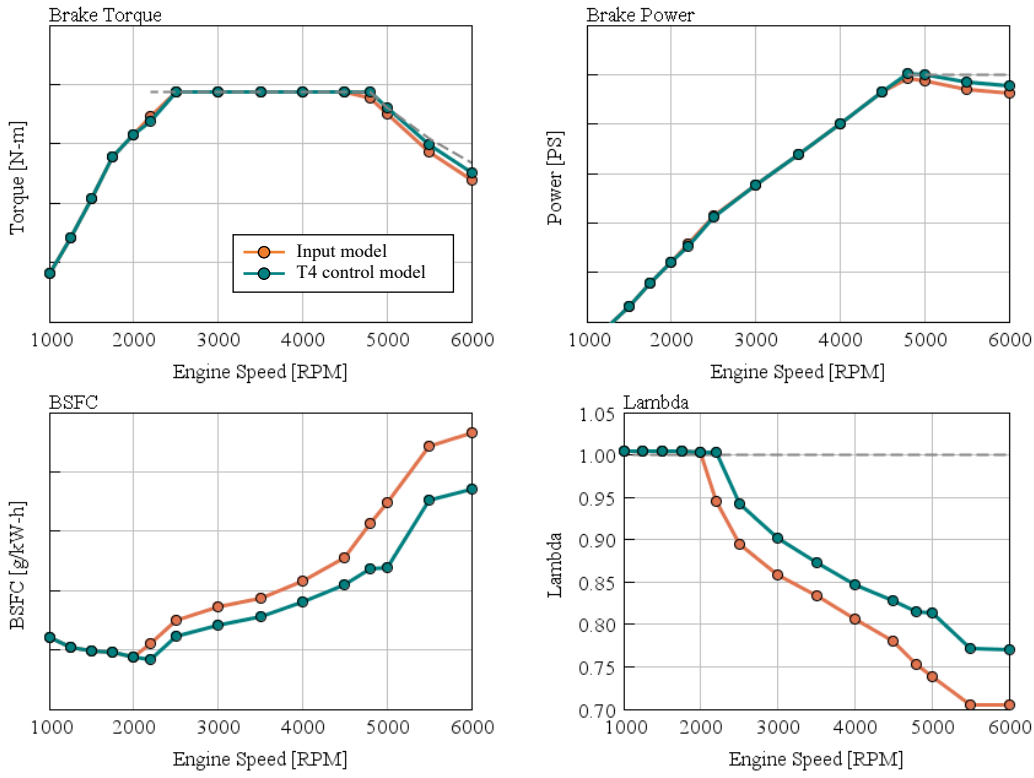

Figure 4.4: Performance of new T_4 lambda control model and of the input model.

4.4. NEW TURBOCHARGER

With the aim of having a strong base to fully exploit the potential of the technologies that are going to be investigated, a new compressor and turbine have been implemented in the model. In Figure 4.5 are reported the compressor and turbine maps of the current engine, where it is possible to highlight the working points of the new model and of the T_4 control model. The current compressor is highly loaded, with operating points very close to the surge line, which gives low margin for the analysis of innovative solutions that may require higher pressure ratio. On the base of this limit, the turbocharger supplier provided a completely new compressor and turbine maps, which represent the state of art of turbocharger development of the supplier. The new turbocharger gives a higher degree of freedom for technologies investigations and furthermore, thanks to the overall higher efficiency of both machines and to the higher compressor pressure ratio, it was possible respectively to have an important gain in fuel enrichment reduction and low-end torque improvement. The engine performance resulting from the new turbocharger maps implementation are reported in Figure 4., where the higher surge limit for low air mass flow rate of the compressor allowed to more than satisfy the low-end torque performance requirement. The relative difference of new compressor and turbine with respect to the original ones, are reported in Table 4.1.

	CURRENT ENGINE	REFERENCE MODEL
Compressor size*	–	+ 4%
Turbine size*	–	+10 %

* Refers to the wheel diameter

Table 4.1: New turbocharger relative dimension.

Since all the investigation that is going to be presented in the next Chapter was performed with lambda controlled on T_4 and with the new turbocharger maps, the so defined engine model will represent the *reference model* upon which all the technologies were tested.

Summing up the characteristic of the reference model:

- The air fuel ratio is controlled to limit the TWC inlet temperature T_4 to 870 °C.
- The boost pressure is controlled to reach the target performance acting on the wastegate valve.
- The combustion anchor angle is controlled to run the engine at knock limited condition.
- New turbocharger maps have been implemented.
- Cam timing has been optimized to have trapping ratio equal to 1 in the whole engine map.
- At peak power (4800 rpm), it is possible to define a target lambda increment of +0.14 which will be used as a technology rating for what lambda potential is concern.

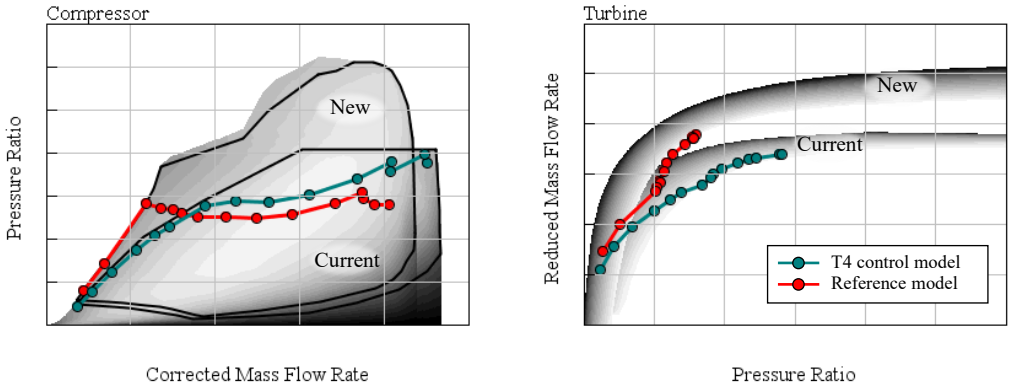

Figure 4.5: Current engine turbocharger maps and new compressor and turbine maps.

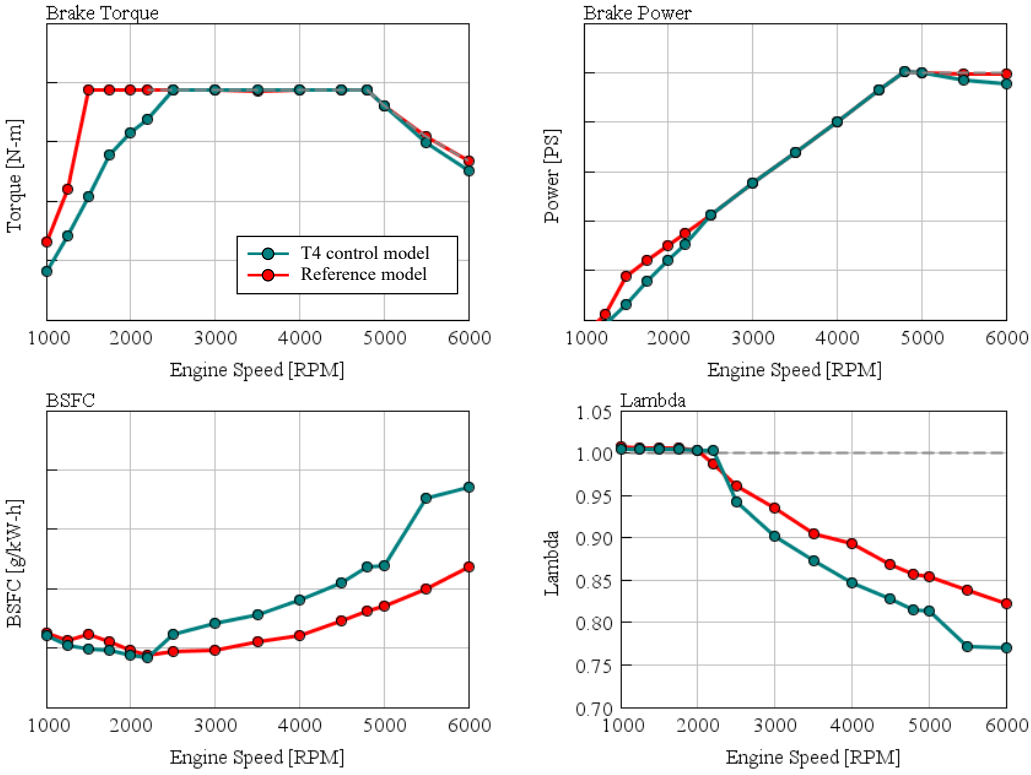

Figure 4.6: Reference model performance.

5. TECHNOLOGIES INVESTIGATION

To the purpose of the thesis, different technologies were investigated with a defined methodology: the single technology was firstly analysed on its own, in order to deeply study its potentialities and possible engine implementation. Successively, the best technologies combinations were investigated to end up with engine concepts Euro 7 compliant, and so capable of working at lambda 1 everywhere in the engine map. The investigated technologies are:

- E-Turbo.
- Miller and Atkinson cycles.
- Turbulent jet ignition.
- Air conditioner supported charge air cooling.
- Water injection.
- Dual lift cam profile.
- Hydrogen assisted combustion.

5.1. E-TURBO

In a common turbocharger group, the compressor and the turbine are installed on the same shaft, which rotate at a speed much higher and disconnected from that of the engine. By means of the turbine, mechanical power is extracted from the exhaust gases and it is used to drive the compressor whose boost pressure will determine the engine rated power. Due to the low friction of the bearings and of the rotating parts in the turbocharger, the mechanical efficiency η_m in power transfer from turbine to compressor is close to 1. Neglecting the heat transfer in both machines, it is possible to write the power balance of the turbocharger with the Formula:

$$P_c = \eta_m P_t \tag{5.1}$$

Being the useful power for a thermal machine equal to:

$$P = \dot{m} \cdot \Delta h \tag{5.2}$$

Formula (5.1) can be rewritten as:

$$\dot{m}_a c_{p,a}(T_2 - T_1) = \eta_m \dot{m}_e c_{p,e}(T_3 - T_4) \tag{5.3}$$

Then, by managing the obtained expression (5.3), it is possible to highlight the pressure ratio, expressing it as function of:

- Constant parameters: $k_c, k_t, c_{p,c}, c_{p,a}, \eta_m, \eta_t, \eta_c$
- Expansion ratio: $\frac{p_4}{p_3}$
- Gases mass flow rate ratio $\frac{\dot{m}_e}{\dot{m}_a}$

$$\left(\frac{p_2}{p_1}\right)^{\frac{k_c-1}{k_c}} = \frac{\dot{m}_e}{\dot{m}_a}\frac{c_{p,e}}{c_{p,a}}\eta_m\eta_c\eta_t\frac{T_3}{T_1}\left[1 - \left(\frac{p_4}{p_3}\right)^{\frac{k_t-1}{k_t}}\right] \tag{5.4}$$

The boost pressure in a turbocharger engine will determine the power output in full load conditions: thus, in order to avoid damage either of engine or of components that may have structural limits to

be respected, the boost pressure is controlled in such a way the engine does not exceed the design conditions. Therefore, it is necessary to implement a control strategy that let the engine run within the prescribed limits, achieving the target performance.

The simplest turbocharger design from the control perspective is the one where the compressor and turbine geometry are chosen in such a way no boost control systems are required, and the level of boost pressure in controlled just by the exhaust mass flow rate through the turbine. This would mean that in Formula (5.4) the mass flow ratio would be close to 1:

$$\frac{\dot{m}_e}{\dot{m}_a} = \frac{\dot{m}_a\left(1+\frac{1}{\alpha}\right)}{\dot{m}_a} = \left(1+\frac{1}{\alpha}\right) \cong 1 \tag{5.5}$$

Of course, such a system does not represent an optimal solution from the performance perspective, because of the big turbine size required, which would lead to very poor low-end torque performance and even more, unacceptable dynamic response. Thus, what is commonly done to control the boost pressure is to use the wastegate valve (WG), usually integrated in the turbine housing, whose actuation allows to control the turbine power bypassing some exhaust gas flowing through it. Such a control strategy is very widely adopted because of its good versatility in turbo matching, low-end torque performances and transient response. Furthermore, it is also the control strategy used in the reference engine. The actuation of the wastegate valve will modify the exhaust mass flow rate through the turbine $\dot{m}_t$, thus the Formula (5.4) can be adjusted as follows:

$$\left(\frac{p_2}{p_1}\right)^{\frac{k_c-1}{k_c}} = \frac{\dot{m}_t}{\dot{m}_a}\frac{c_{p,e}}{c_{p,a}}\eta_m\eta_c\eta_t\frac{T_3}{T_1}\left[1-\left(\frac{p_4}{p_3}\right)^{\frac{k_t-1}{k_t}}\right] \tag{5.6}$$

Where $\dot{m}_t$:

$$\dot{m}_t = \dot{m}_e - \dot{m}_{WG} \tag{5.7}$$

Only part of the exhaust stream is expanded in turbine and if the temperature after the expansion is measured $T_{4,t}$, it will result to be lower than that at the inlet of the TWC T_4, because of the mixing among exhaust expanded gas and WG bypassed gas, which is at higher temperature (close to T_3). A small scheme is shown in Figure 5.1.

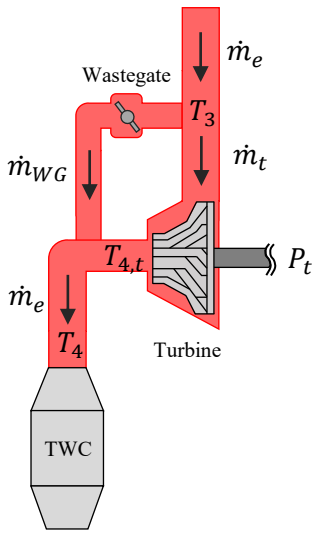

Figure 5.1: Schematic representation of turbine and wastegate exhaust gas mass flow rate.

Whereas the major concern for Euro 7 engine concept development is the temperature at catalyst inlet T_4 to control the enrichment, short-circuiting some exhaust gas leads not only to an increase of T_4 but also to an energy waste, because of the high enthalpy of the exhaust gas bypassed and the throttling losses through the wastegate valve. Thus, in order to have the best energy exploitation, and so to maximize the system efficiency to reduce the enrichment, the optimum would be to have a system that allows to eliminate the wastegate, enabling the expansion of the whole exhaust mass flow without compromising the performance.

The solution proposed in this work provides the use of the E-Turbo, which has an electric machine (EM) installed on the same shaft of the turbocharger group as shown in Figure 5.2, that would electrically assist the turbocharger operations. In particular, the presence of the electric motor allows at high loads to expand all the exhaust gas mass flow in such a way the extra power generated by the turbine can be recovered as electric power. Thus, the turbine size can be optimally chosen for the best trade-off of enrichment and low-end performance, where the electric motor can assist the low-end torque and transient operations. Moreover, the boost control can rely just on the electric power recovery, removing the constraint of the wastegate valve needs.

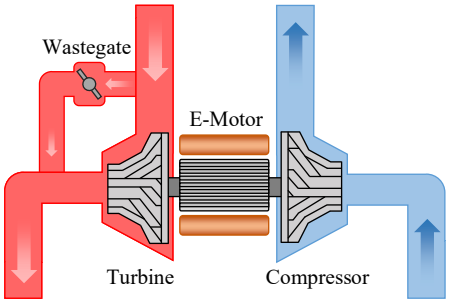

Figure 5.2: E-Turbo illustration.

The idea of E-Turbo implementation on the reference engine can be the following:

- Increase the turbine size, reducing the exhaust backpressure and thus the in-cylinder exhaust gas residual content, beneficial for the enrichment reduction.
- Electrically boost at low-end torque, where the power extracted by the turbine from the exhaust gas is not enough to reach the target boost pressure.

The mentioned solution has already been studied by some turbocharger manufacturer [10]. The lower residual content gives a lot of benefit in terms of enrichment reduction, thanks to the better combustion stability and lower knock tendency, which allows to advance MFB50 improving engine efficiency. However, this solution was not considered in this work because of two reasons:

- It is very effective in enrichment reduction especially when enrichment depend on T_3, while in the reference model it depends on T_4.
- Low-end torque and transient performance strictly depend on the vehicle battery state of charge (SOC), which is undesired.

The implementation proposed for the reference model indeed, allows to remove the dependency from the battery state of charge, providing a standalone solution able to reduce the fuel enrichment keeping the maximum T_4 below the fixed threshold.

5.1.1. E-TURBO MODEL IMPLEMENTATION

The solution used in the reference model exploits the presence of the P2 EM in the vehicle in order to modify the system hybridization by electrically coupling the E-Turbo EM with the P2 EM as shown in Figure 5.3.

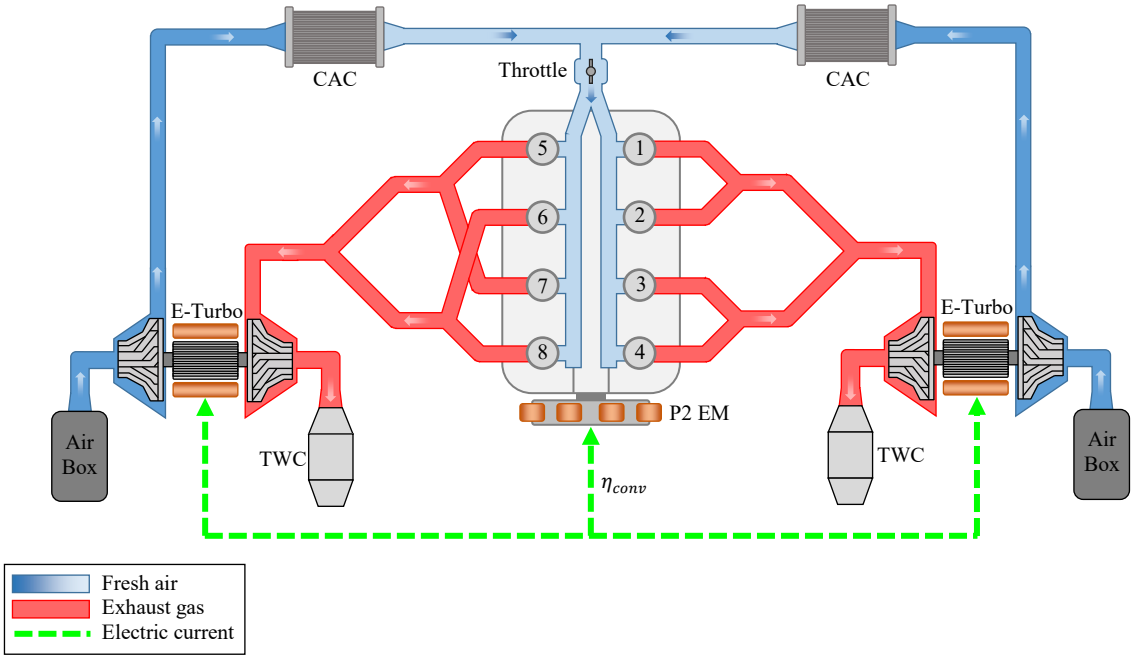

Figure 5.3: E-Turbo technology powertrain implementation scheme.

The resultant hybrid system can work in full load condition with the wastegate completely closed (ideally it can be even removed), controlling the target boost pressure by means of the E-Turbo EM. The EM and P2 EM electrical connection allows to realize a SOC independent system where:

- If to reach the target boost pressure, the compressor requires an input power P_c higher than what the turbine can provide P_t, the extra power will be supplied to the EM by the P2 EM and so from ICE, which works at higher load.
- If the turbine extract from the exhaust gas more power of the one the compressor needs, the extra power is converted in electric power that is delivered to the P2 EM where it becomes traction power reducing ICE load.

It is possible then to define an electric power conversion efficiency η_{conv} in the connection among electric machines, that was assumed:

$$\eta_{conv} = \eta_{P2\,EM} \cdot \eta_{EM} \cdot \eta_{electronics} = 80\% \tag{5.5}$$

$$\eta_{P2\,EM} = 92\,\% \tag{5.6}$$

$$\eta_{EM} = 92\,\% \tag{5.7}$$

$$\eta_{electronics} = 95\,\% \tag{5.8}$$

Closing the wastegate and recovering electric power with the EM, adds a further term in the Formula (5.1), that becomes:

$$P_{EM} + P_c = \eta_m P_t \tag{5.9}$$

Since the reference engine is twin-turbocharged, $P_{P2\,EM}$ will be then:

$$P_{P2\,EM} = \eta_{conv}(P_{EM1} + P_{EM2}) \tag{5.10}$$

The brake power P_b of the described system, and so at gearbox input shaft, will be:

$$P_b = P_{ICE} + P_{P2\,EM} \tag{5.11}$$

In Figure 5.4 are reported the turbocharger powers comparison between the reference model, where the boost pressure is controlled with the wastegate and the E-Turbo model, where the wastegate is completely closed and the boost controlled with the electric motors. The turbine power difference between the two models can be quantified as the extra energy produced by the turbine due to the higher exhaust mass flow, which is converted in electric power in the EM (E-Turbo EM Power plot). Compressor powers are almost the same, demonstrating that the increased turbine backpressure due to the higher expansion ratio is compensated by the ICE load reduction. In the bottom right plot the P2 EM power is shown, computed according to Formula (5.10): it is possible to notice that P2 EM power is always positive, which means that the engine does not have to increase the load to boost the EM.

The system performances are reported in Figure 5.5, where it can be observed an important gain in fuel enrichment reduction simply recovering the exhaust gas wasted energy and converting it in traction power. The increased lambda value (+0.08) is reflected in a considerably improved brake specific fuel consumption (BSFC).

However, the solution investigated so far requires a very powerful EM, which for a mild hybrid application represents a challenge in the turbocharger manufacturing, and so to work with such power levels it would be required higher voltage systems. According to the turbocharger supplier, the state of the art of mild hybrid E-Turbo technology is represented by an EM operating at 48V with a maximum rated power of 10 kW. Therefore, this component was used in the following investigation. With such a component, the turbine will extract too much power from the exhaust gas that cannot be fully recovered in the EM. So, the wastegate needs to be operated to control the boost pressure, introducing an energy loss. To avoid that, the turbine size was scaled so that the maximum power that it can extract at full load and maximum speed is limited to 10 kW, removing the need of a wastegate valve. The new scaled turbocharger specifications are reported in Table 5.1.

	REFERENCE MODEL	**E-TURBO 10KW MODEL**
Compressor size*	Ref	Ref
Turbine size*	Ref	+ 25 %
Wastegate	Boost control	Completely closed
Electric machine	Absent	48V – 10 kW

*Refers to the wheel diameter

Table 5.1: E-Turbo model turbocharger specifications.

An increased turbine size causes a reduction of in-cylinder burned gases residual, which have a positive effect on fuel enrichment reduction, compensating the negative impact on lambda improvement due to the reduced turbine expansion ratio, as confirmed by the similar lambda and BSFC values at high engine speed, observed in the results reported in Figure 5.6. The higher BSFC values at low engine speed are justified by the need of a higher ICE load to boost the compressor.

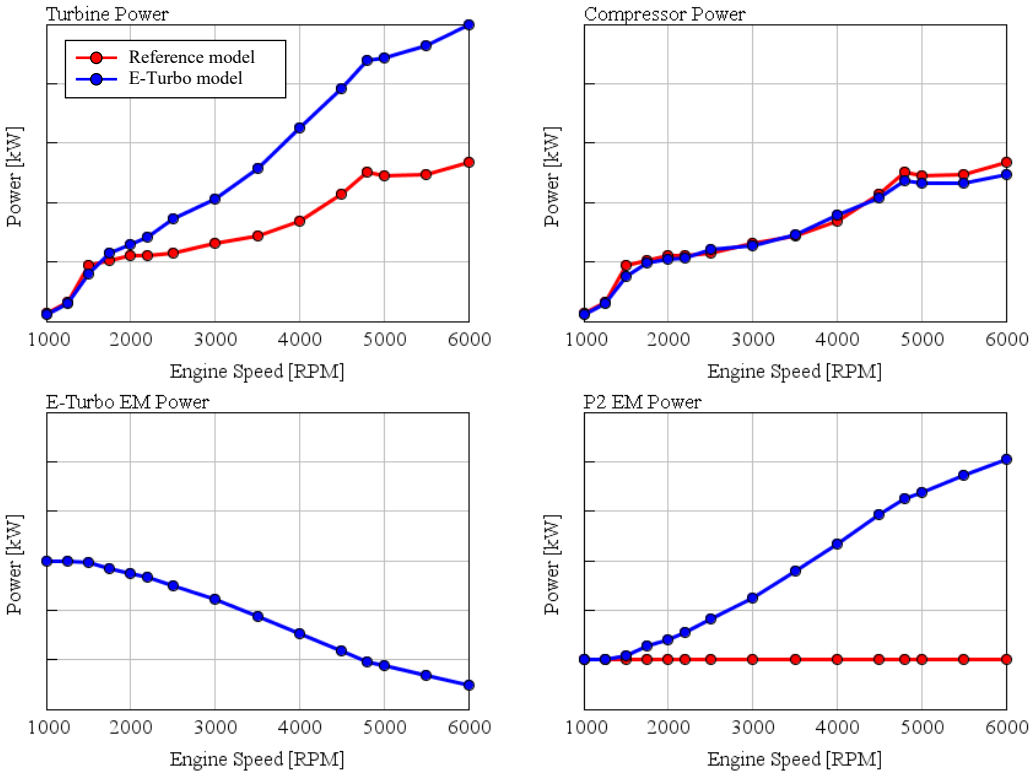

Figure 5.4: Reference and E-turbo model turbocharger powers.

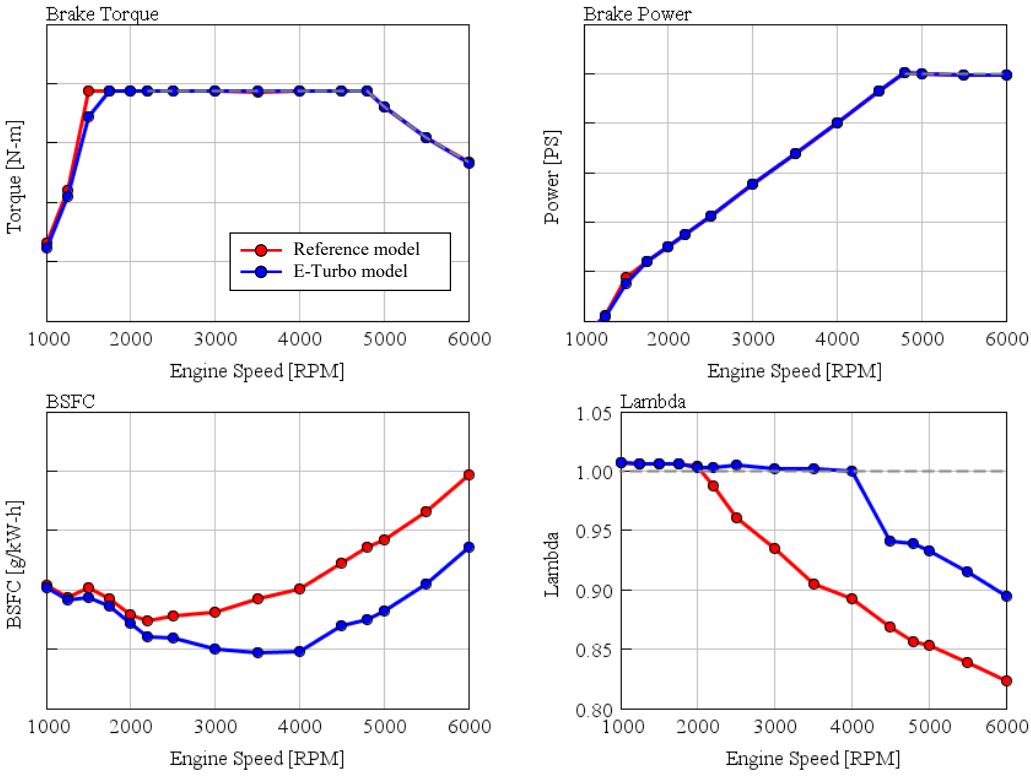

Figure 5.5: E-Turbo technology implementation performance.

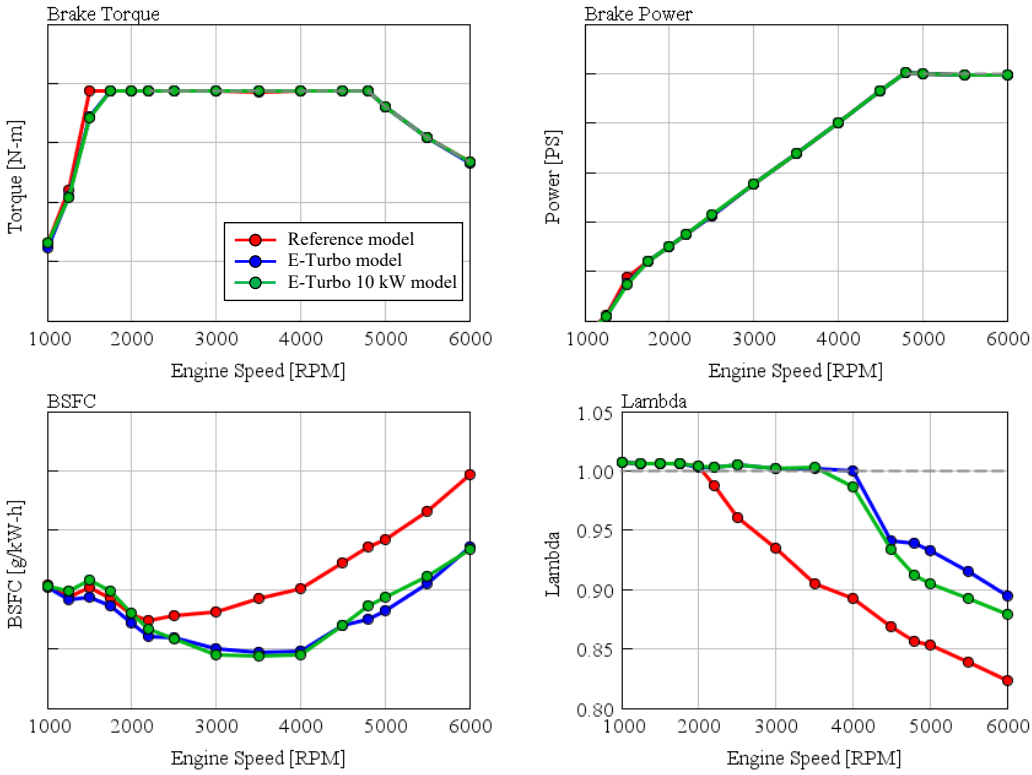

Figure 5.6: E-Turbo technology implementation with scaled turbine and 48V – 10 kW electric motor performance.

To conclude, the E-Turbo technology has shown great potentialities in fuel enrichment reduction, further enhanced by a series of advantages:

- Optimal turbo matching, with a turbine sizing able to reduce exhaust back pressure.
- Improved transient response, because of the electric motor assistance.
- Possible turbine energy recovery not in full load operation to recharge the battery.
- No dependency on battery state of charge.
- High versatility.
- Higher system efficiency.

The main limitation could be imposed by the need of a hybrid system which however can be simpler than that used in the reference engine. For instance, a P1r or a P1f hybrid system, according to the application, can be enough to be coupled with the E-Turbo technology.

5.2. MILLER AND ATKINSON CYCLES

An effective way to increase the knock resistance of a GDI turbo engine so that the fuel enrichment in WOT operation can be reduced, is by means of the adoption either of a Miller or Atkinson cycle [11] [12]. As it is well known, the increase of engine geometrical compression ratio (CR) is very effective in efficiency improvement [13], in fact about 3% of efficiency increase corresponds to one point of compression ratio rise in the range of CR from 9 to 12. However, with higher CR also comes

an increased knock tendency that would lead to a combustion phasing retard, detrimental for exhaust temperatures and for component protection requirement. Many attempts were done with the aim of mechanical varying the effective CR making it lower than the expansion ratio [14] [15], so that knock likelihood is reduced and engine efficiency is increased. Both Miller and Atkinson cycles allows to achieve similar results just acting on the intake valve (IV) opening duration, where respectively an *early intake valve closure* (EIVC) and *late intake valve closure* (LIVC) strategy are realized. A comparison on the p-V diagram of both cycles with respect to the traditional Otto cycle is illustrated in Figure 5.7.

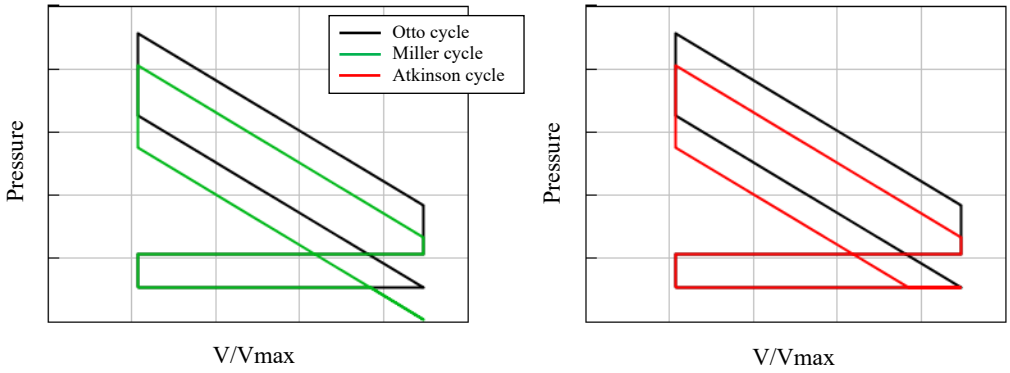

Figure 5.7: Working principle of Miller and Atkinson cycles.

Thanks to the reduced effective CR, the decreased temperature at the end of compression stroke will positively affect the knock resistance of the engine, for which then, in fuel enrichment reduction perspective it is worth to increase the geometrical CR, so that the gas temperature at the end of the expansion stroke will be reduced. The effect on the p-V diagram of the increased CR is reported in Figure 5.8.

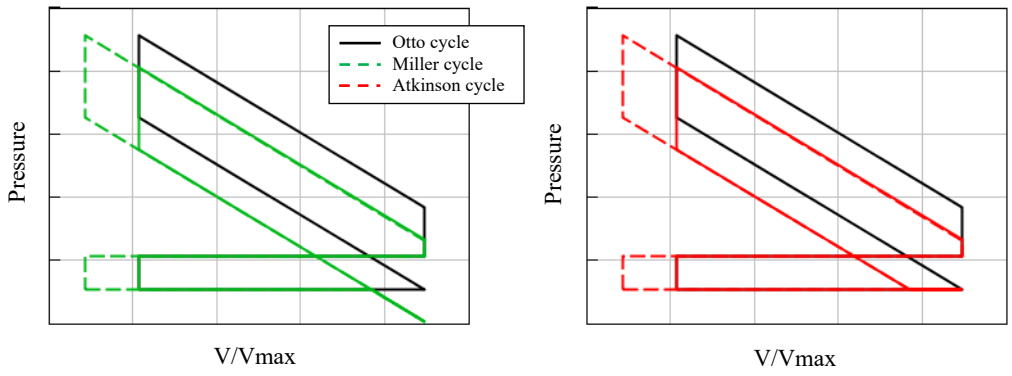

Figure 5.8: p-V diagram for Miller and Atkinson cycles with increased compression ratio.

In this case, ideally, the effective CR will be similar to the original CR of the standard Otto cycle and so the combustion anchor ancle phasing will be similar to the original case as well, but less fuel enrichment will result due to the higher expansion ratio.

A short analysis of both cycles is here reported, highlighting their pros and cons:

- *Miller cycle* (EIVC): the shorter intake event duration worsens the volumetric efficiency which would require an increased boost level especially at high engine speed, where a longer intake valve duration would be the optimum. At low-end torque, the smaller intake cam prevents the backflow through the valve indeed, which somehow improves the volumetric efficiency and so reduces the amount of boost required. However, since the intake valve closes before the BDC, the fresh air is expanded into the cylinder up to the BDC to be then compressed again, reaching the same initial condition before the expansion. This in-cylinder expansion perturbate the charge turbulences, which results to be reduced at the spark time, deteriorating the burn duration (MFB1090).
- *Atkinson cycle* (LIVC): as opposed to the Miller cycle, the longer intake event will worsen the volumetric efficiency at low engine speed, where high backflows occurs, and high boost pressure are required. By convers, at high engine speed, higher air mass flow rate and low boost pressure is required compared to Miller case. Moreover, since the intake valve is kept open longer than the standard case, the tumble motion is not affected, and therefore the turbulence intensity at spark time will not be adversely modified.

5.2.1. MILLER & ATKINSON CYCLE MODEL IMPLEMENTATION

As a first analysis, a design of experiment (DOE) was set up to study the potentialities of both Miller and Atkinson cycles on the reference model. Furthermore, since both cycles would have required a higher boost level, it was thought to perform the investigation on the formerly analysed E-Turbo model, where the E-Turbo EM can compensate eventual lack of boost that cannot be provided by the standard wastegate controlled turbocharger.

The DOE was set up swapping the compression ratio and the intake valve duration, where the intake cam profile was modified acting on the intake valve angle multiplier (IVAM), a parameter which scales the intake cam angle, and the intake valve lift multiplier (IVLM) that in turns scales the intake valve lift. Specifically, to keep constant the valve acceleration, the following relation was used to link the two multipliers:

$$IVAM = IVLM^{\frac{1}{2}} \tag{5.12}$$

All the assumption done for the Miller and Atkinson cycle DOE set up are summarized here:

- Low-end torque at 2200 rpm and peak power at 4800 rpm conditions were tested.
- The same turbocharger size of reference model was considered.
- E-Turbo technology was considered to supply extra boost if required. In this regards, E-Turbo EM power was not limited to 10 kW as previously stated in Paragraph 5.1.1.
- As a first approximation the burn duration increase caused by Miller cycle was not considered, since it strongly depends on engine geometry, ports design etc. and so correlation and prediction are difficult.

High-end torque results are reported in Figure 5.9 and low-end torque results in Figure 5.10. The dashed black curves were used to divide the region where the performance requirements are meet and the region where they do not. At 4800 rpm are present 2 zones where the lambda value reaches the unity, corresponding to extreme short and long IV opening duration, and thus they identify two islands of stoichiometric operation. The Atkinson lambda 1 island results much bigger than the one

of Miller cycle and moreover, there the engine efficiency is the higher. At low engine speed, Atkinson cycle evidence limits in torque output, whereas even boosting with the E-turbo EM the target torque is not reached. With Miller cycles indeed, lambda 1 operation is reachable meeting the target performance in both operative conditions. Thus, the criteria adopted to define the intake valve duration and the CR for both cycles are finalized to reach the target torque and lambda one minimizing the BSFC, while for what it concerns the P2 EM power the criteria were:

- At 4800 rpm, minimize the P2 EM power, so that higher turbine expansion ratio reduces the maximum T_4.
- At 2200 rpm, maximize the P2 EM power, so that lower E-Turbo electric boost is required.

The specification for possible Miller or Atkinson cycle implementation are reported in Table 5.2.

CYCLE	SPEED	IVAM	IV DURATION	CR
Atkinson	4800 rpm	1.3	262 CAdeg	10.5
	2200 rpm	1.0	190 CAdeg	9.5
Miller	4800 rpm	0,8	140 CAdeg	9.5 ÷ 10.5
	2200 rpm	0,8	140 CAdeg	9.5 ÷ 10.5

Table 5.2: Miller and Atkinson optimal implementation specifications.

It is possible to conclude that for Atkinson cycle, a dual lift cam profile will be necessary, due to the lack of low-end torque (the solution is going to be investigated in Paragraph 5.6), while for Miller cycle the shortest intake cam duration would be the optimum for reaching lambda 1 in both considered conditions.

However, Miller cycle burn duration variation was not considered and also, to have the fairest comparison it is important to point out that the engine is embedded with the twisted camshaft to counteract the blowdown interferences as introduced in Chapter 3. The cam angle deltas of the component were designed according to the standard IV duration of 190 CAdeg and so, the shortening of the intake event with Miller cycle, might prematurely cut off the filling of that cylinders for which the cam deltas were negative (IV opening occurs earlier). This does not happen with Atkinson cycle, since the cylinder filling is always accomplished, whereas it might change the amount of reverse flow, which affect the boost pressure. With these regards, a further DOE was performed removing the intake and exhaust twisted camshafts and keeping unchanged all the other assumptions considered so far. The results for the model without twisted camshaft are reported in Figure 5.11 at peak power condition and in Figure 5.12 at low-end torque.

The new analysis shows a completely different behaviour at peak power condition, where now the most favourable region is just the one with shorter intake cam duration and higher compression ratio. By converse, the engine efficiency as well as the lambda value is now negatively affected by EIVC strategy due to the lack of blowdown interferences optimization and thus, to compensate the different cylinders IMEP variations, a new set of twisted camshaft design, optimized for shorter intake cams is required.

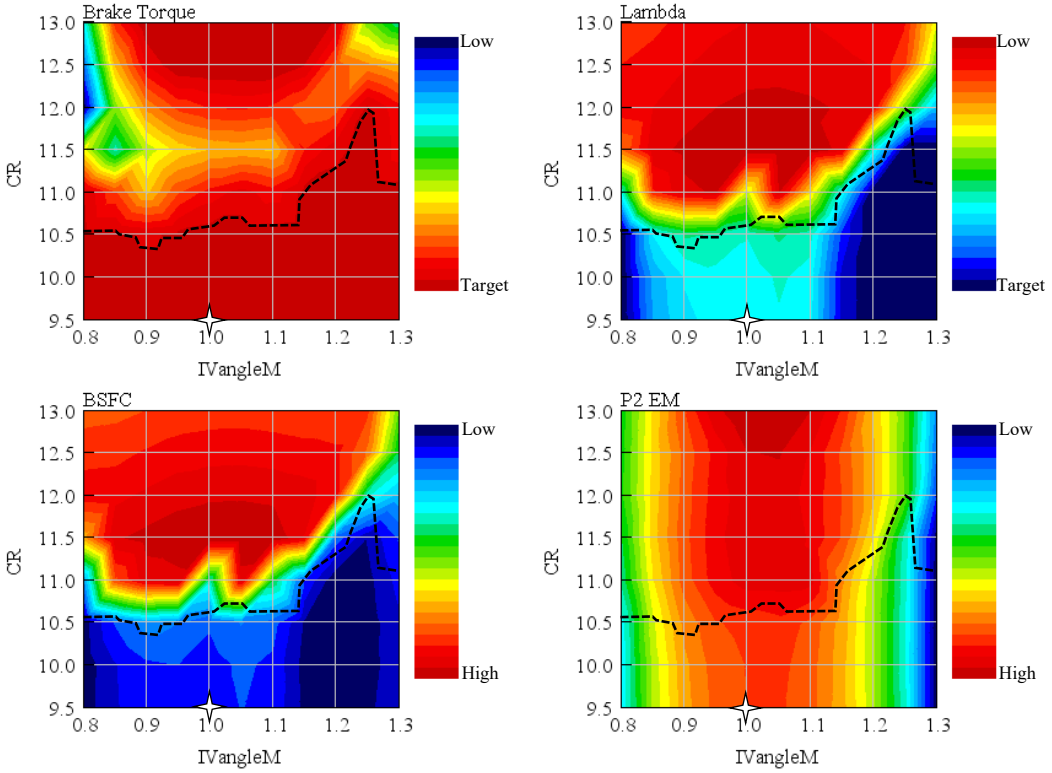

Figure 5.9: Effects of IVAM and CR on brake torque, lambda, BSFC and P2 EM at 4800 rpm and full load.

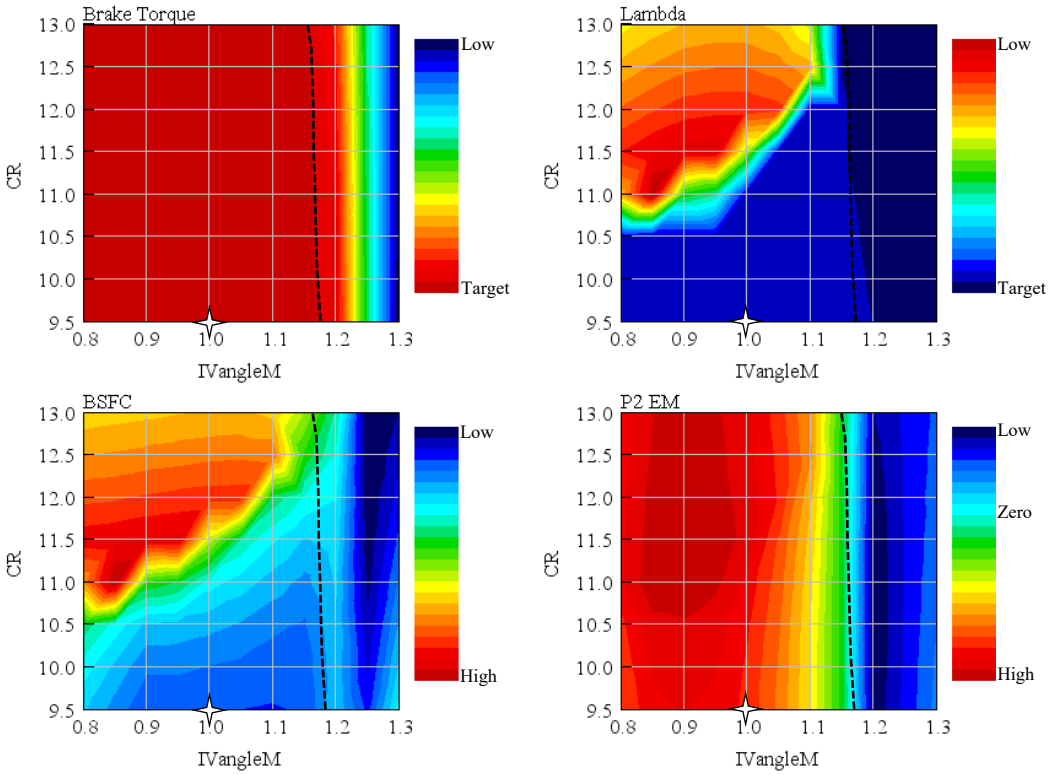

Figure 5.10: Effects of IVAM and CR on brake torque, lambda, BSFC and P2 EM at 2200 rpm and full load.

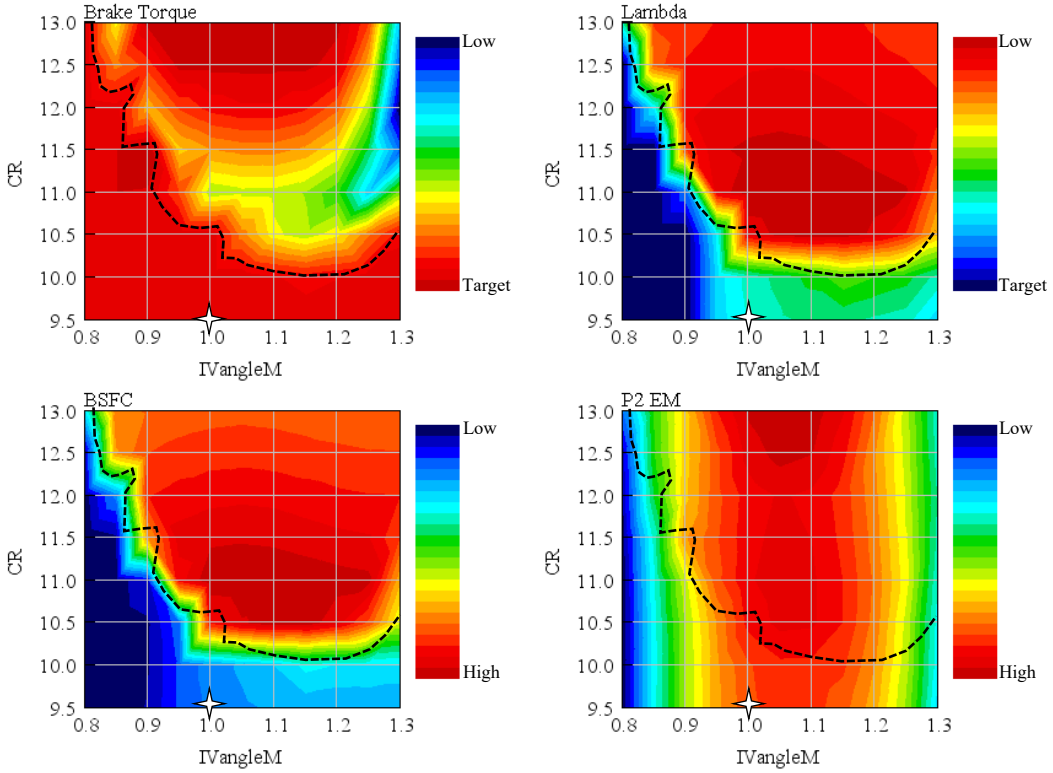

Figure 5.11: Effects of IVAM and CR on brake torque, lambda, BSFC and P2 EM at 4800 rpm and full load without twisted camshaft.

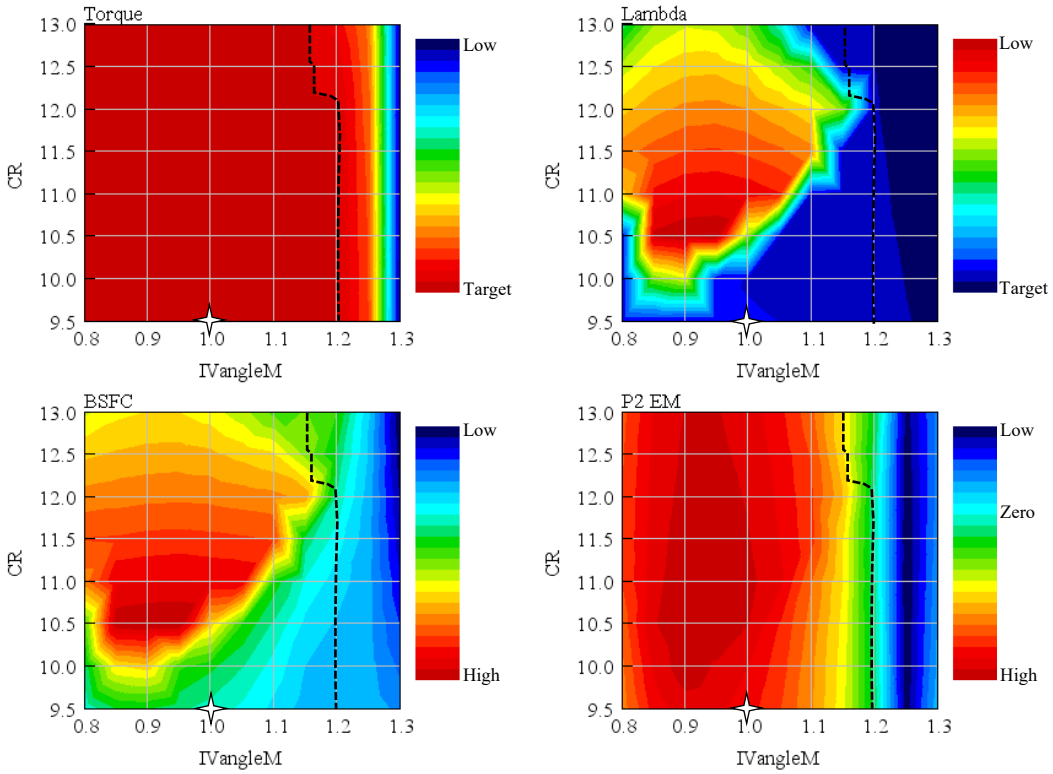

Figure 5.12: Effects of IVAM and CR on brake torque, lambda, BSFC and P2 EM at 2200 rpm and full load without twisted camshaft.

5.2.2. OPTIMIZED TWISTED CAMSHAFT FOR MILLER CYCLE

The optimal design of new twisted camshaft would require a big amount of time which goes beyond that available for the thesis work and furthermore, it would go over the actual thesis target. Therefore, it was adopted a simplified reduced methodology which is able to provide very good results in a short amount of time. The parameter at disposal on which it was possible to act for the camshafts optimization are 18 and summarized in Table 5.3.

PARAMETERS	DESCRIPTION	RANGE OF VARIATION
8	Delta* intake cam	-20° ÷ 20°
8	Delta* exhaust cam	-20° ÷ 20°
1	Intake Valve Angle Multiplier	0.8 ÷ 1
1	Compression Ratio	9.5 ÷ 13

*Refers to the angular position variation of the cam with respect to the standard position of a traditional camshaft.

Table 5.3: Optimization parameters of Miller twisted camshaft.

To simplify the analysis, the cam timing was kept constant. Nevertheless, it is clear that the number of designs which are possible to realize is incredibly high, and although the 1D-CFD simulation powerfulness that allows short simulation times, testing all the possible solutions within the time at disposal for the analysis was not feasible. In this regard, an automatized approach, based on a genetic algorithm (GA) was used, where a coupled interaction between GT-POWER and Simulia ISight™ was necessary to short the design process. Since the design process for every engine speed, even with a simplified methodology requires a lot of efforts, it was decided to perform the optimization at low-, mid- and high-end torque, so respectively at 2200rpm, 3500rpm, 4800rpm, with the methodology illustrated in Figure 5.13

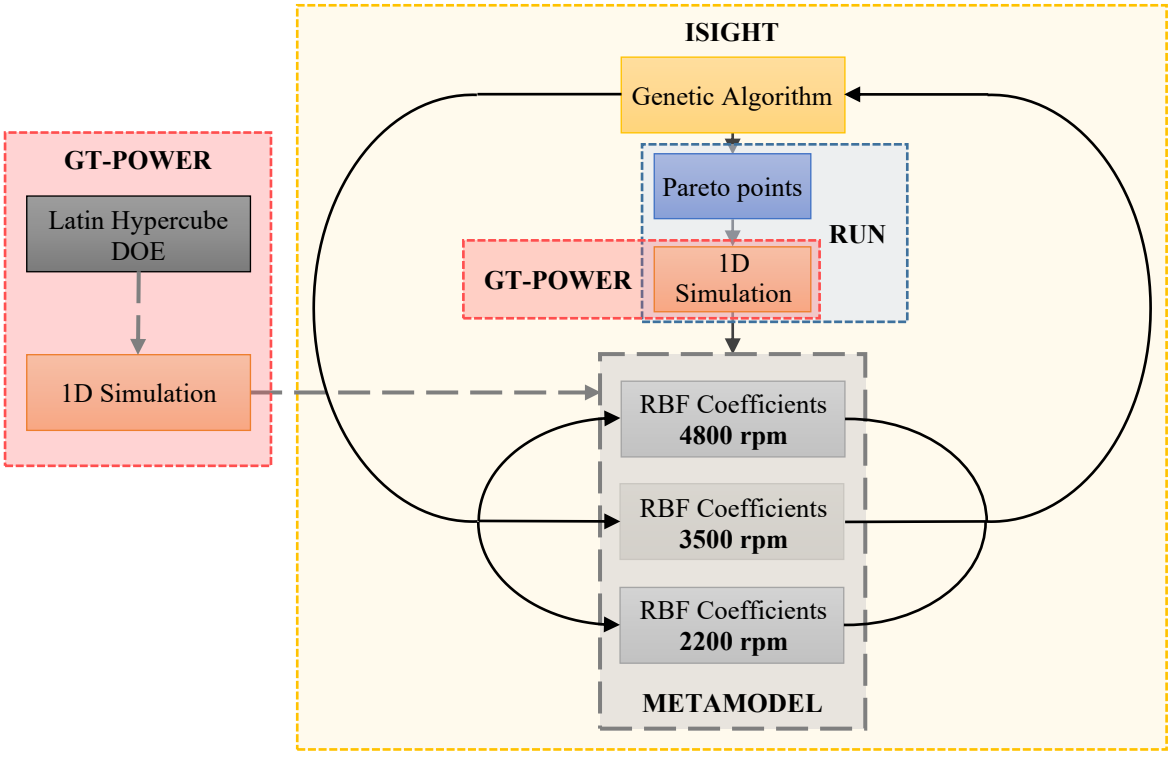

Figure 5.13: Miller cycle twisted camshaft optimization methodology.

Initially a huge Latin Hypercube DOE was generated starting from the 18 design parameters, realizing an initial design sets necessary to compute the RBF coefficients. Metamodels were then generated (one per each engine speed) from the GT-POWER simulations results of the Latin Hypercube DOE input. By using the metamodels it was possible to dramatically cut-down the simulation time, since if correctly trained, they are able to accurately predict the real simulation results with times that are different order of magnitude shorter than a standard 1D-Simulation, thus the huge DOE was mandatory to increase the metamodels accuracy. Once the RBF coefficients were available, in ISight, the genetic algorithm was implemented, for which an optimization target function was defined to guide it toward the optimal design direction. In doing so, it was chosen to minimize the BSFC in each tested engine speed, with higher importance for low- and high-end torque as a target objective. The reason is that the BSFC reduction is strongly correlated to the lambda value, to the engine residual contents that will be minimized and to the exhaust temperature as well, so a loop of engine beneficial effects is triggered by the BSFC reduction. The GA starts the optimization phase computing the feasible designs using the metamodels, obtaining as result of a single optimization phase a series of optimal suggested solution based on constraint compliance and target function value. From the suggested designs, the pareto designs were screened and individually computed in GT-POWER; then the 1D results of this optimization run were used to further increase the metamodel accuracy, recomputing the RBF coefficient. The procedure is repeated for a total of 3 run, since thanks to the big input DOE results, the metamodels were capable of very good results prediction already at run 2, so that the third run was used to select the best 10 designs, which then had been computed in GT-POWER for a complete full load curve, in order to decree the best design.

In Figure 5.14 (a) are reported all the BSFC values at 4800 rpm and 2200 rpm resultant from the runs and from the DOE, while in Figure 5.14 (b) the 3-dimension plot with BSFC result at 4800, 3500 and 2200 rpm are reported just for run 3 for the sake of visualization simplicity. Finally, the new twisted camshaft design was obtained, where the optimum values for a Miller cycle implementation in the reference engine corresponds to an IVAM of 0.8 (IV duration of 140 CAdeg) and a CR of 10.5.

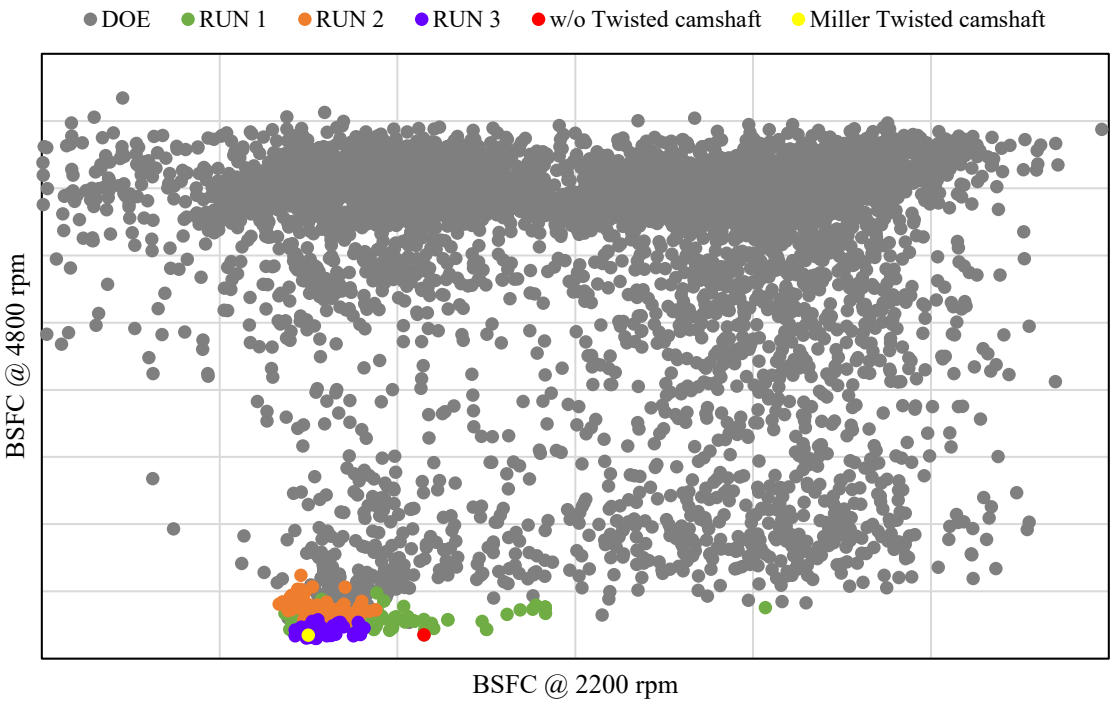

(a)

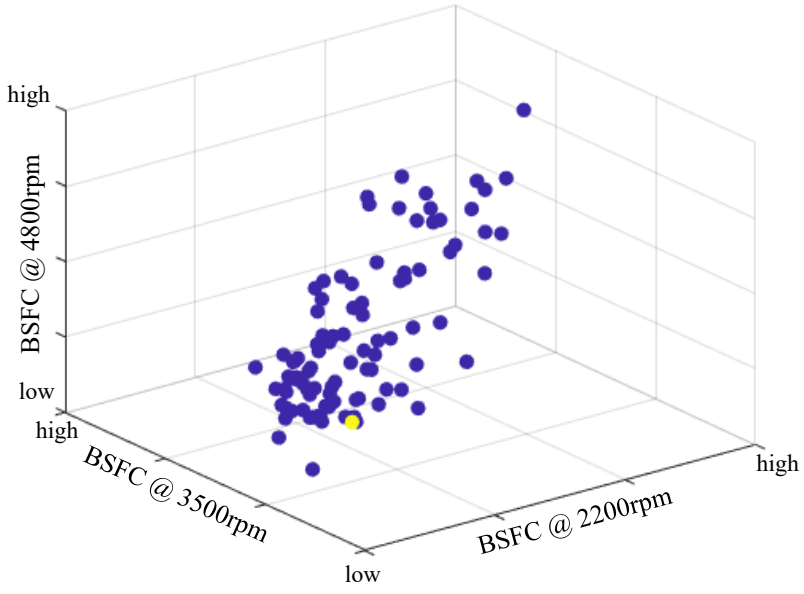

(b)

Figure 5.14: (a) Miller cycle twisted camshaft optimization BSFC full results at 4800 rpm and 2200 rpm. (b) Run 3 results at 4800 rpm, 3500 rpm and 2200 rpm.

5.3. TURBULENT JET IGNITION

Gasoline spark ignition internal combustion engine are by definition ignited by the spark plug, which has been introduced in the second half of the XVII century and it is still now the more widespread ignition mean. Although the excellent characteristics of the spark plug, the low cost and simplicity, today is becoming of high interest the need of letting the SI engine working with very lean air fuel ratio mixture, in order to increase engine brake efficiency and reduce pollutant formation [16] [17]. Enabling lean stoichiometric operation is not an easy task for such engines, because of the combustion instabilities that will arise for value of $\lambda > 1$ up to $\lambda = 1.2$ where misfire is very likely to occur [4].

In a very simplified manner, when the spark occurs a small amount of electric energy of about 25-50 mJ is released in the cylinder and the direct consequence is the formation of a flame kernel which starts to ignite the surrounding mixture. The flame front starts to propagate and because of the charge motion it is being corrugated, enhancing the burn speed of the bulk mixture up to the combustion ends, where the burning speed decreases due to the descended piston motion and mixture depletion.

The introduction of prechamber turbulent jet ignition (TJI) systems opened new horizons in the realization of gasoline engine able to run with very lean mixture, with a significant decrease in specific fuel consumption and emissions [18] [19] [20].

Prechamber systems substitute the spark plug in the combustion chamber and allow to ignite the mixture in multiple sites by means of multiple turbulent jets. The spark plug has been relocated inside the prechamber where it ignites the close to stoichiometry mixture. Depending on the mixture formation in the prechamber, a distinction can be made between active and passive prechambers:

- *Active prechamber* jet ignition: the main direct or port injector, injects the fuel for charging the air into the combustion chamber. A second fuel injector is located in the prechamber as well as the spark plug and it is responsible of injecting a very small amount of fuel necessary for the turbulent jet formation.
- *Passive prechamber* jet ignition: only the spark plug is located into the prechamber, which is fuelled by fresh mixture during the piston compression stroke. The fuel in the main chamber can be port or direct injected.

The working principle is similar for both and a simplified scheme of a passive prechamber jet ignition system is represented in Figure 5.15.

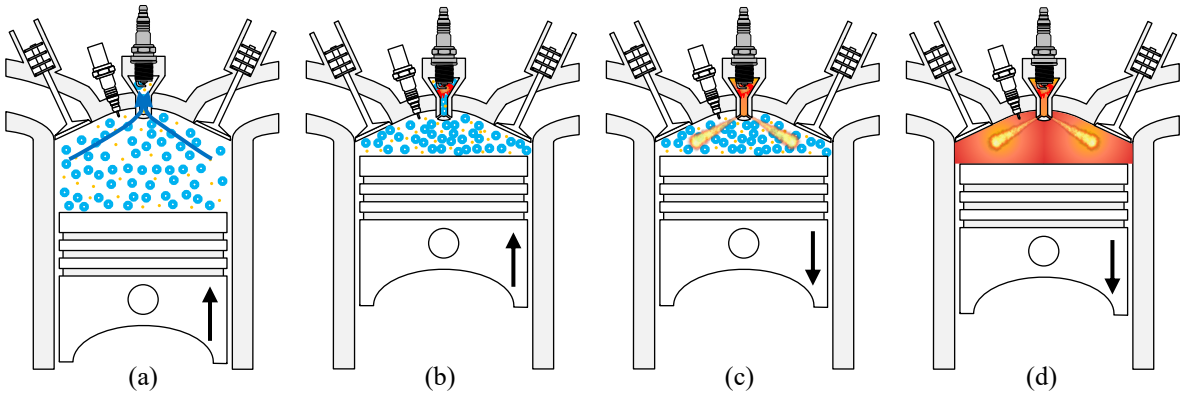

Figure 5.15: Passive prechamber TJI working principle. (a) Fresh mixture flows into the prechamber during compression stroke. (b) Prechamber mixture is spark ignited. (c) Turbulent jets propagate into the main chamber. (d) Turbulent jets ignite the bulk mixture.

During the compressor stroke the air fuel mixture is forced to flow through the calibrated holes of the prechamber (only fresh air in case of active prechamber) filling the whole volume. To ignite the bulk charge, the spark plug ignites the prechamber mixture that is close to stoichiometric condition (for both active and passive) which burns almost instantly and due to the pressure differential, that arise between pre and main chambers, the flames are forced to exit from the calibrated holes where develops in turbulent jets [21]. The ignition of the bulk charge occurs in multiple points with an overall faster combustion and also a lower knock tendency than the standard spark case.

The advantages of such a faster combustion, beyond the increased knock resistance and combustion stability, do also regards the enrichment reduction thanks to the possibility to advance the combustion anchor angle. A more advanced combustion phasing causes the increase of engine thermodynamic efficiency, and whilst the efficiency increases the charge boost pressure decreases. Since the boost level is controlled acting on the power generated by the turbine, the lower power demand reduces the p_3 and T_3 with a reduction of T_4 as well. Furthermore, the higher knock tendency allows to increase the compression ratio which would further expand the exhaust gas into the cylinder with a further T_3 reduction.

Although the huge potentialities of TJI system, it has the drawbacks of a reduction of effective compression ratio due to the presence of the prechamber volume and of an increased heat loss, because of the small amount of mixture that is burning into the prechamber without producing useful work. Anyhow the gain in engine efficiency deriving from the possibility to increase the compression ratio and to advance the combustion phasing, in WOT operations more than overcompensate the before mentioned phenomena. The true limitation of the system may be found on the poor catalyst warm-up capability and the low combustion stability at low loads [20]. The reduced intake air pressure within the cylinder at low load operations makes difficult the mixture to flow into the prechamber and even more to obtain the ideal air fuel ratio in it.

5.3.1. TJI MODEL IMPLEMENTATION

In the reference model a passive prechamber has been considered. Active prechambers are more expensive than passive ones and although they allow to have higher lambda lean limits and higher combustion speed, up to 40% [21] more than a spark ignition case in lean operation, being the work target to run at lambda one in the whole engine map, it would be useless to implement an active system. Furthermore, it may seem to be more convenient to exploit higher lambda value in terms of fuel economy but for lambda values higher than 1 the three way catalytic converter will be not efficient at all, and a diesel like after treatment system would be required with a further cost increase.

Passive prechamber are cheaper (additional injector not needed and the dimension are lower than an active system) and at stoichiometric conditions have almost the same benefit of the active prechamber case, which according to Porsche experience can be quantified to about a 20% of reduction in burn duration at full load conditions.

For the TJI implementation, since at the moment of the work GT-POWER did not have a dedicated combustion model for such technology, only an MFB1090 decrease of 20% was considered, as shown in Figure 5.16, where burn rate and burned fraction at 4800 rpm and peak power are shown.

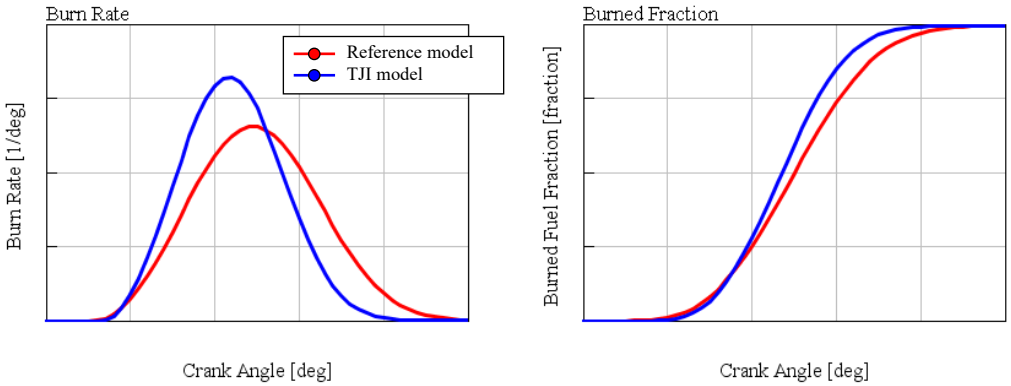

Figure 5.16: TJI burn rate and burned fuel fraction variation at 4800 rpm with respect to a standard spark plug.

In the TJI model, as a first approximation, the thermodynamic efficiency loss due to higher heat rejection and effective compression ratio reduction were not considered.

The full load results of the TJI technology implemented on the reference model are reported in Figure 5.17. As expected, from the lambda plot it is possible to observe a higher benefit at low and mid-engine speed, while increasing the speed the lambda gain tend to reduce. This is justified by the higher engine knock tendency at low speed and there the TJI system can better exploit its knock mitigation capabilities, as further evidenced by the T_4 reduction in that region. At higher speed, enrichment just depend on component protection and the lambda gain from TJI implementation is marginal (+0.02 at 4800 rpm). However, the TJI technology arouses a lot of interest thanks to its positive effects on combustion, conveying a big potential in enrichment reduction whether coupled with other technologies.

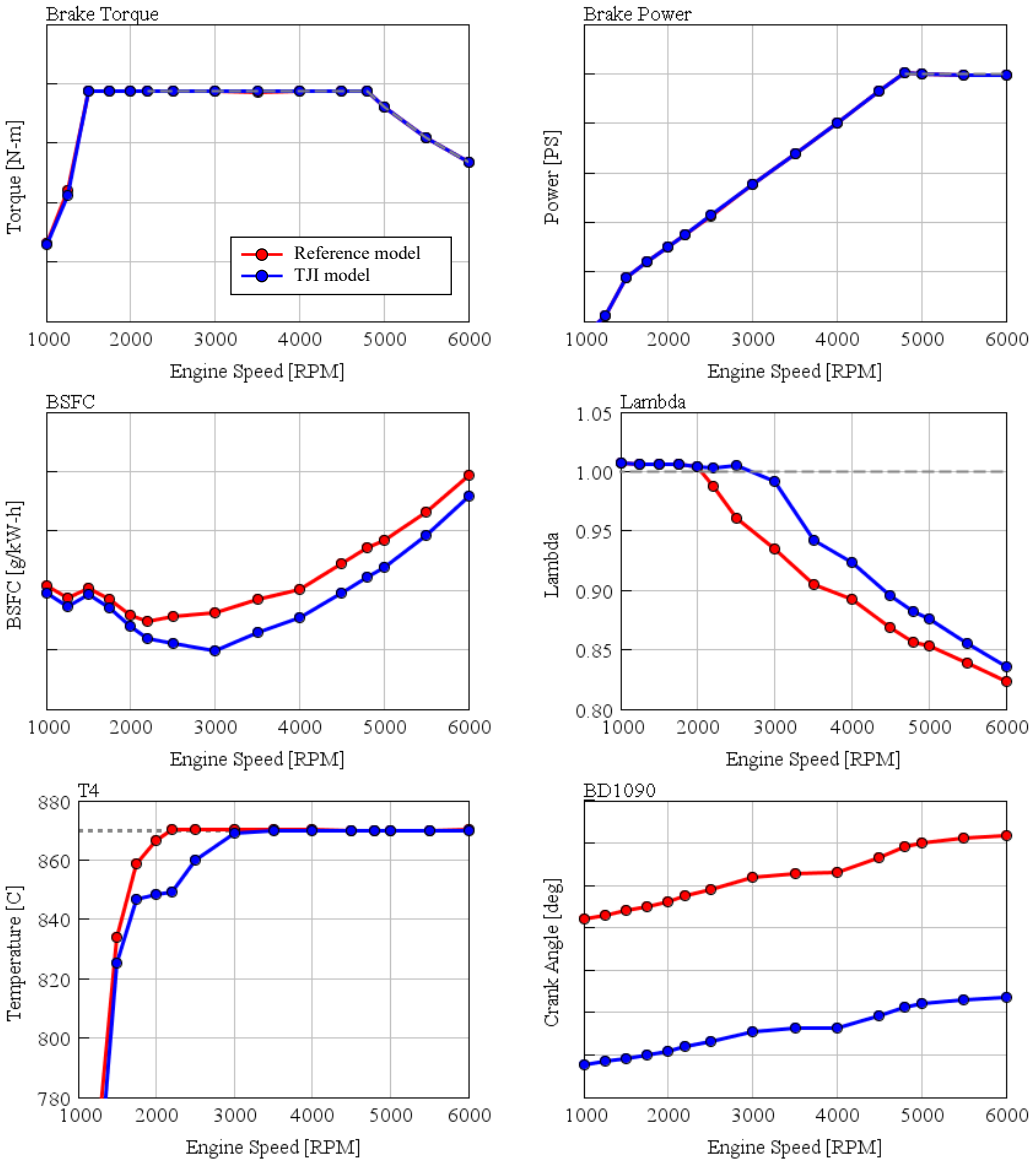

Figure 5.17: Passive prechamber TJI technology implementation performance.

5.4. A/C SUPPORTED CHARGE AIR COOLER

Turbocharging the internal combustion engine is one of the best solutions to increase the specific power by increasing the fresh air density. However, compressing the intake air would not only increase its pressure p_2 but also the temperature T_2, which is not desired whenever the performances are the major concern. The higher knock tendency and the reduced volumetric efficiency caused by the lower air density are the direct consequences of the increased T_2. In order to limit this phenomenon, charge air coolers (CAC) are used to cool down the compressed air before to get it into the cylinders. For a conventional CAC the effectiveness η_{CAC} can be expressed with the formula:

$$\eta_{CAC} = \frac{T_{in} - T_{out}}{T_{in} - T_{cool}} \tag{5.13}$$

Although the very high effectiveness reachable by the charge air coolers, it is physically impossible to approach a charge temperature which goes below the temperature of the cooling fluid T_{cool}, that in common CAC correspond to the ambient temperature. In this regard, an effective solution to further cool down the fresh air would be to use a different cooling mean, able to reach temperature below the one of the ambient. In this sense, an additional charge air cooler exploiting the air conditioning (A/C) system is employed. The advantages deriving from a lower than ambient charge temperature at engine inlet are:

- Increased air density, that improves the volumetric efficiency and knock resistance.
- Overall positive balance between the power cooling necessary and so the power subtracted by the A/C compressor and the engine power gain from lower T_2.

Automotive air conditioning systems are generally designed for the worst conditions, with vehicle still and extremely high ambient temperature [23] [24]: in such conditions, the compressor power required by the A/C system will be the maximum available, of about 10 kW in case of a high segment car. As soon as the vehicle starts to move, the increasing air flow rate through the A/C condenser radiator, significantly decreases the request of power to the A/C compressor. According to Porsche experience, in normal driving conditions, an average of 5 kW compressor power will be enough to keep the climate into the passenger compartment and, the higher the relative speed of the wind to vehicle, the lower will be the cooling power demand. Therefore, being half of the compressor power usually available in normal driving condition, it can be exploited in order to further cool down the fresh air charge so that to realize an air conditioner supported charge air cooler (A/C CAC). A schematic integration of the system is reported in Figure 5.18.

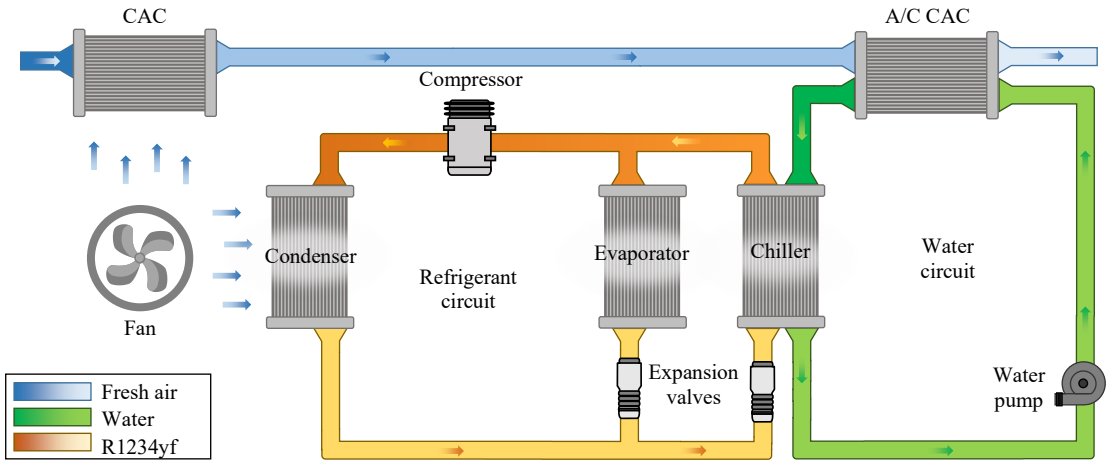

Figure 5.18: Schematic representation of an air conditioner supported charge air cooling system.

An additional evaporator is added to the traditional air conditioning circuit, which allows to reduce the temperature of the water in the water circuit, that is connected to the A/C CAC. The amount of cooling power transferred either to the cabin or to engine intake can be controlled by mean of the expansion valves.

The cooling capacity of the system $\dot{Q}_{cooling}$ is related to the power required to drive the compressor $P_{A/C}$ by the coefficient of performance COP:

$$\dot{Q}_{cooling} = P_{A/C} \cdot COP \tag{5.14}$$

The assumption done for the implementation of the A/C CAC in the reference model are reported in Table 5.4.

COP	Calculated from R1234yf refrigerant p-h diagram
A/C compressor isentropic efficiency	0.5
Maximum refrigerant fluid pressure	20 bar
Heat exchanger effectiveness	0.98

Table 5.4: Assumptions for A/C supported CAC model implementation.

The assumed isentropic compressor efficiency of 0.5 represents a pessimistic case, since for such kind of application a value of 0.65 is typically considered [25].

The cooling power required to cool down the intake air into the A/C CAC is expressed by the formula:

$$\dot{Q}_{air} = \dot{m}_a c_p (T_{A/C\ CAC,in} - T_{A/C\ CAC,out}) \tag{5.15}$$

where $T_{AC\ CAC,in}$ is the temperature at the A/C CAC inlet and $T_{A/C\ CAC,out}$ is the temperature at A/C CAC outlet.

Combining the formula (5.14) and (5.15) and considering the heat exchanger effectiveness $\eta_{chiller}$ and $\eta_{A/C\ CAC}$ it is possible to compute the temperature $T_{A/C\ CAC,out}$:

$$T_{A/C\ CAC,out} = T_{A/C\ CAC,in} - \frac{P_{A/C} \cdot COP}{\dot{m}_a c_p} \cdot \eta_{chiller} \cdot \eta_{A/C\ CAC} \tag{5.16}$$

5.4.1. A/C CAC MODEL IMPLEMENTATION

The increased ρ_a that can be obtained by the application of the A/C CAC technology may be exploited increasing the compression ratio and thus improving the engine efficiency. The idea of increasing the compression ratio in such a way the end-compression temperature remains the same of the standard case could be reasonable. However, in doing so the benefit in terms of enrichment reduction derives from the high in cylinder gas expansion, since the combustion anchor angle will be close to the standard case or slightly retarded. The increase of compression ratio causes an almost linear combustion phasing retard, while the lower end-compression temperature, thanks to the increased knock resistance, allows to advance the MFB50. Thus, the combination of both effects which are not linearly dependent, cause a slight improvement in enrichment reduction at high engine speed as proved Figure 5.19 (b),where the compression ratio variation with the maximum A/C cooling power at peak power is represent; this solution however forces to use cooling power also at low speeds where the knock tendency increase because of the higher compression ratio is significant. Therefore, being the lambda gain deriving from compression ratio increase negligible if compared with the gain obtained with the only A/C CAC technology implementation as reported in Figure 5.19 (a), it was decided to keep the standard CR, preventing low engine speed power cooling usage. In the A/C CAC model, a control strategy was implemented that controls the A/C cooling power, and so the A/C compressor power, in order to reach lambda 1, up to the maximum available cooling power of 10 kW. The power necessary to drive the compressor is subtracted from the engine.

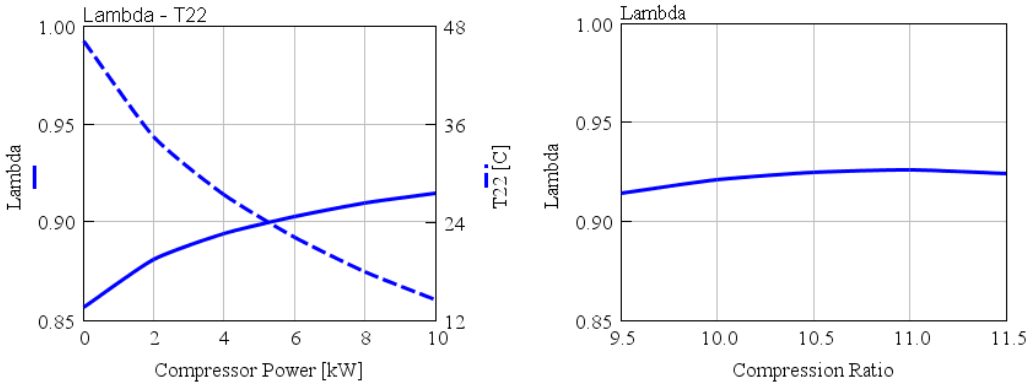

Figure 5.19: (a) Lambda gain and corresponding T_{22} reduction varying the A/C compressor power at 4800 rpm. (b) Lambda gain with max cooling power (10 kW A/C compressor power) varying the CR at 4800 rpm.

The results of A/C CAC technology investigation are reported in Figure 5.20. It can be observed the effectiveness of the system in reducing the T_{22}, which in turns reduces the need of enrichment up to +0.07 lambda increase. However, even with very high inlet air temperature reduction, which can achieve value below 0 °C exploiting the maximum cooling power available, it is not possible to approach lambda 1 at high engine speed, where further knock mitigation means are needed.

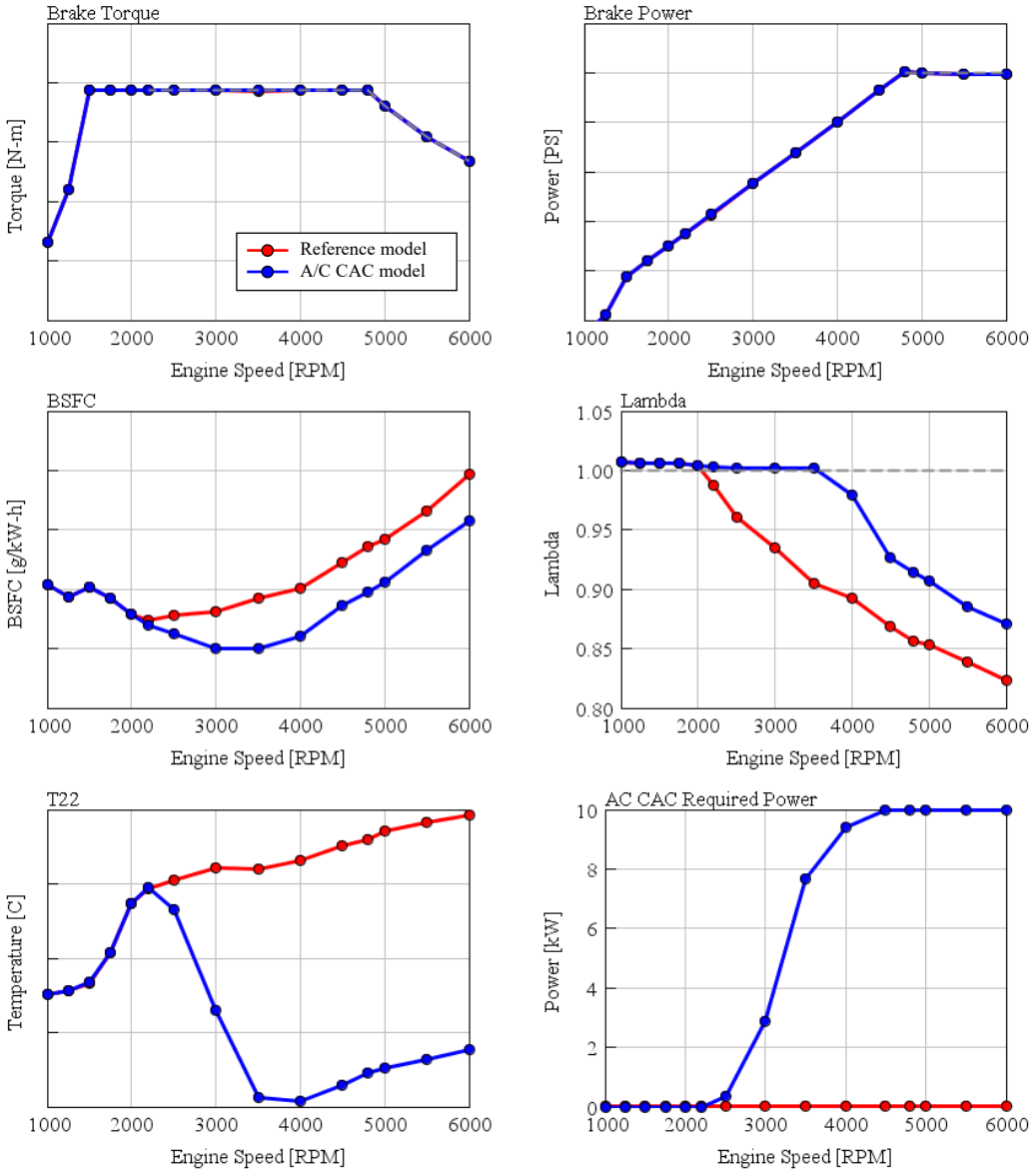

Figure 5.20: A/C supported charge air cooler technology implementation performance.

5.5. WATER INJECTION

One of the technologies that nowadays is showing a great interest in automotive field is the Water Injection (WI), seen as one of the most promising solutions for knock mitigation. Exploiting the high latent heat of vaporization of water, it allows to efficiently reduce the intake charge temperature with an important improvement in knock resistance. Furthermore, the increased heat capacity of the charged air, gives an additional cooling effect during compression and combustion phase with a further knock mitigation effect. As a matter of fact, great fuel enrichment reduction potentiality has been shown [26], thanks to its strong knock resistance capabilities, which allow to improve the combustion phasing and to increase the compression ratio, to achieve a higher engine efficiency.

Two main WI systems can be adopted: *direct water injection* (DWI) and *port water injection* (PWI). Despite their high cost (water tank, water circuit, water pump, water injectors etc are required), the good performances may be significantly affected by the design of the WI system and by its calibration parameters, like for example the location and the targeting of the injector [27]. An incorrect water injection phasing may also cause oil dilution with possible engine damage, because of water impingement on the cylinder liner [28].

For what PWI is concern, the injection phasing affects the knock mitigation capability, acting on the water film that usually is formed in the intake port, and so on the charge cooling. Thanks to the low water pressure system required, PWI has the advantages of simplicity, lower cost and robustness for corrosion and freezing issues but, on the contrary, the disadvantages of an higher water consumption in comparison with direct injection systems, mainly because of port and valve wall wetting phenomena [29], [30], [31]. These disadvantages may be partially reduced by means of a proper spray targeting and with the reduction of the droplet size, which is linked to the nozzle design and to the injection pressure [32].

Additionally, for both systems, the mixture dilution will negatively affect the combustion process, reducing the laminar burning speed of the gasoline. Thus, considering all the above-mentioned effects, a 1D approach for WI modelling requires reliable sub-models that allow to take into account the effects on turbulence, combustion, wall film formation, heat transfer, Cycle to Cycle Variability (CCV) and knock phenomena.

5.5.1. WI MODEL IMPLEMENTATION

Port Water injection was implemented in the reference model. In the PWI system, the injection events start approximately in correspondence of the intake valve opening, aiming to entrain all the water mass into the cylinder during the intake stroke and, although all the efforts in design and calibration, a water wall film formation in the intake port is very likely to occur. The thickness of such layer mainly depends on the heat transfer with the walls and on the dynamic fresh air pressure variation.

In order to consider all the mentioned effects, a proper 1D-CFD Water injection simulation set up and calibration would have required an important amount of time, and it would have gone beyond the thesis target as well. Therefore, a simplified methodology was adopted, as proposed by [30], in such a way to reduce computational efforts and to provide reliable results, allowing to quantify the potentiality of such technology, taking also into account the water wall film formation in the intake port and the water vaporization into the cylinder during intake and compression phase.

In GT-POWER, the use of just a port injector for each cylinder will cause the bulk water mass to evaporate into the intake port, subtracting heat from the fresh gases, which in turn will have a lower temperature at intake valve opening. Therefore, in order to better approximate the injection dynamic, a fictitious direct injection was added, and the injection event was calibrated as follows:

- *Port Injection*: since the simulation calculation is performed in steady state condition, the water film thickness is assumed to remain constant, with a constant balance between evaporated and deposited water. A constant mass flow rate injector is used to simulate the water film mass that evaporate and that slightly reduces the intake air temperature. The constant indirect injected water mass flow rate is indicated as $\dot{m}_{w,i}$.
- *Direct Injector*: a pulse injector is used to simulate the entrainment of water droplets into the cylinder during intake event and their further evaporation in the cylinder. The direct injected water mass flow rate is indicated as $\dot{m}_{w,d}$.

Such a water injection system required a fine-tuned control strategy, which was meant to control the water mass in order to reach the Lambda 1 operation. A schematic representation of water controller strategy is reported in Figure 5.21.

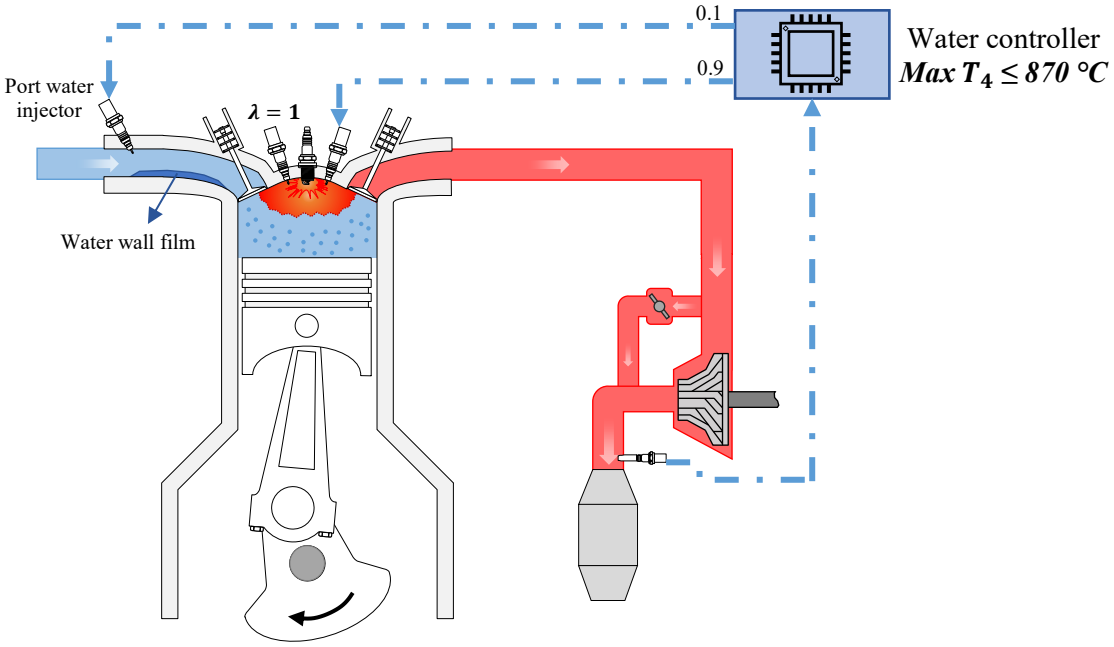

Figure 5.21: Water injection technology control strategy scheme.

The engine is set to run at Lambda 1, deactivating the PID controller of the maximum T_4. A water PID controller is added, and it controls the maximum T_4 acting on the overall water mass flow rate $\dot{m}_w$ into the engine that can be expressed as:

$$\dot{m}_w = i \cdot \dot{m}_{w,cyl} \tag{5.17}$$

Where i is the number of cylinder and $\dot{m}_{w,cyl}$ is the water mass flow rate for each cylinder, that can be divided in:

$$\dot{m}_{w,cyl} = \dot{m}_{w,d} + \dot{m}_{w,i} \tag{5.18}$$

It was assumed:

$$\dot{m}_{w,d} = 0{,}9\ \dot{m}_{w,cyl} \tag{5.19}$$

$$\dot{m}_{w,i} = 0{,}1\ \dot{m}_{w,cyl} \tag{5.20}$$

Furthermore, a sensor is used to record the IV opening (IVO) of each cylinder and the engine speed, so that the direct injector is timed to start the injection at intake valve opening, with a time duration equal to the intake event t_{intake}, and a mass flow rate computed by the controller as follows:

$$\dot{m}_{w,d,inj} = \frac{\dot{m}_{w,d}}{\frac{n}{2}} \cdot t_{intake} \tag{5.21}$$

The effects of considering two injectors to model a single port water injection is shown in Figure 5.22, where temperature during compression is reported in the left plot and pressure for compression and expansion in the right plot. The red curve refers to the case where just a port injector is used while the blue curve is the result of the presented methodology, with 10% of water mass port injected and 90% direct injected. As can be observed, being in the red curve the water fully vaporized before to enter into the cylinder, the lower temperature at the compression start enhances the knock resistance due to low temperature at compression-end. In the blue curve indeed, the larger water mass evaporates within the cylinder, where part of the vaporization heat is supplied to the water by the combustion chamber walls, with a less effective mixture temperature reduction and higher water consumption. The benefit of higher knock resistance of the red case can be even seen in the pressure plot, where combustion can be advanced, increasing the peak pressure.

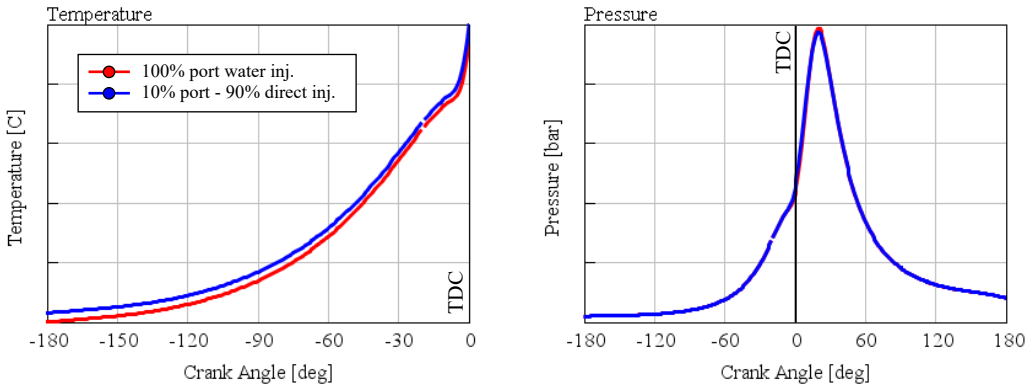

Figure 5.22: Effects of 100% port injected water mass modeling with respect to 10% port injected and 90% direct injected water mass modelling on in-cylinder temperature and pressure at high load – high speed.

Moreover, in order to take into account the effects on combustion, a correlation table between water to fuel ratio and combustion duration have been generated, according to the results of [30] [33], and it is reported in Figure 5.23.

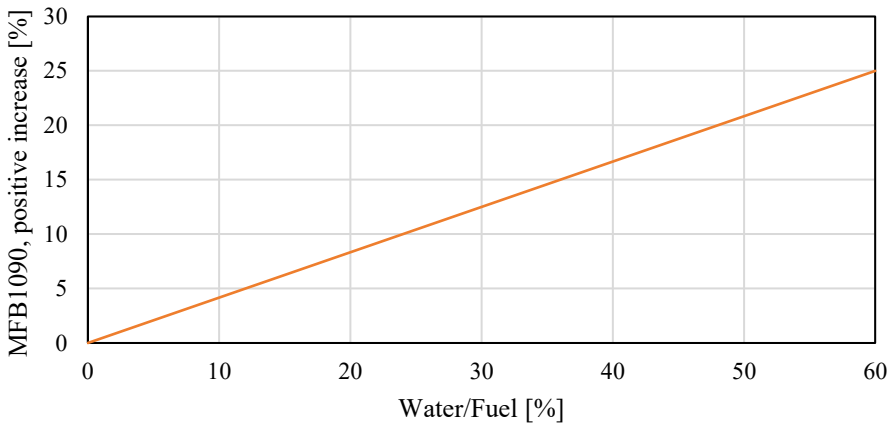

Figure 5.23: Burn duration increase with water/ratio, model assumption.

A burn duration controller is used to continuously computing the water to fuel fraction, necessary to adjust, by means of the correlation table, the burn duration variation using an actuator connected to each cylinder.

Water injection has been finally tested in the reference model, with the proposed methodology and results are shown in Figure 5.24. As anticipated, a very effected fuel enrichment reduction has been achieved, enabling stoichiometric operation in the whole engine map. However, the price to pay in order to have such lambda gain is a quite high water demand, quantifiable in a water to fuel ratio approaching 50 %, which would require the installation of a big water tank (it can even be unfeasible for packaging reasons) in order to limit the customers dissatisfaction, due to closer water refill operation. Nevertheless, the WI potentialities are evident, where although the longer combustion duration, the boost pressure p_2 is reduced, indicating a slightly increased spark advance.

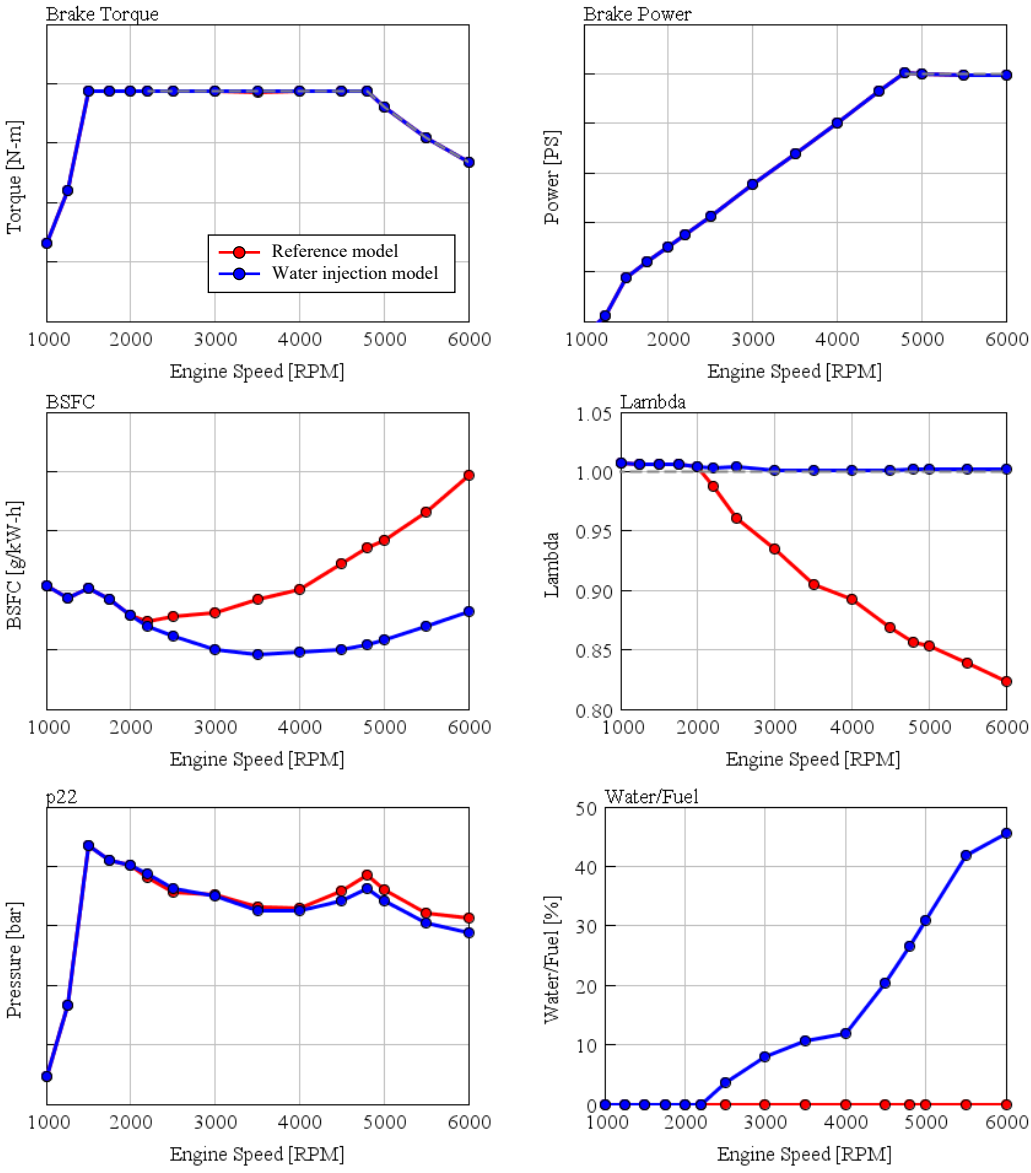

Figure 5.24: Water injection technology implementation performance

5.6. DUAL LIFT CAM PROFILE

Dual lift cam profile allows to compensate the lack of torque caused by the Atkinson cycle, as discussed in Paragraph 5.2. This technology has been widely adopted in light duty engine because of its relative simplicity and ease of application [34]. It consists in realizing an intake camshaft where two cam lobes are present for each intake valve and by means of a slider mechanism, the camshaft can slide changing the cam profile. In this regard, the idea of application is to exploit a smaller cam profile for low engine speeds and a bigger cam profile able to realize a LIVC strategy at higher engine speed.

5.6.1. DUAL LIFT CAM PROFILE MODEL IMPLEMENTATION

According to the results obtained for Atkinson cycle in Paragraph 5.2.1, the big cam profile is chosen, and due to the presence of the smaller cam to guarantee low end torque performances, different boost needs are now present with the two cams and therefore, the turbo matching is revised. Furthermore, in the dual lift model was also implemented the E-Turbo technology, in order to provide the required boost pressure in any condition. The technical specifications of the dual lift model are reported in table

	SPECIFICATION	DETAIL	DATA
Engine	Compression ratio		10.5
Camshaft	Small cam	IV duration	190 CAdeg
	Big cam	IV duration	263 CAdeg
	Crossover speed		4000 rpm
Turbocharger	E-Turbo	Compressor size*	-
		Turbine size*	+ 18 %
		Boost control	48V – 10 kW EM

* Refers to the wheel diameter, compared to the reference model.

Table 5.5: Dual lift cam profile model specifications.

The results of the dual lift cam profile model are reported in Figure 5.25. Lambda 1 operation was reached up to 5000 rpm, demonstrating the effectiveness of the solution. From the P2 EM power it is clear the switch to from the smaller cam up to the big one, since the electric power suddenly change its value, due to the different boost demand of the Atkinson cycle. However, no further investigations were done with the dual lift cam technology, since it is a very well-known and mature technology, that moreover has a limited potential for future development.

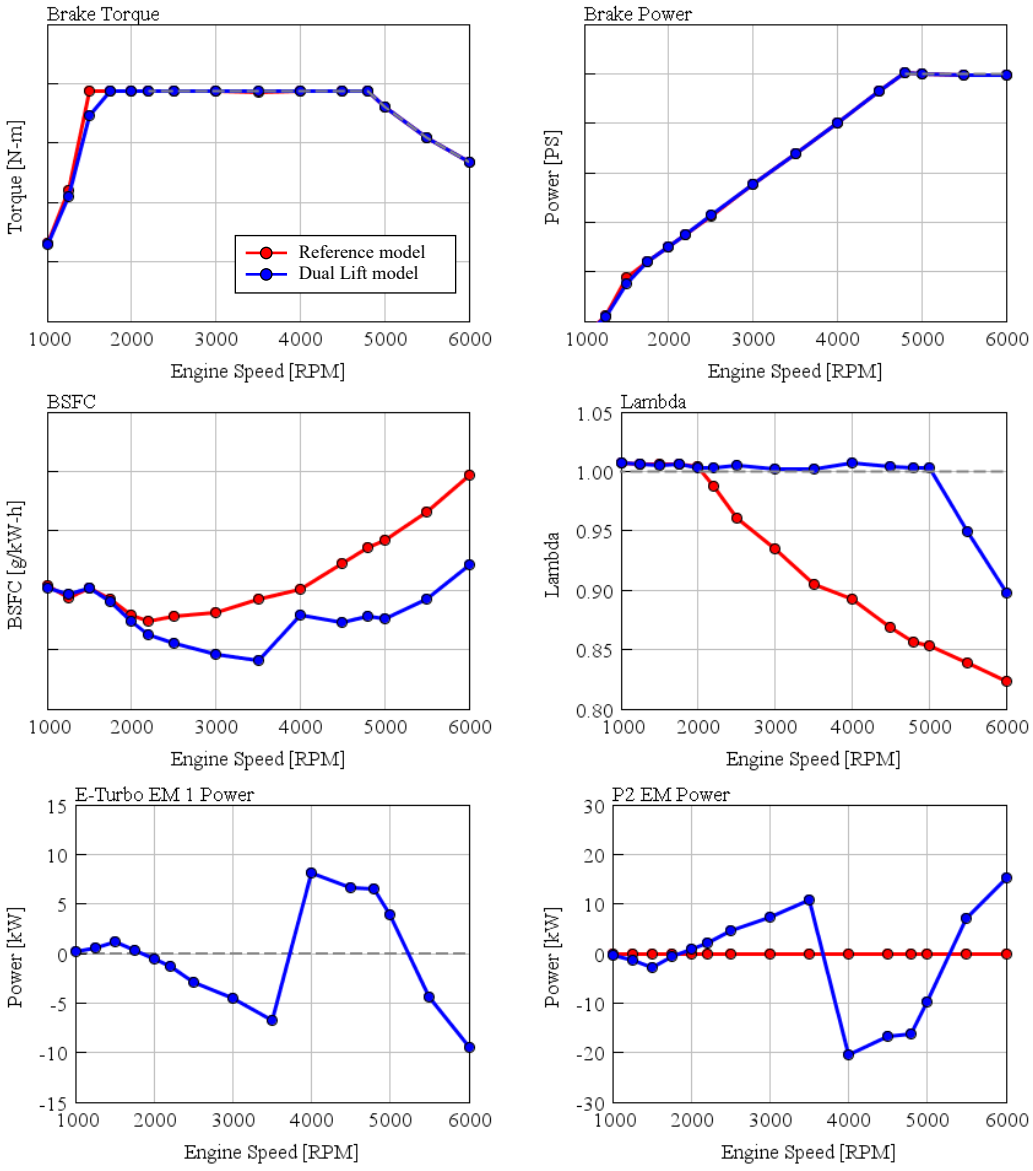

Figure 5.25: Dual lift cam profile technology implementation performance.

5.7. HYDROGEN ASSISTED COMBUSTION

As emerged during the study of the different engine technology, the main target which it is willing to achieve is an important knock mitigation, of paramount importance to increase engine efficiency and thus to reduce fuel enrichment. In this paragraph will be described a rough investigation on the addiction of a hydrogen fraction in the air fuel mixture in order to study the knock tendency reduction potentialities. Hydrogen was and still is a very interesting combustion means thanks to its good combustion properties. In Table 5.6 are reported gasoline and hydrogen characteristics, showing the hydrogen very high RON and lower heating value compared to gasoline, which make it very interesting for ICE combustion.

	GASOLINE	HYDROGEN
Molecular weight	110 ÷ 150	2
Stoichiometric A/F ratio	34.2	14.6
Minimum ignition energy	0.24 mJ	0.02 mJ
Laminar flame speed	40 cm/s	185 cm/s
Lower heating value	42 ÷ 44 MJ/kg	120 MJ/kg
RON	95 ÷ 98	140

Table 5.6: Gasoline and Hydrogen characteristics.

According to its excellent properties, the implementation idea thought for the thesis was to add a small fraction of H_2 so that to reduce the knock tendency as suggested by many researches [35] [36] [37] [38] [39], since beyond the higher RON, it also allows to increase the burning speed and the combustion stability. Furthermore, the idea is supported by the possibility to produce hydrogen on bord vehicle by means of a fuel reformer, which starting from gasoline, convert it into CO and H_2 and according to [35] [38] the presence of the CO does not affect the knock mitigation qualities of hydrogen. The positive effects of hydrogen addiction reported in the [36] [37] [38] [39], are here summarized:

- Overall higher RON of the total mixture.
- Improved knock resistance, especially at low engine speed while improved engine brake efficient at high engine speed.
- Anti-knock potential is affected by the hydrogen distribution.
- Increased burning speed.
- Slower autoignition chemistry due to the inhibition of fuel decomposition and hydroxyl radical production.
- Lower CO and HC emissions but higher NOx.
- Increased combustion stability.
- Extended lean limit.

With this in mind, it become clear as a 1D approach might be insufficient to evaluate all the hydrogen addiction effects on combustion process and being most of the studies cited carried out at relatively low engine speed and load, considering the engine operations under investigation in this work, it could be tentative to undertake a deeper analysis, relying on 3D simulations with dedicated combustion sub-models able to account for the hydrogen presence in the mixture. Nevertheless, a brief fluid dynamic investigation attempt was done, aiming to explore the hydrogen enhanced combustion potential in a very simplified manner.

5.7.1. H2 ASSISTED COMBUSTION MODEL IMPLEMENTATION

The engine model used for hydrogen implementation is different from the ones adopted in the analysis of the previous engine technologies. The reason is that, the Kinetics Fit Gasoline knock model used in the reference model is not capable of perform with a fuel different from gasoline and so the original engine model with Douaud and Eyzat knock model was used, with some modifications:

- Scavenging was removed.
- T_3 lambda control was deactivated.
- New T_4 lambda control was implemented.
- E-Turbo was added.

The E-turbo technology was added to compensate eventual boost needs due to the high stoichiometric air fuel ratio of hydrogen, which is more than twice the one of gasoline. Initially a port hydrogen injection was implemented, with the aim of studying the technology that require less engine hardware modification. However, it had been quickly rejected due to the huge volumetric efficiency reduction, caused by the low hydrogen density. In this regard, it was opted for a direct hydrogen injection where a second injector was placed in the cylinder chamber, injecting hydrogen during the compression stroke. Due to the complexity of hydrogen enhanced combustion 1D simulation, where detailed combustion sub-models should be defined, able to account the different laminar flame speed and so forth, some simplified assumptions were done. Firstly, it was defined the *hydrogen fraction* δ as the ratio of H_2 over gasoline mass flow rate, as expressed in the Formula:

$$\delta = \frac{\dot{m}_h}{\dot{m}_g} \tag{5.22}$$

Therefore, in order to consider the combustion improvement due to H_2 addiction, it was assumed that the burn duration is reducing as the hydrogen fraction is increasing. The correlation among burn duration reduction versus hydrogen fraction was defined according the results obtained in [36] [38] [39] and it is reported in Figure 5.26.

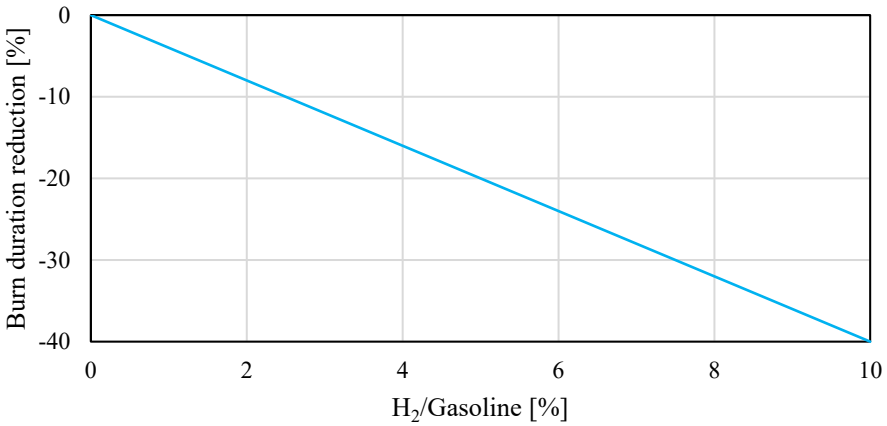

Figure 5.26: Burn duration decrease with hydrogen fraction.

The hydrogen exploitation as an anti-knock agent could be meaningful whether just little fractions of hydrogen are injected, so that either two solutions can be realized: or to store small quantity of hydrogen on vehicle or to directly produce hydrogen on board, by means of a fuel reformer. Thus, to simplify the investigation, it was neglected the H_2 supply mean, while just small hydrogen fractions were investigated.

Since two fuels are now burning in the combustion chamber, it was necessary to correctly compute the lambda value of the system, in other to ensure the correct working of the TWC. Therefore, a series of assumption were. A simplified scheme of the mixture composition during the compression stroke is reported in Figure 5.27.

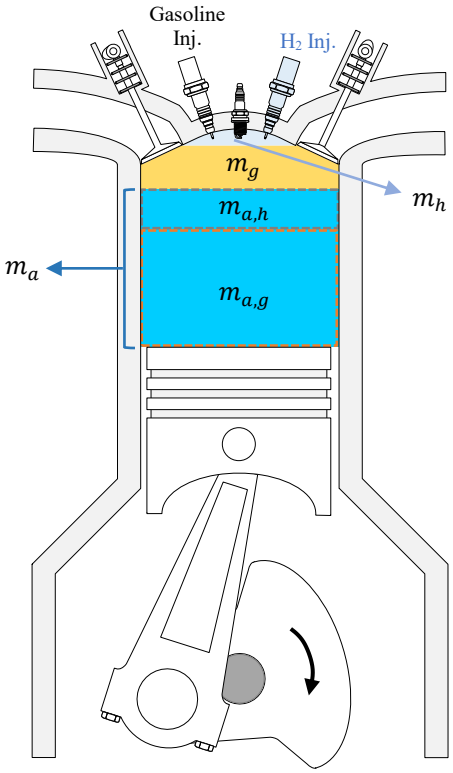

Figure 5.27: Hydrogen enhanced combustion, in-cylinder gas composition.

Since hydrogen burns very easily, the assumption for the lambda computation was that the hydrogen mass m_h burns completely. Then the total air mass flow rate is the sum of the air mass necessary to the hydrogen to burn completely and the air mass necessary to burn the gasoline, as expressed in formula:

$$\dot{m}_a = \dot{m}_{a,h} + \dot{m}_{a,g} \tag{5.23}$$

Then is possible to define the stoichiometric air fuel ratio as:

$$\alpha_{h,st} = \left(\frac{\dot{m}_{a,h}}{\dot{m}_h}\right)_{st} = 34{,}2 \tag{5.24}$$

$$\alpha_{g,st} = \left(\frac{\dot{m}_{a,g}}{\dot{m}_g}\right)_{st} = 14{,}6 \tag{5.25}$$

And in the same manner:

$$\lambda_h = \frac{\frac{\dot{m}_{a,h}}{\dot{m}_h}}{\alpha_{h,st}} = 1 \tag{5.26}$$

$$\lambda_g = \frac{\frac{\dot{m}_{a,g}}{\dot{m}_g}}{\alpha_{g,st}} \tag{5.27}$$

The lambda of hydrogen λ_h is set to 1 because of the assumption that hydrogen burns completely, while the lambda of gasoline λ_g is PID controlled according to the maximum T_4.

However, since the hydrogen fraction is imposed, a fine tuning of the injector was required, due to the fact that for the software, inside the cylinder just an air-fuel mixture is present and it does not consider the different stoichiometric value of the two fuels. Thus, it was necessary to compute the overall stoichiometric value of the mixture starting from the equations (5.22), (5.23), (5.24), (5.25) as function of constant parameters, which results in a constant value as well:

$$\alpha_{m,st} = \frac{\alpha_{g,st}}{1+\delta} + \frac{\alpha_{h,st}}{1+\frac{1}{\delta}} \tag{5.28}$$

Then, for both hydrogen and gasoline injectors in the model the lambda value is computed respectively as:

$$\lambda_{h,inj} = \frac{\frac{\dot{m}_a}{\dot{m}_h}}{\alpha_{m,st}} \tag{5.29}$$

$$\lambda_{g,inj} = \frac{\frac{\dot{m}_a}{\dot{m}_g}}{\alpha_{m,st}} \tag{5.30}$$

With regard on lambda control, the PID lambda controller acts on λ_g, which is different from what the injector compute. Defining two constant parameters λ_{g*}, λ_{h*} as the ratio between the stoichiometric respective air-fuel ratio over the mixture stoichiometric air-fuel ratio:

$$\lambda_{g*} = \frac{\alpha_{g,st}}{\alpha_{m,st}} \tag{5.31}$$

$$\lambda_{h*} = \frac{\alpha_{h,st}}{\alpha_{m,st}} \tag{5.32}$$

It is then possible to rewrite the injectors lambda just as function of λ_g, while all the other parameters are constant:

$$\lambda_{g,inj} = \lambda_{g*} \cdot \boldsymbol{\lambda_g} + \lambda_{h*} \cdot \delta \tag{5.33}$$

$$\lambda_{h,inj} = \lambda_{h*} + \frac{\lambda_{g*} \cdot \boldsymbol{\lambda_g}}{\delta} \tag{5.34}$$

With the shown methodology it was possible to keep constant the hydrogen fraction so that the direct effect of enrichment reduction caused by the hydrogen addiction can be better analyzed. Finally, the overall lambda value at catalyst will simply be:

$$\lambda = \frac{\frac{\dot{m}_a}{\dot{m}_g + \dot{m}_h}}{\alpha_{m,st}} \tag{5.35}$$

The product of hydrogen combustion will be just water, do not affecting the TWC function. Furthermore, due to the higher RON of hydrogen, it has been completed the equivalent RON of the mixture according to an energy balance as proposed by [35], and so the RON_{eq} is:

$$RON_{eq} = \frac{Q_{LHV,g} \cdot RON_g + Q_{LHV,h} \cdot RON_h \cdot \boldsymbol{\delta}}{Q_{LHV,g} + Q_{LHV,h} \cdot \boldsymbol{\delta}} \tag{5.36}$$

The results of the hydrogen injection for different hydrogen fraction, with the following methodology are reported in Figure 5.28.

It can be observed an increased lambda value with the hydrogen addiction but however not a huge step as it was expected. The reduced fuel enrichment is achieved thanks to the knock mitigation effect derived from the higher RON_{eq} of the mixture as well as from the burn duration reduction. What it seems to increase a lot is the engine efficiency, since an important reduction of BSFC is observed. Nevertheless, the BSFC reduction is somehow misleading because it is due to the overall higher Q_{LHV} of the mixture. In fact, being the BSFC defined as:

$$BSFC = \frac{\dot{m}_f}{P_{ICE}} = \frac{1}{\eta_b Q_{LHV}} \tag{5.37}$$

The lower heating value of the mixture will be:

$$Q_{LHV} = \frac{Q_{LHV,g} \cdot \dot{m}_g + Q_{LHV,h} \cdot \dot{m}_h}{\dot{m}_g + \dot{m}_h} = \frac{Q_{LHV,g} + Q_{LHV,h} \cdot \delta}{1 + \delta} \tag{5.38}$$

As an example, considering a hydrogen fraction $\delta = 5\%$ the Q_{LHV} will then be:

$$Q_{LHV} = \frac{44\frac{MJ}{kg} + 120\frac{MJ}{kg} \cdot 0.05}{1 + 0.05} = 47.6\frac{MJ}{kg} \tag{5.39}$$

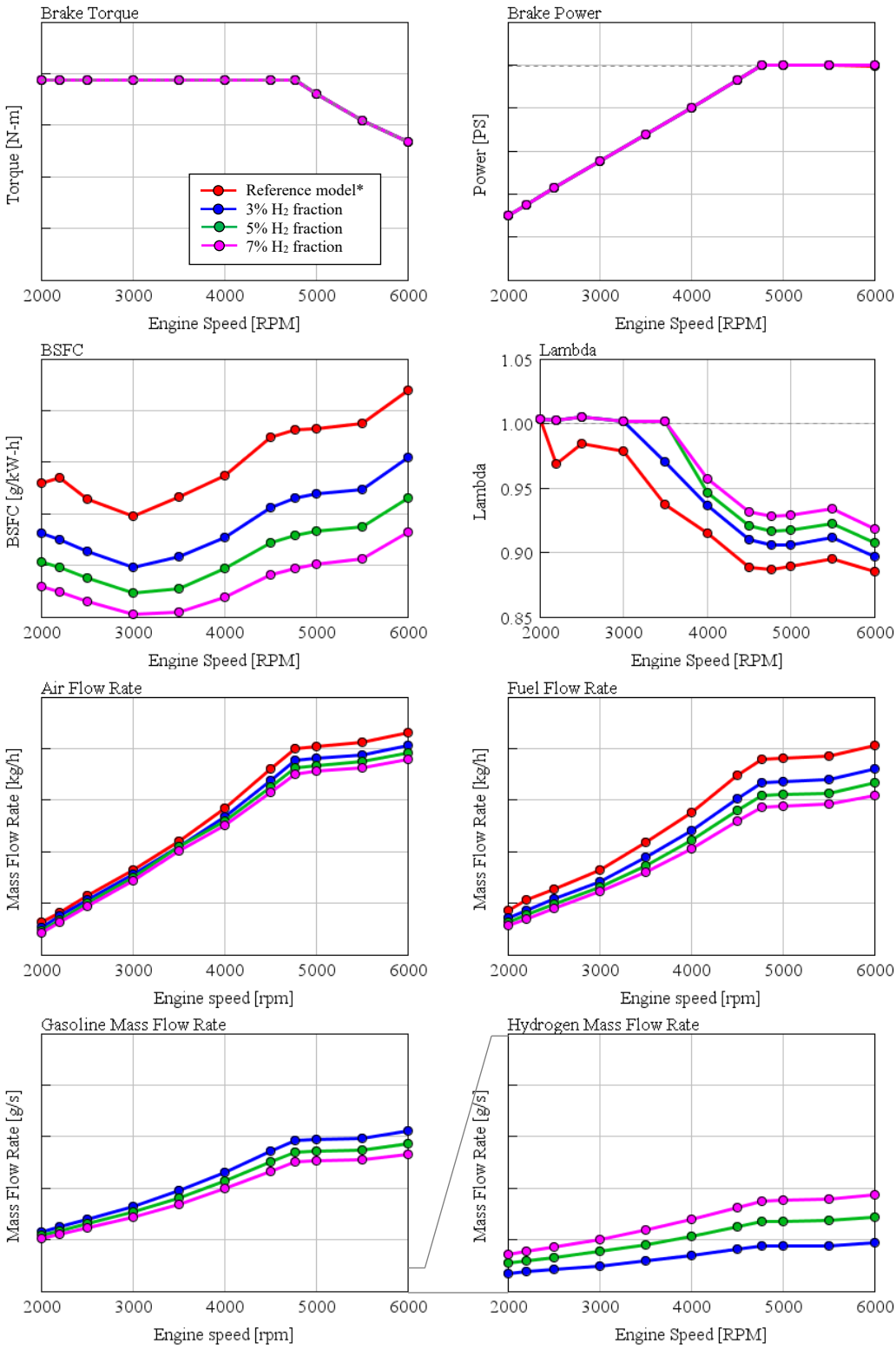

*Model with Douaud and Eyzat knock model and E-Turbo.

Figure 5.28: Hydrogen enhanced combustion technology implementation performance.

5.7.2. H2 ASSISTED COMBUSTION CONSIDERATIONS

Although the hydrogen enhanced combustion investigation was hugely simplified to make it feasible to be performed in short times, by means of a 1D-CFD simulation code, some considerations can be drowned, according to the results obtained and assumption done:

- Simplified assumption was done for combustion modelling, so with a more accurate methodology, higher knock mitigation potentials are plausible.
- The higher lower heating value of the system may be beneficial in CO_2 abatement optics, due to the reduced specific fuel consumption.
- The reduced specific fuel consumption also compensates for the need of higher compressor boost, as it might be expected from the higher stoichiometric hydrogen air-fuel ratio.
- The higher combustion stability reported by the cited studies, may also open the way for leaner engine operation, interesting for other ICE applications.
- The hydrogen assisted combustion, with a different approach, could be adopted for low load efficiency increase, where combustion stability is a concern and higher compression ratio may be allowed.

Regardless the simplified investigation, hydrogen enhanced combustion was a very interesting topic to analyze, for which further detailed simulation or experimental test may be carried on, in order to analyze its true potential, especially for the application on high performance engine.

6. EURO 7 ENGINE CONCEPTS

In Chapter 5 different engine technologies have been analyzed to evaluate their potential in fuel enrichment reduction. The result is that most of them (except for water injection and dual lift cam profile) showed certain level of enrichment reduction that alone was not big enough to allow lambda 1 operation at peak power. With this regard, a combination of different engine technologies is necessary to approach the stoichiometric operation, realizing Euro 7 engine concepts.

Euro 7 compliant engine concepts were defined proposing two different engine versions:

- *Standard version:* low- and high-end torque requirements are meet, whereas engine can work at lambda 1 at peak power. The approach adopted in standard concepts definition was aimed at minimizing the number of technologies to be implemented, considering costs, technologies compatibility and overall system potential.
- *Evo version:* technologies were chosen with the aim to increase specific power and letting the engine run at lambda 1 in the whole engine map. Costs did not play an important role, while just performance was researched.

Engine concepts with their technologies combinations are reported in Table 6.1.

VERSION	CONCEPT	TECHNOLOGIES
Standard	Concept 1	E-Turbo + Miller cycle + Turbulent Jet Ignition
	Concept 2	E-Turbo + A/C CAC
	Concept 3	E-Turbo + Water Injection
Evo	Evo 1	E-Turbo + Miller cycle + Turbulent Jet Ignition + AC CAC
	Evo 2	E-Turbo + Miller cycle + Turbulent Jet Ignition + Water Injection

Table 6.1: Euro 7 engine concepts, standard and Evo versions.

6.1. STANDARD VERSIONS

The standard versions engine concepts definition was the main target of the thesis work, since they represent feasible solutions which satisfy engine performance targets and Euro 7 fuel enrichment restrictions. Therefore, their definition and analysis were the major concern in such a way that, not only WOT operations were considered, but also part load and transient operations, to deeply compare and analyze their potential and characteristics. Moreover, in Paragraph 6.1.4, possible catalyst heating issues and improvements due to the new technologies are going to be discussed.

6.1.1. CONCEPT 1

The Concepts 1 adopts the E-Turbo, the Miller cycle and the Turbulent Jet Ignition.

For what Miller cycle is concern, it was adopted the optimized twisted camshaft presented in Paragraph 5.2.2, as well as the same IVAM and CR were maintained. However, in the Miller cycle technology analysis presented, the effect of burn duration deterioration was not considered, because of the difficulties related to an accurate analytical quantification. Therefore, in Concept 1 it was assumed that the negative effect on combustion caused by the EIVC can be well compensated by the TJI technology, which showed promising results in combustion speed up. The worsening of the volumetric efficiency caused by Miller cycle required to optimize the turbo matching, which was done scaling the turbine size so that to obtain a maximum recoverable power from the E-turbo EM equal to 10 kW, thus the highest exhaust gas expansion with the implemented E-Turbo is achieved. The technical specifications of the technologies adopted in Concept 1 are reported in Table 6.2.

TECHNOLOGY	SPECIFICATION	REFERENCE MODEL	CONCEPT 1
E-Turbo	Compressor size*	–	–
	Turbine size*	–	+ 9 %
	Boost control	Wastegate actuation	48V – 10 kW EM. Wastegate closed
Miller Cycle	IVAM	1	0.8
	IV opening duration	190 CAdeg	140 CAdeg
	CR	9.5	10.5
Turbulent Jet Ignition	Ignition	Spark Plug	Passive Prechamber Jet Plug

* Refers to the wheel diameter

Table 6.2: Concept 1 technologies specifications.

In Figure 6.1 are reported the performance results of Concept 1. The lambda 1 operation in the whole engine map is accomplished and accompanied by an important engine efficiency improvement, as can be observed from the significant BSFC reduction. The Miller cycle knock mitigation, which is more effective especially at low-end torque where knock is most likely to occurs, reduces the boost needs in that region, resulting in E-Turbo EM power lower or at most equal to zero. It means the turbine is always recovering power from the exhaust gas, with positive effect for T_4 reduction, which then reaches value even lower than the maximum threshold. For what T_3 is concern, a maximum value of 1000 °C is approached at maximum speed, value far from the previously set 1030°C limit, and thus the T_3 lambda controller does not need to intervene.

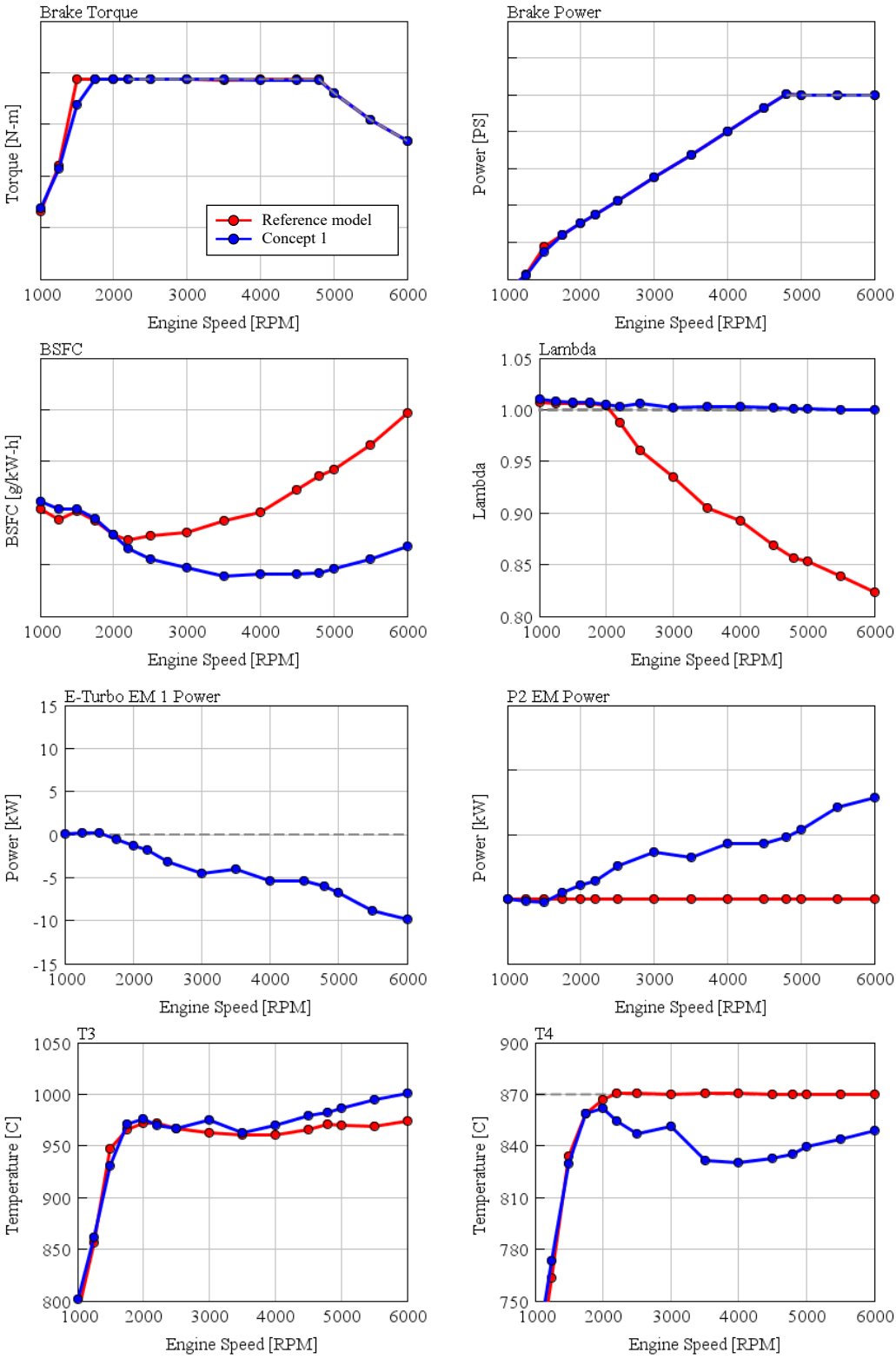

Figure 6.1: Concept 1 performance, main results.

6.1.2. CONCEPT 2

The Concepts 2 adopts the E-Turbo and the A/C supported charge air cooler.

The A/C cooling power is controlled in order to reach lambda 1 and the respective compressor power required is extracted from the engine. The technical specifications of the technologies adopted in Concept 2 are reported in Table 6.3.

TECHNOLOGY	SPECIFICATION	REFERENCE MODEL	CONCEPT 2
E-Turbo	Compressor size*	–	–
	Turbine size*	–	+ 26 %
	Boost control	Wastegate actuation	48V – 10 kW EM. Wastegate closed
A/C CAC	Charge cooling	Standard	A/C supported
	A/C cooling power	–	up to 10 kW

* Refers to the wheel diameter

Table 6.3: Concept 2 technologies specifications.

In Figure 6.2 are reported the performance results of Concept 2. The target of no fuel enrichment is reached up to peak power, which satisfy the requirements. However, at higher engine speed, even using the maximum available cooling power, lambda 1 operation is not achieved. Nevertheless, to increase the lambda value at maximum speed, the maximum power can be reduced up to a level where stoichiometric operation is enabled. Focusing on the ET EM power, some boost is required at low-end torque due to the bigger turbine size compared with that of Concept 1 and to the lack of knock mitigation, since A/C CAC is not exploited in those speeds. The maximum T_3 is comparable with that of the reference model, which represent a very safe operation for the component.

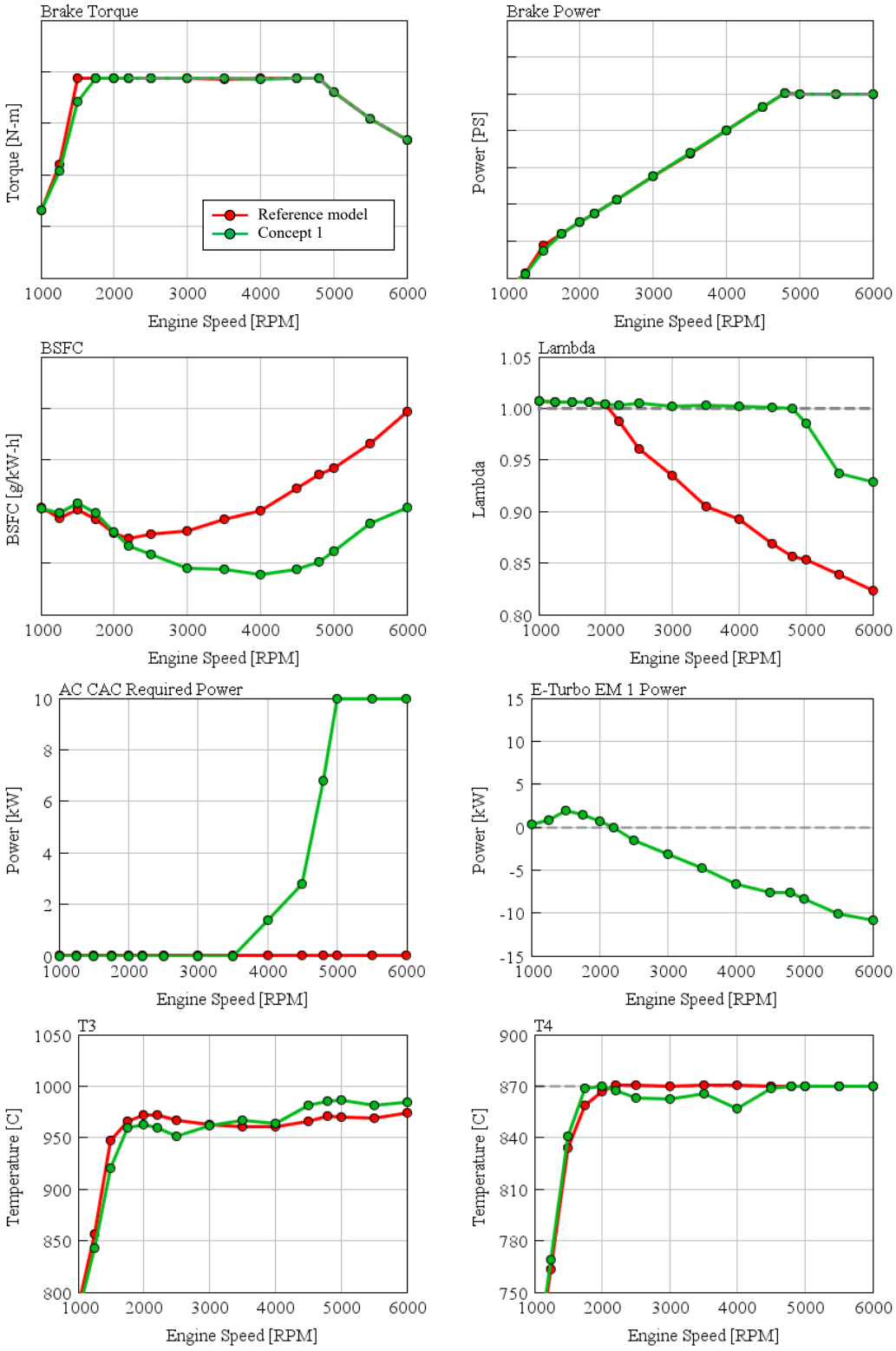

Figure 6.2: Concept 2 performance, main results.

6.1.3. CONCEPT 3

The Concepts 3 adopts the E-Turbo and the water injection.

The concept is very similar to Concept 2, where just the charge cooling mean is different. The technical specifications of technologies adopted in Concept 3 are reported in Table 6.4.

TECHNOLOGY	SPECIFICATION	REFERENCE MODEL	CONCEPT 3
E-Turbo	Compressor size*	–	–
	Turbine size*	–	+ 26 %
	Boost control	Wastegate actuation	48V – 10 kW EM. Wastegate closed
Water Injection	Water Injector	–	Port Injector

* Refers to the wheel diameter

Table 6.4: Concept 3 technologies specifications.

In Figure 6.3 are reported the performance results of Concept 3. According to the results showed in Paragraph 5.5.1, water injection technology alone was already capable of reaching lambda 1 in the whole engine map. However, an important water consumption close to a maximum value of water-fuel ratio of 45% had to be paid for such a result, which is somehow uncomfortable for what water tank refilling is concern. Thus, with Concept 3, thanks to the coupling with the E-Turbo technology, a significant reduction of water consumption is achieved, increasing the concept potentialities. Effectiveness of water injection in knock mitigation is evidenced also from the quite high BSFC reduction as well as from the maximum T_3 values, which are comparable to the reference model.

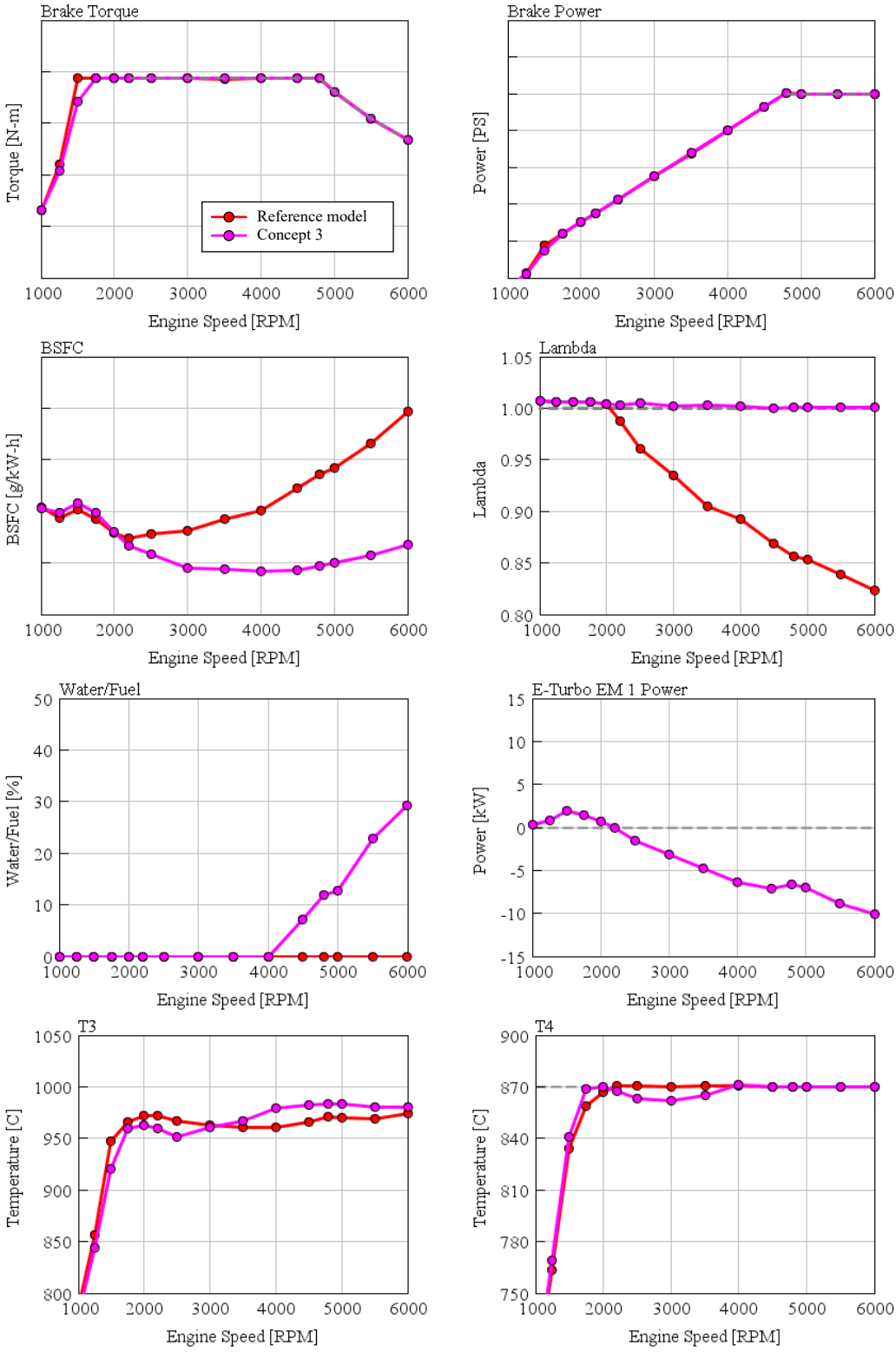

Figure 6.3: Concept 3 performance, main results.

6.1.4. CATALYST HEATING

With concern in coming Euro 7 emission regulation, an important topic beside the fuel enrichment reduction regards the TWC heating strategies, also known as *cat heating*. Type approval emission tests are performed with cold start and thus, in the initial stage, where the TWC has not reached yet the light-off temperature, the tailpipe emissions are the highest, due to the inactivity of the TWC. Therefore, the largest part of pollutant emission during the tests are concentrated in the initial cat heating stage (up to 80%) [40], which is something the car manufacturers struggle to avoid. In fact, many solutions have been introduced to speed up the cat heating phase, and one above all is the spark retard, which is aiming of postponing the combustion as much as combustion stability is acceptable, so that the exhaust temperature increases, with beneficial effect for cat heating [41]. However, the only spark retard may not be enough, so that further strategies for catalyst heating up are used by car manufacturers to speed up the process. Being the topic very wide and beyond the task of the thesis, just a brief description of the possible solutions are provided:

- *Active methods*: includes electrically heated catalyst, where resistors are integrated in the catalyst washcoat increasing the walls temperature; secondary air injection, that sustain the exothermal CO and HC oxidation reaction; catalyzed fuel burner.
- *Passive methods*: include close coupled catalyst installation, use of pre-catalysts, air gap insulation, phase change material and variable conductance insulation.

In Euro 7 perspective, the trend will be to feature electrically heated cat, which will require a certain gas mass flow through the cat itself, in order to prevent resistors damage and to better distribute the heat into the component. With this regard, electric pumps are adopted, which are responsible of pumping fresh air into the catalyst, but since the TWC has to work with stoichiometric mixture, the fresh air in the exhaust system would increase the lambda value. To avoid that, the engine during the cat heating runs with rich mixture to compensate the leaning caused by the fresh air. Furthermore, the rich mixture will increase the engine out CO and HC emission, that are further oxidated in the catalyst increasing its temperature [42]. Unfortunately, this strategy involves some limits: electric catalysts typically requires very high electric power, with high battery energy consumption and therefore large batteries are required, to ensure the correct working in any condition. In addition, the electric air pumps adopted to increase the air mass flow are usually not able to withstand high exhaust back pressure, which would cause the component to stuck: hence, if the engine load is increased, cat heating may be prevented.

After the above simply overview, it is interesting to analyze the effects of the technologies implemented in the Euro 7 engine concepts in cat heating condition. Being the engine at idle, many of the technologies in the concepts do not intervenes in this condition. Starting from Concept 2 and 3, the A/C CAC and water injection technologies are not active at low loads, while the E-Turbo may be exploited. For what it concerns Concept 1 instead, all the technologies included may affect the cat heating. Hence, it is possible to analyze the effects of the mentioned technologies in cat heating:

- *E-Turbo*: this technology may be beneficial in cat heating. In fact, the compressor can be exploited in pumping fresh air in the TWC, thanks to the EM that can electrically boost the compressor, which can easily withstand the exhaust back pressure.
- *TJI*: as mentioned in Paragraph 5.3.1, this technology does not provide stable low load operation, requiring a second spark plug. However, some studies demonstrated the correct operation of the component coupled with Miller cycle at idle [22].
- *Miller cycle*: the lower in-cylinder turbulences may be detrimental for spark retard.

6.2. EVO VERSIONS

Evo versions engine concepts definition was motivated by the research of performance, combining the different technologies so that also lambda 1 operation can be guaranteed. According to the results from standard concepts, it was chosen to base the high-performance concepts on Concept 1, where Miller cycle and TJI can be exploited for further efficiency improvement due to their compatibility with the charge cooling technologies adopted in the other concepts.

6.2.1. EVO 1

The Evo 1 adopts the E-Turbo, the Miller cycle, the Turbulent Jet Ignition and the A/C supported charge air cooler.

Since higher specific power was desired, according to what highlighted in Chapter 2, higher fresh air density is required at engine inlet. Therefore, the turbo matching was revised with this target, and in fact bigger compressor size was implemented. Moreover, in order to avoid too high boost pressure due to the higher air density and to the quite short intake valve opening duration present in Concept 1, the Miller grade had been relaxed, keeping anyway the same CR. The technical specifications of technologies adopted in Evo 1 are reported in Table 6.5.

TECHNOLOGY	SPECIFICATION	REFERENCE MODEL	EVO 1
E-Turbo	Compressor size*	–	+ 7 %
	Turbine size*	–	+ 13 %
	Boost control	Wastegate actuation	48V – 10 kW EM. Wastegate closed
Miller Cycle	IVAM	1	0.85
	IV opening duration	190 CAdeg	152 CAdeg
	CR	9.5	10.5
Turbulent Jet Ignition	Ignition	Spark Plug	Passive Prechamber Jet Plug
A/C CAC	Charge cooling	Standard	A/C supported
	A/C cooling power	–	up to 10 kW

* Refers to the wheel diameter

Table 6.5: Evo 1 technologies specifications.

In Figure 6.4 are reported the performance results of Evo 1. Thanks to the combination of a higher number of technologies it was possible to increase the specific power of 17% keeping lambda 1 in the whole engine map. The higher power also raised the compressor pressure ratio, with a limited increase thanks to the lower Miller grade and the presence of the A/C supported CAC. For what is concern the cooling power required, the presented concept has a quite low compressor power demand, due to the parallel effect of all the implemented technologies. What may alert is the maximum T_3, which now reaches value close to 1030°C, that can be dangerous for the turbine.

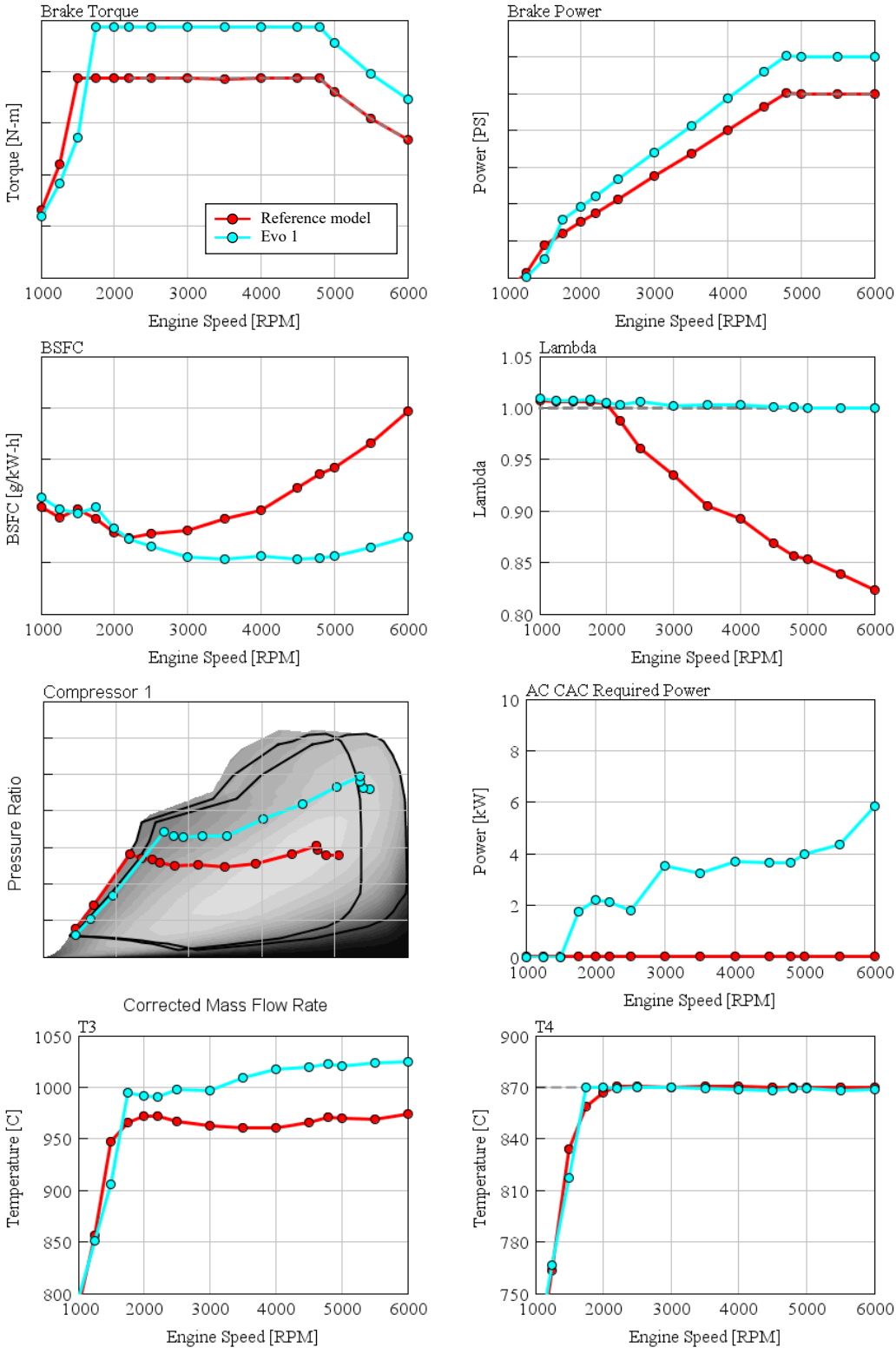

Figure 6.4: Evo1 performance, main results.

6.2.2. EVO 2

The Evo 2 adopts the E-Turbo, the Miller cycle, the Turbulent Jet Ignition and the water injection.

Evo 2 has the same technologies specification of Evo 1, except for the A/C CAC that here was substituted with the water injection. The technical specifications of the technologies adopted in the concept are reported in Table 6.6.

TECHNOLOGY	SPECIFICATION	REFERENCE MODEL	EVO 2
E-Turbo	Compressor size*	–	+ 7 %
	Turbine size*	–	+ 13 %
	Boost control	Wastegate actuation	48V – 10 kW EM. Wastegate closed
Miller Cycle	IVAM	1	0.85
	IV opening duration	190 CAdeg	152 CAdeg
	CR	9.5	10.5
Turbulent Jet Ignition	Ignition	Spark Plug	Passive Prechamber Jet Plug
Water Injection	Water Injector	–	Port Injector

* Refers to the wheel diameter

Table 6.6: Evo 2 technologies specifications.

In Figure 6.5 are reported the performance results of Evo 2. Also for this concept an increase of 17 % of specific power can be easily reached, and the combination of the four engine technologies, despite the higher performances, allows to reach lambda 1 with very low water consumption levels. In detail, in the concept water is required starting from a lower engine speed if compared to Concept 3, but the peak requirement stays below the 15% of water-fuel ratio. In closing, as formerly highlighted, the water injection effectiveness in knock mitigation allows to reach very good results with maximum T_3 value limited within the fixed threshold of 1030 °C.

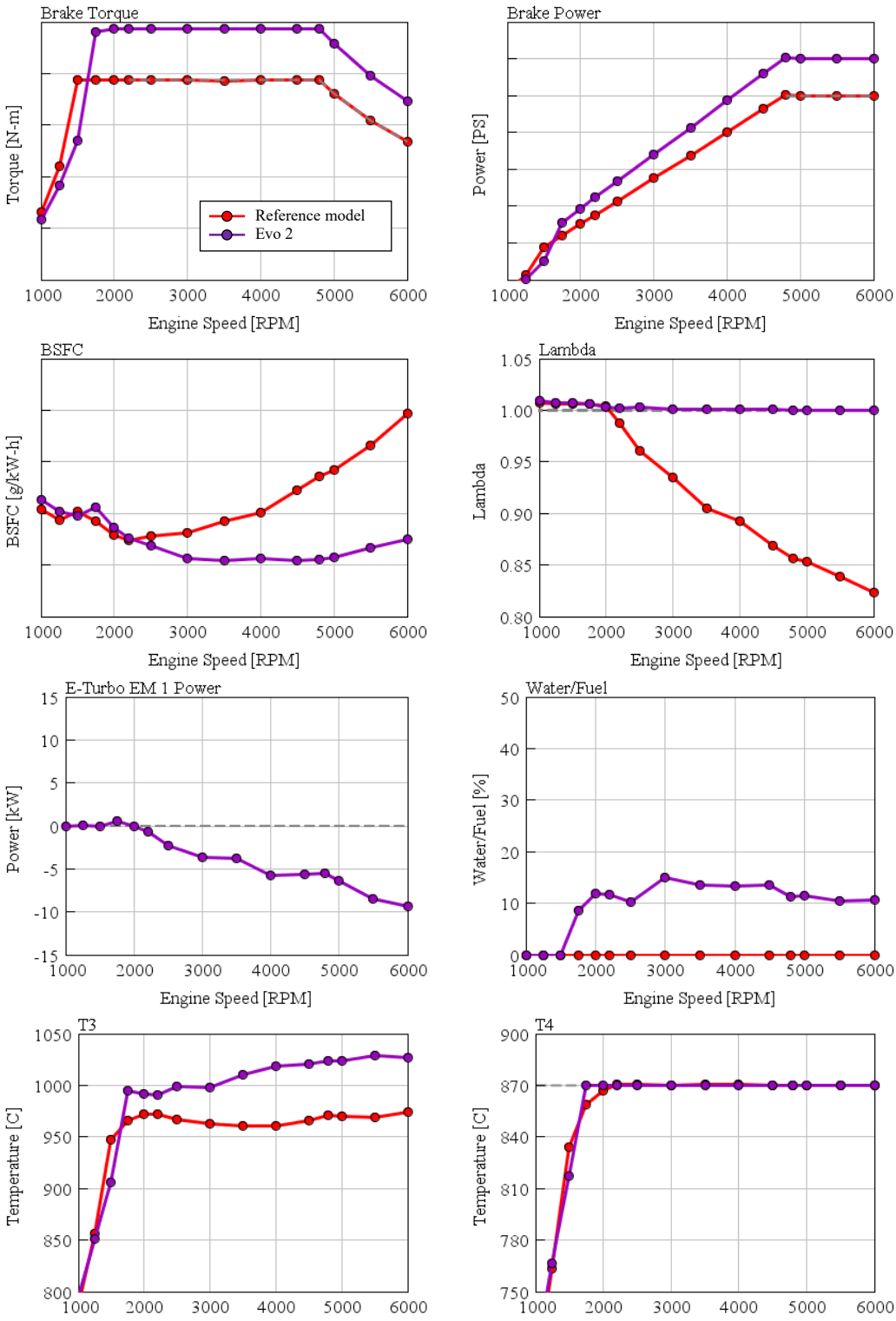

Figure 6.5: Evo 2 performance, main results.

7. PART LOAD ANALYSIS

Part load investigation was performed on standard version engine concept proposed in Paragraph 6.1, being them of higher interest for the thesis work. For the analysis, the typical low urban load condition corresponding to a load of 2 bar of BMEP was considered.

In part load operation, the load is controlled by means of the throttle valve that with the aim of reducing the pressure in the intake manifold, introduces throttling losses which reflect in a higher pumping work of the engine (PMEP). The consequence of such an increase of PMEP and reduction of IMEP due to the load control, is a worsening of the engine specific fuel consumption as depicted in Figure 7.1. Furthermore, being the intake and exhaust mass flows rate dramatically reduced, also the turbo speed will be reduced as well, that is a factor of paramount importance for what transient response is concern.

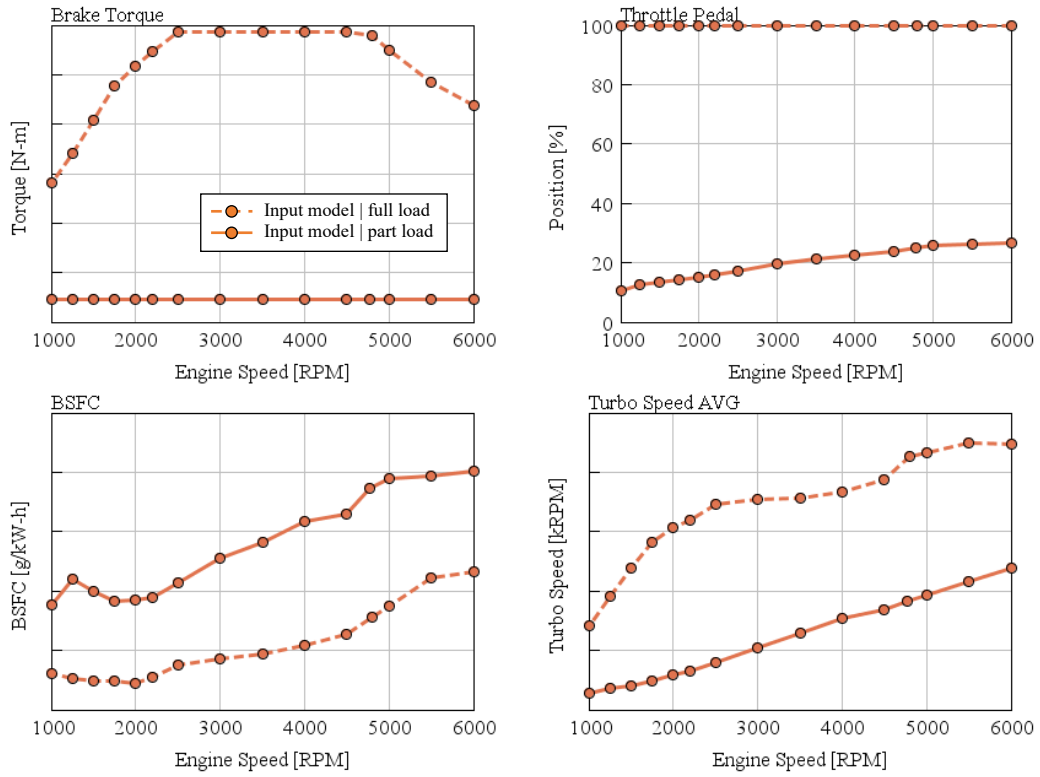

Figure 7.1: Reference engine, load sweep from WOT to part load (2 bar BMEP). Worsening of BSFC and turbo speed.

In the part load analysis, the reference engine was considered instead of the reference model reported so far: in fact, the reference model was introduced and used as reference in the technologies investigation because of the new turbocharger and of the new control on T_4, which were present in every model analyzed in full load. In part load, the technologies enabling knock mitigation do not play any role, since the load and mixture composition are controlled respectively by the throttle valve and by the engine residual content, which affect the combustion stability. Thus, it makes more sense to compare the standard engine concept with the reference engine. In this regard, considering

the standard version concept, it is possible filter the technologies that affects the part load behavior and the those who do not. A summary of the technologies on each concept which plays a role in part load is reported in Table 7.1.

	1	PL ROLE	2	PL ROLE	3	PL ROLE
Concept 1	E-Turbo	**Yes**	Miller cycle	**Yes**	TJI	No*
Concept 2	E-Turbo	**Yes**	A/C CAC	No		
Concept 3	E-Turbo	**Yes**	WI	No		

* Requires standard spark plug for part load

Table 7.1: Summary of standard concepts technologies that affect the part load operations.

Concept 2 and 3 results very similar at a first glance due to the only presence of E-Turbo which affect the part load operation and in detail, from the Table 7.1 it is possible to conclude that both concepts behave in the same manner, because of the same turbocharger size. Therefore, the part load analysis can be reduced just to reference engine, Concept 1 and Concept 2, the latter representative for Concept 3.

7.1. SIMULATION METHODOLOGY

In full load operation, thanks to the double VVT present in the reference engine, the cam timing is optimized to improve the volumetric efficiency as well as to prevent scavenging. However, in part load operation, since the BSFC is increased by the throttle losses through the throttle valve, an effective way to optimize the fuel consumption is to change the cam timing in order to worse the volumetric efficiency, so that an wider throttle angle is required. The cam timing was then changed in this sense, ensuring to have a maximum residual limit close to 25% value that according to Porsche represent the combustion stability limit.

For what turbocharger is concern, it was thought to perform the analysis with the wastegate valve completely closed. In doing so, the turbocharger speed is higher, useful for the following transient analysis. An operation with the wastegate completely open would have improved the specific fuel consumption, due to the lower p_2, which would have required more throttle angle with then less pumping work. Nevertheless, it was privileged the dynamic response, which captured more interest because of the high degree of freedom allowed by the E-Turbo technology.

Part load results are reported in Figure 7.2, where is evidenced the better fuel consumption of Concept 1 with respect of Concept 2. The advantage is mainly due to the Miller cycle, that thanks to the shorter intake cam reduces the volumetric efficiency and so lead to wider throttle angle. Comparing Concept 2 with the current engine, it can be observed the positive effect of its bigger turbine size on the BSFC, caused by the lower p_2. By convers, the bigger turbine reduces the turbo speed that shows the lowest values, therefore the combined effects of the bigger dimension of the turbocharger group with the low turbo speed may portend a worst dynamic response.

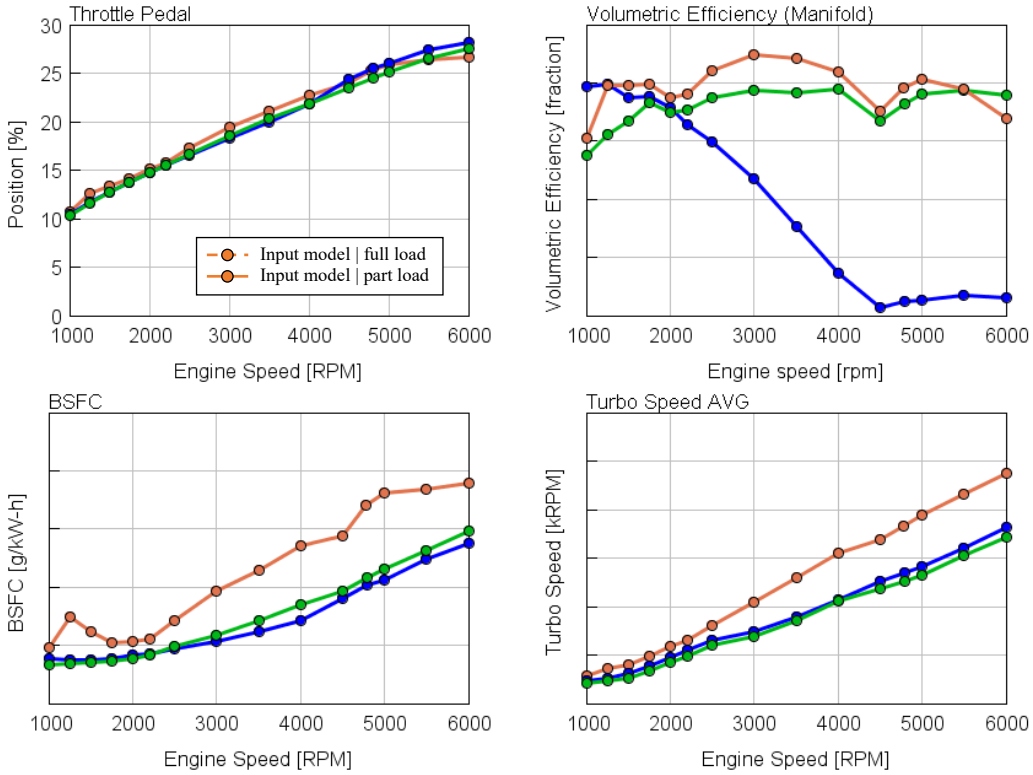

Figure 7.2: Part load 2 bar BMEP standard concept results compared to reference engine.

8. TRANSIENT ANALYSIS

Whenever high-performance engines are developed, not only the full load performance is the major target but also the transient response, which is very important to satisfy customer requirement and expectation. In this regard, the transient behavior of the Euro 7 standard version concepts was analyzed in a tip-in maneuver, where the load demand is abruptly changed from a low load condition to full load. In fact, during the tip-in, at time instant $t = 0\ s$ the throttle valve position varies from a part load angle up to the maximum opening angle in $t = 0.15\ s$. During this short time, the engine undergoes a series of delays which all together determine the time necessary to complete the maneuver; the most important are: the *fluid dynamic delay*, which refers to the time needed to build up the pressure in the manifolds and ducts, and the *mechanical delay*, mostly linked to the turbocharger group acceleration. As a matter of fact, in a turbocharger group, neglecting the mechanical friction, the angular acceleration is described by the formula:

$$\frac{T_T - T_C}{J_{TC}} = \frac{d\omega_{TC}}{dt} \tag{8.1}$$

Where T_T and T_C are respectively the turbine toque and compressor resistant torque, while J_{TC} is the polar moment of inertia of the turbocharger. Thus, the TC acceleration is inversely proportional to the J_{TC}, which is proportional to the wheel diameter D at power of five:

$$J_{TC} \propto \rho D^5 \tag{8.2}$$

It follows that the moment of inertia of the group hugely affects the mechanical delay in the transient response. Moreover, due to the presence of the electric motor in the Euro 7 concepts turbochargers, Formula (8.1) needs also to take into account the polar moment of inertia J_{EM} of it. Thus, the formula become:

$$\frac{\boldsymbol{T_{EM}} + T_T - T_C}{\boldsymbol{J_{EM}} + J_{TC}} = \frac{d\omega_{TC}}{dt} \tag{8.3}$$

Since the EM can provide a torque T_{EM} during the TC acceleration, the term T_{EM} can compensate the higher resultant moment of inertia of the whole group, due to the EM and the bigger component dimensions. In Table 8.1 are reported the relative inertia of the turbocharger group of the current engine and of the standard version engine concepts.

MODEL	TURBOCHARGER	GLOBAL TC INERTIA
Current Engine	Standard, wastegate controlled	–
Concept 1	E-Turbo	+ 92 %
Concept 2	E-Turbo	+ 214 %
Concept 3	E-Turbo	+ 214 %

Table 8.1: Current engine and Euro 7 engine concepts turbocharger polar moment of inertia.

8.1. SIMULATION METHODOLOGY

The tip-in maneuver was investigated at three different engine speed: 1500 rpm, 2000 rpm and 4000 rpm. During the maneuver, the speed remains constant while the load is sweep from 2 bar of BMEP

up to WOT. The same reasoning done in Chapter 7 was adopted for the transient analysis, where again the current engine will be considered instead of the reference model. For what it concerns the Euro 7 engine concepts, as for part load analysis, also in transient the Concepts 2 and 3 have the same dynamic response, due to the fact that both A/C CAC and water injection stay inactive in the considered conditions. Therefore, just Concept 1 and 2 will be investigated, with the latter representative also for Concept 3.

As illustrated in Figure 3.3 and deeply discussed in the E-Turbo analysis in Paragraph 5.1, the reference powertrain is hybrid with a P2 electric motor. Therefore, the P2 EM can currently be exploited in transient operations, improving the overall performance during the maneuver, while in the analysis carried out indeed, it was decided to do not consider the P2 EM aid in transient. The decision is motivated by the fact that regardless of the concept and configuration considered, the P2 EM can give a constant advantage, as it does in the current engine. Thus, the P2 EM was just considered in the E-Turbo technology, where the system hybridization is present according to the configuration shown in Figure 5.3.

With these assumptions, on the base of the high number of possible strategies enabled by the E-Turbo technology present in all Euro 7 concepts, three different *engine modes* were investigated, which mainly differs for electric motors and battery vehicle power split:

- *Normal mode*: before the maneuver starts the engine is at 2 bar BMEP load, where the wastegate is completely closed and the EMs power equal to zero. At the start of the tip-in, the E-turbo EM is electrically accelerated suppling the maximum power to the EM (according to the EM power map) and subtracting the electric power for the P2 EM, which increases the engine load. As soon as the maximum torque is reached, the E-Turbo EM starts to regulate the boost to do not exceeded the target value. The main advantage of such a strategy is that the maneuver feasibility does not depend on the battery SOC.
- *Sport mode*: the operation is very similar to normal mode but now, during the transient maneuver the battery supply the power to the E-turbo EM and, up to the approach of the maximum torque the P2 EM does not intervenes. At maximum torque, the EM starts to regulate the boost and the recovered or supplied energy to the EM will be provided or subtracted to the engine by means of the P2 EM. In sport mode the dynamic response is much better with respect to the normal one, due to the reduced engine load. However, battery energy is required and so its operation strongly depend on the battery SOC.
- *Sport Plus mode*: the transient performance is here brought to the extreme. The simultaneous combination of P2 and E-Turbo EM operation also in part load makes this engine mode more complicated, for which it was decided to describe it in a dedicated Paragraph 8.1.1.

In Figure 8.1 are reported the torque values of the models during the tip-in in the tested engine speeds and in the three-engine mode. At a first glance of the results, it emerges that comparing Concept 1 and Concept 2 in the same engine mode, the latter shows longer times to reach the target torque. This is mainly due to the higher turbocharger inertia of Concept 2 with respect to Concept 1, as reported in Table 8.1. Comparing then the performance of both concepts in normal mode with that of the current engine, it is interesting to notice how the aid of the E-Turbo significantly improves the tip-in at low engine speeds (2000 rpm and 1500 rpm), where the turbocharger speed is quite low. On the contrary, at 4000 rpm where the turbo speed is higher, the higher inertia in case of Concept 1 and 2 lead to a tip-in performance worse than the current engine case. However, the positive effect of the E-Turbo technology comes with the possibility to exploit different transient strategies. As a matter of fact, switching to Sport mode or even better to Sport Plus mode, very good results are obtained. At 4000 rpm it is possible with the Sport Plus mode to fully recover the current engine

performance while an excellent response is obtained at low engine speeds, where the improvement from normal mode is maximized.

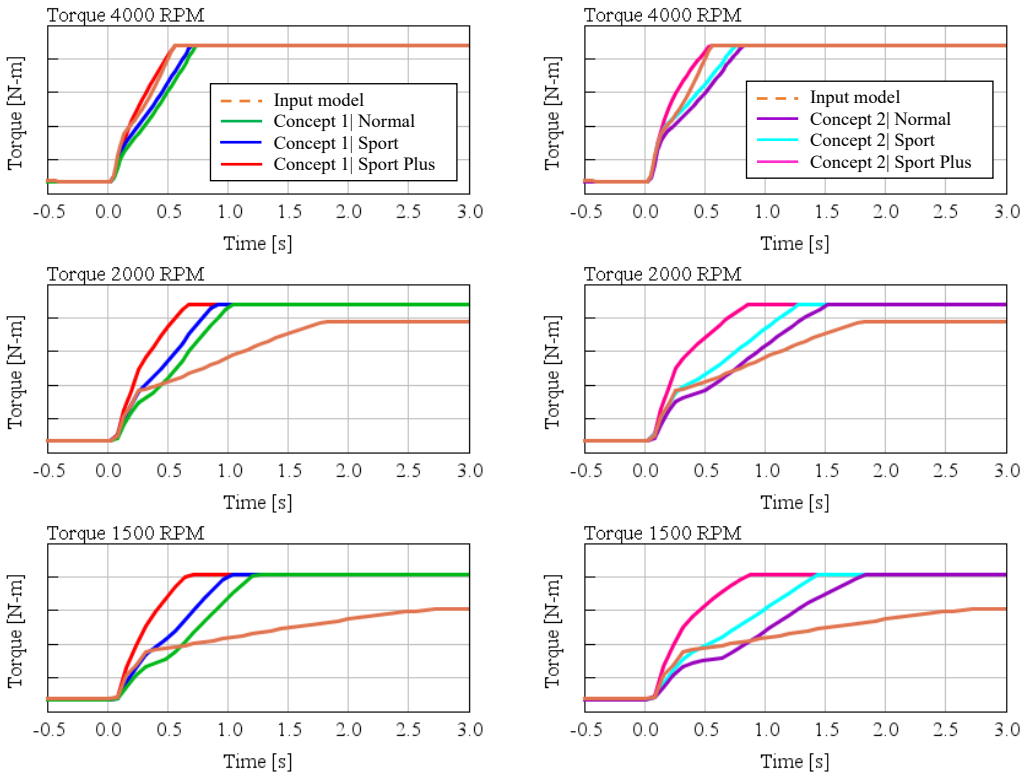

Figure 8.1: (a)Torque build up during tip-in maneuver of Concept 1 compared to reference engine. (b)Torque build up during tip-in maneuver of Concept 2 compared to reference engine.

The performance in torque build up are also reported in Figure 8.2 where three indexes are used:

- *Time to max torque*: is the time in seconds required to complete the tip-in, which means the time to reach the target torque.
- *Time to torque 1090*: is the time in seconds necessary to move from the 10% of the maximum torque up to the 90% of the maximum torque.
- *Torque integral* at 1.2 s: is a parameter which indicates the capability of torque build up in 1.2s. Introduced by Porsche Engineering, it qualitatively indicates the engine promptness felt by the driver. It follows that the higher the torque integral, the higher the acceleration feeling. In formula:

$$Torque\ integral = \int_{0\ s}^{1.2\ s} T_{ICE} \cdot dt \tag{8.4}$$

Hence, the attention goes to the torque integral, where again very good values emerge from low speeds tip-in while at 4000 rpm just Sport Plus mode is capable of perform better than the current engine.

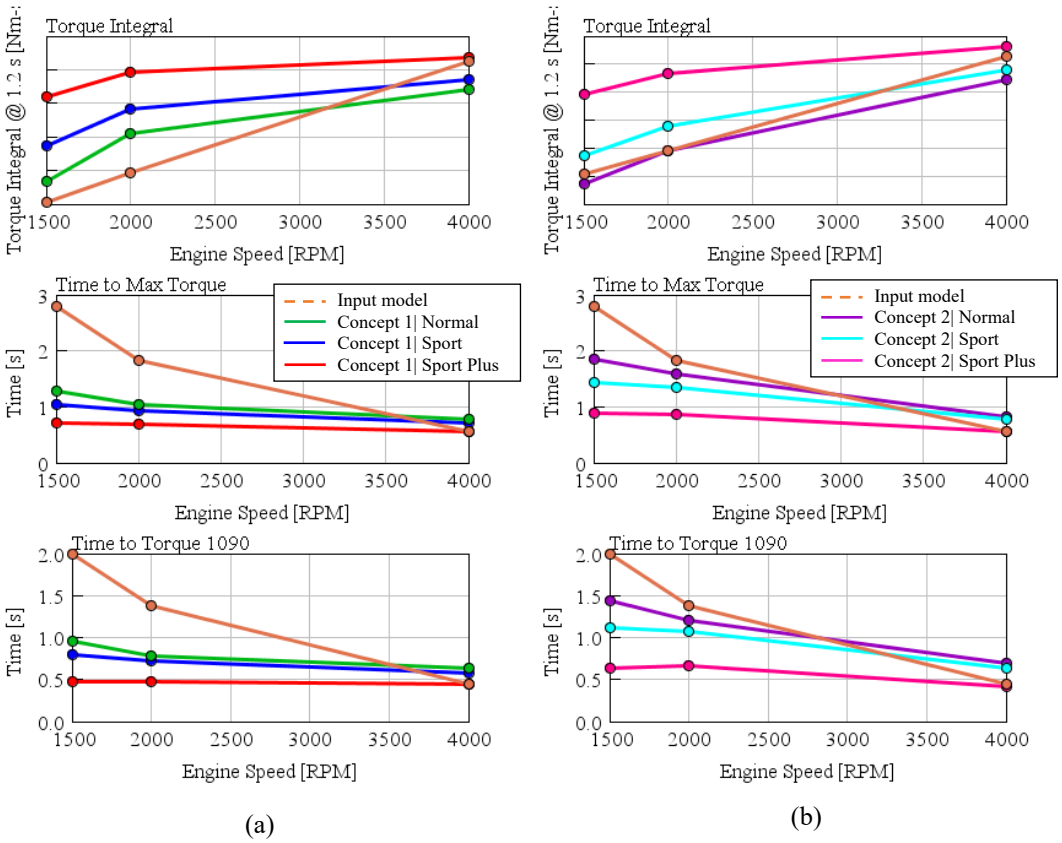

Figure 8.2: (a) Concept 1 transient performance indexes compared to reference engine. (b) Concept 2 transient performance indexes compared to reference engine.

8.1.1. SPORT PLUS ENGINE MODE

In Sport Plus mode, excellent transient performances are obtained in both Concept 1 and Concept 2 tip-in maneuver, as highlighted in Figure 8.1. However, the price to pay of these high performances are an increased part load fuel consumption and the battery energy usage in transient.

In part load in order to minimize the time to maximum torque, the idea is to keep the turbocharger "awake" by keeping the turbo speed at high values. In order to do so, simply driving the turbocharger with the E-turbo EM would have led to move the compressor operating point in the surge region and thus, it would have been dangerous for the component. It was thought indeed, to exploit the compressor blow-off valve, that is kept open while the compressor is electrically driven with the EM. Furthermore, instead of discharging the battery in part load operation, the P2 EM provides the energy to the E-Turbo EM, and so the engine load increases. The part load results just for Concept 1 as an example are reported in Figure 8.3, where also the normal part load mode is shown. It can be observed that the EM power is positive since it is driving the compressor while the P2 EM power is now negative. The electric efficiency in the connection among the two electric motors is now decreased to 50% as a worst case, considering the lower electric motor efficiency at low loads. The BSFC increases a lot because of the higher engine load but it is beneficial for the turbo speed, which is significantly higher than the normal mode.

In transient instead, the blow-off valve is being closed with the same speed at which the throttle valve is wide opened, the P2 EM power goes to 0 and it does not intervene during the tip-in, while the E-Turbo EM is battery boosted. The described working principle is shown in Figure 8.4: EM power is positive before the tip-in starts and by convers the P2 EM is negative, since it is boosting the E-Turbo EM. The turbo speed is already high before the maneuver starts and as soon as the throttle is wide opened, P2 EM power goes to 0 and E-Turbo EM increases up to the maximum value. Reached the maximum torque, the E-Turbo starts to regulate the boost pressure.

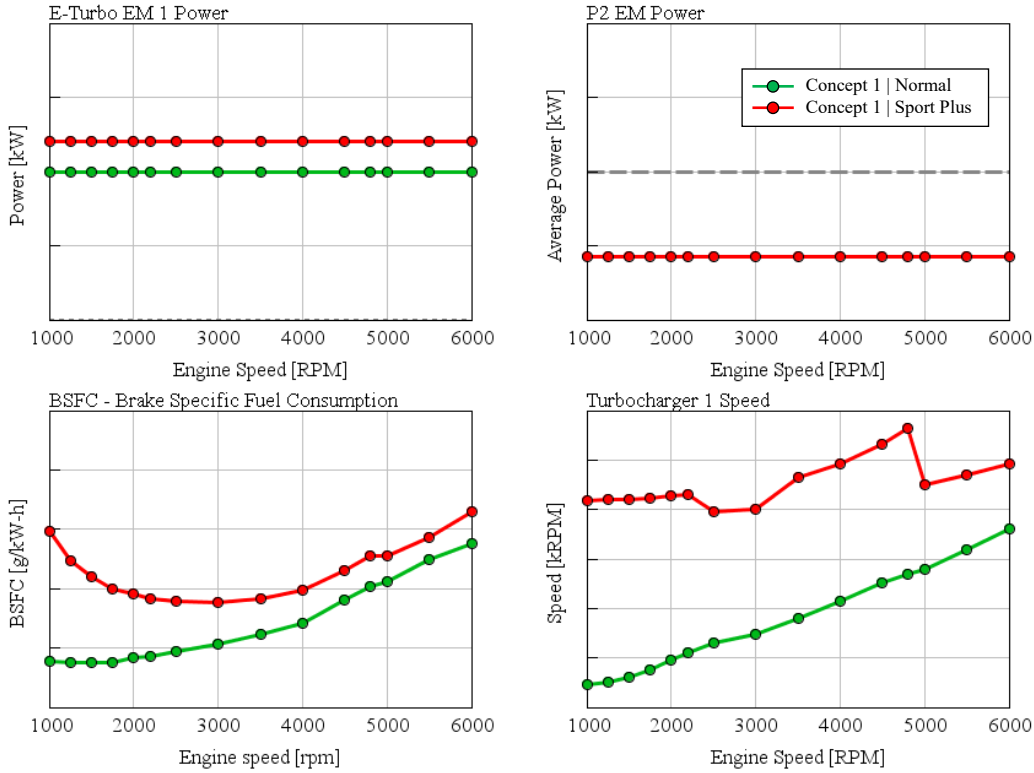

Figure 8.3: Concept 1 Sport Plus mode in part load (2 bar BMEP) operation performance. E-Turbo operation details.

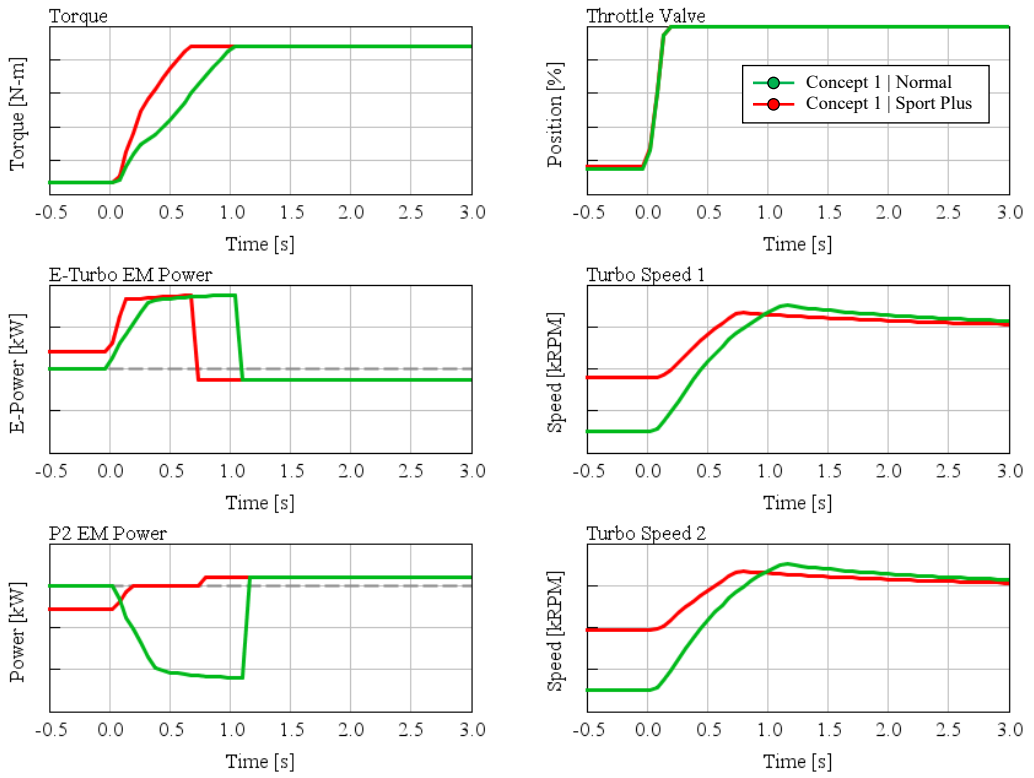

Figure 8.4: Concept 1 Sport Plus mode during 2000 rpm transient operation performance. E-Turbo operation details.

9. CONCLUSIONS

The future Euro 7 emission standard, which will come into force from 2025, will prohibit the fuel enrichment strategy, widely adopted in gasoline ICE to prevent component damage. Moreover, the TWC conversion efficiency strongly depend on the lambda value, reinforcing the requirement of stoichiometric operations even in the near future. Therefore, the work was motivated by the need of completely remove the fuel enrichment in the whole engine map and thus the full load conditions, which are the most demanding of enrichment, were considered. In this regard, the 1D CFD simulation code was used to perform the investigations on the reference engine, a V8 twin-turbocharged GDI engine, on which several updates were done. Initially, the enrichment causes were studied in order to consider the latest components limits developments, then the engine model was modified accordingly. The result was an update in the lambda control strategy, being the TWC the component exposed to the highest risk of damage, due to the increased turbine thermal resistance: hence the enrichment is now controlled according to the maximum T_4 of 870 °C.

With the new lambda control strategy, a series of innovative engine technologies were individually investigated, aiming at minimize the exhaust temperature and therefore to maximize engine efficiency:

- *E-Turbo*: it is a very promising technology, especially thanks to its increased flexibility in the powertrain power management and to the improved transient behavior.
- *Miller and Atkinson cycles*: allow a very effective knock mitigation. However, their standalone application may be insufficient. Their potential is maximized if coupled with other technologies.
- *TJI*: its improvement in combustion, its ease of implementation and low cost make it a very promising technology for the future of gasoline engine. Part load operation might impose some limitation.
- *A/C CAC*: it is a very solid technology, capable of important enrichment reduction without the need of big engine layout modification, since the A/C system is already present in vehicle and properly dimensioned.
- *WI*: widely studied, it showed the highest knock mitigation potential due to the high vaporization heat of the water. However, the high implementation cost and the water consumption are its major weakness.
- *Dual lift cam profile*: a well-known technology, widely adopted that allows to reach lambda 1 with proper cam profiles. However, it has no more potential of improvements.
- *H2 assisted combustion*: deeper analysis is necessary to clearly understand the true potential, especially at high load and high speed. Nevertheless, promising results have been obtained.

By the combination of the technologies that showed the higher potential and the higher margin of future improvement, two versions of Euro 7 engine concepts have been defined: *standard version*, characterized by the minimum number and technology combination and the *Evo version*, where performances were researched. Three standard versions concepts and two Evo versions have been proposed, all capable to reach the target even with the higher specific power of +17% of the Evo versions. The standard versions represent output of the thesis work, thus additional analysis were performed on them, investigating the part load operation and the transient behavior, where a tip-in maneuver was simulated. According to the results obtained for such concepts it is possible to conclude: The E-Turbo technology is present in each concept and therefore it can be considered as

a constant for what cost and installation is concern. Concept 1 showed the best performance in full load operation, where the maximum T_4 was even below the threshold, as well as in part load and transient operations, where respectively the Miller cycle and the smaller turbocharger inertia positively affected the performances. Furthermore, considering the concepts technologies installations costs, Concept 3 results to be the worst, due of the water injection that requires a lot of sub-systems that significantly increase the overall cost, while both Concept 1 and 2 require a comparable implementation effort. However, despite the similar cost of both concepts, the Concept 2 showed limited performance in fuel enrichment reduction at maximum speed, which would have limited the maximum power. Thus, the Concept 1 can be decreed the best in Euro 7 optic, thanks to the combination of promising technologies that make it future proof for further development and capable of ensure very good performances. Finally, for what Evo versions is concern, similarly to the standard versions, concept Evo 1 can be selected as the preferred among the two, because of the A/C CAC technology robustness and relative low implementation cost, especially if compared with water injection.

In closing, the tightening of the emission restrictions will definitely require an increase in internal combustion engine efficiency and in this regard, the technologies analyzed showed a promising potential, which however will introduce new challenges in packaging, implementation and costs. Furthermore, the fact that all the concepts adopt the E-Turbo technology, suggest that in the next future, to meet the emission standards, some level of hybridization will probably be required.

10. BIBLIOGRAPHY

[1] Joshi, A."Review of Vehicle Engine Efficiency and Emissions", SAE Journal Article, 2019-01-0314 - doi.org/10.4271/2019-01-0314, 2019.

[2] Commission Regulation (EU) 2009/443, OJ L140, 5.6.2009, p. 1-15..

[3] Joshi, A."Review of Vehicle Engine Efficiency and Emissions", SAE Journal Article, 2020-01-0352 - doi.org/10.4271/2020-01-0352, 2020.

[4] J. Heywood, Internal Combustion Engine Fundamentals 2E, McGraw-Hill Education, 2018.

[5] V. Bevilacqua, E. Jacobs, G. Grauli, J. Wüst, "Future of Downsizing: Fuel Consumption Improvement in NEDC as well as in Customer Operating Conditions", SIA SI Engine Int. Conf, Strasburg, n. 2019-06-30, 2013.

[6] K. Grote e J. Feldhusen, Dubbel: Taschenbuch für den Maschinenbau, Springer-Verlag Berlin Heidelberg, 2007.

[7] G. Corvaglia, «Optimization of the gas exchange of a cross-plane V8 engine,» 2015.

[8] Gamma Technologies, GT-POWER User Manual, 2019.

[9] G. Woschni, «A Universally Applicable Equation for the Instantaneous Heat Transfer Coefficient in the Internal Combustion Engine,» SAE Transactions, vol. 76, p. 3065, 1967.

[10] Bontemps N., Bas A., Ladonnet M., Zecchetti D., Heintz S., Davies P., "Electric turbo, a key technology to achieve Eu7 hybridized powertrain (lambda 1, performance and energy efficiency)", Internationaler Motorenkongress, Springer Vieweg, Wiesbaden - doi.org/10.1007/978-3-658-26528-1_6, 2019.

[11] Millo F., Luisi S., Borean F., Stroppiana, A., "Numerical and experimental investigation on combustion characteristics of a spark ignition engine with an early intake valve closing load control", Fuel,Vol. 121, Pages 298-310 - doi:10.1016/j.fuel.2013.12.047, 2014.

[12] Luisi, S., Doria, V., Stroppiana, A., Millo, F. et al."Experimental Investigation on Early and Late Intake Valve Closures for Knock Mitigation through Miller Cycle in a Downsized Turbocharged Engine", SAE Technical Paper, 2015-01-0760 - doi.org/10.4271/2015-01-0760, 2015.

[13] G. Ferrari, Motori a Combustione Interna, Esculapio, 2005.

[14] Schernus et al.: “Methods to Reduce End Gas Temperatures for Lower Knocking Sensitivity - A Simulation Study”, SIA SI Engine Int. Conf., Strasbourg, France, 2013.

[15] Wittek, K., and al.: “CO2-potential of a two-stage VCR system in combination with future gasoline powertrains”, 33rd Intern. Vienna Motor Symposium, Austria, 2012.

[16] Stadler, A., Sauerland, H., Härtl, M., and Wachtmeister, G."The Potential of Gasoline Fueled Pre Chamber Ignition Combined with Elevated Compression Ratio", SAE Technical Paper, 2020-01-0279 - doi.org/10.4271/2020-01-0279, 2020.

[17] Bozza, F., Tufano, D., Malfi, E., Teodosio, L. et al."Performance and Emissions of an Advanced Multi-Cylinder SI Engine Operating in Ultra-Lean Conditions", SAE Technical Paper, 2019-24-0075 - doi.org/10.4271/2019-24-0075, 2019.

[18] Bunce, M., Blaxill, H., and Cooper, A.,"Development of both Active and Passive Pre-Chamber Jet Ignition Multi-Cylinder Demonstrator Engines," presented at in the 28th Aachen Colloquium Automobile and Engine Technology, 2019.

[19] A. A. Yontar, "A comparative study to evaluate the effects of pre-chamber jet ignition for engine characteristics and emission formations at high speed", Energy Procedia, Volume 81, Pages 826-835 - doi.org/10.1016/j.egypro.2015.12.091, 2015.

[20] Bunce, M. and Blaxill, H."Sub-200 g/kWh BSFC on a Light Duty Gasoline Engine", SAE Technical Paper, 2016-01-0709 - doi.org/10.4271/2016-01-0709, 2016.

[21] B. S., Physics of turbulent jet ignition: mechanisms and dynamics of ultralean combustion, Springer, 2018.

[22] Cooper, A., Harrington, A., Bassett, M., Reader, S. et al."Application of the Passive MAHLE Jet Ignition System and Synergies with Miller Cycle and Exhaust Gas Recirculation", SAE Technical Paper, 2020-01-0283 - doi.org/10.4271/2020-01-0283, 2020.

[23] R. Dingelstadt, P. Wieske e A. Eilemann, «Refrigerant-based Charge Air Subcooling,» MTZ worldwide, vol. 76, pp. 36-41, 2015.

[24] A. Eilemann, P. Wieske and R. Dingelstadt, "Interaction between Charge Air Cooling and Vehicle Air Conditioning," ATZ Worldwide, vol. 118, pp. 48-53, 2016.

[25] A. Gomaa, «Performance Characteristics of Automotive Air Conditioning System with Refrigerant R134a and Its Alternatives,» International Journal of Energy and Power Engineering, vol. 4, pp. 168-177, 2015.

[26] Tornatore, C., Siano, D., Marchitto, L., Iacobacci, A. et al."Water Injection: a Technology to Improve Performance and Emissions of Downsized Turbocharged Spark Ignited Engines", SAE Journal Article, 2017-24-0062 - doi.org/10.4271/2017-24-0062, 2017.

[27] Berni F, Breda S, Lugli M, Cantore G. "A numerical investigation on the potentials of water injection to increase knock resistance and reduce fuel consumption in highly downsized GDI engines", Energy Procedia; 81:826–35, 2015.

[28] Millo, F., Mirzaeian, M., Porcu, D., "Knock Mitigation Techniques for highly boosted downsized SI engines", 29th SIA Powertrain Congress – June 06-07, Paris, 2017.

[29] Hoppe F, Thewes M, Baumgarten H, Dohmen J. Water injection for gasoline engines: Potentials, challenges, and solutions. Int J Engine Res, 2016.

[30] Cavina, N., Rojo, N., Businaro, A., Brusa, A. et al."Investigation of Water Injection Effects on Combustion Characteristics of a GDI TC Engine", SAE Journal Article, 2017-24-0052 - doi.org/10.4271/2017-24-0052, 2017.

[31] Zhu, S., Hu, B., Akehurst, S., Copeland, C., Lewis, A., Yuan, H., Kennedy, I., Bernards, J., Branney, C., "A review of water injection applied on the internal combustion engine", Energy Conversion and Management,Vol. 184, Pages 139-158, doi:/10.1016/j.enconman.2019.01.042, 2019.

[32] Battistoni, M., Grimaldi, C., Cruccolini, V., Discepoli, G. et al."Assessment of Port Water Injection Strategies to Control Knock in a GDI Engine through Multi-Cycle CFD Simulations", SAE Technical Paper, 2017-24-0034 - doi.org/10.4271/2017-24-0034, 2017.

[33] Paltrinieri, S., Mortellaro, F., Silvestri, N., Rolando, L. et al."Water Injection Contribution to Enabling Stoichiometric Air-to-Fuel Ratio Operation at Rated Power Conditions of a High-Performance DISI Single Cylinder Engine", SAE Technical Paper, 2019-24-0173 - doi.org/10.4271/2019-24-0173, 2019.

[34] M. Sellnau, T. Kunz, J. Sinnamon e J. Burkhard, «2-step Variable Valve Actuation: System Optimization and Integration on an SI Engine,» SAE Technical Paper 2006-01-0040 - doi:10.4271/2006-01-0040, 2006.

[35] Topinka, J., Gerty, M., Heywood, J., and Keck, J."Knock Behavior of a Lean-Burn, H2 and CO Enhanced, SI Gasoline Engine Concept", SAE Technical Paper, 2004-01-0975 - doi.org/10.4271/2004-01-0975, 2004.

[36] Shinagawa, T., Okumura, T., Furuno, S., and Kim, K."Effects of Hydrogen Addition to SI Engine on Knock Behavior", SAE Technical Paper, 2004-01-1851 - doi.org/10.4271/2004-01-1851, 2004.

[37] Gerty, M. and Heywood, J."An Investigation of Gasoline Engine Knock Limited Performance and the Effects of Hydrogen Enhancement", SAE Technical Paper, 2006-01-0228 - doi.org/10.4271/2006-01-0228, 2006.

[38] Ashida, K., Hoshino, M., Maeda, H., Araki, T. et al."Study of Reformate Hydrogen-Added Combustion in a Gasoline Engine", SAE Technical Paper, 2015-01-1952 - doi.org/10.4271/2015-01-1952, 2015.

[39] Kim, J., Chun, K., Song, S., Baek, H. et al."Effect of Hydrogen as an Additive on Lean Limit and Emissions of a Turbo Gasoline Direct Injection Engine", SAE Technical Paper, 2015-01-1886 - doi.org/10.4271/2015-01-1886, 2015.

[40] Heimrich, M., "Air Injection to an Electrically-Heated Catalyst for Reducing Cold-Start Benzene Emissions from Gasoline Vehicles," SAE Technical Paper 902115 - doi.org/10.4271/902115, 1990.

[41] Heller, S. and Wachtmeister, G., "Analysis and Modeling of Heat Transfer in the SI Engine Exhaust System During Warm-Up," SAE Technical Paper 2007-01-1092 - doi.org/10.4271/2007-01-1092, 2007.

[42] Sendil velan, S., Jeyachandran, K., and Bhaskar, K., "Experimental Investigation of Emission Control from Spark-Ignition Engine Using Electrically Heated Catalyst," SAE Technical Paper 2001-01-2000 - doi.org/10.4271/2001-01-2000, 2001.


PORSCHE
STUTTGART